

SOOT FORMATION

B. S. HAYNES* and H. GG. WAGNER

Institut für Physikalische Chemie der Universität Göttingen, 3400 Göttingen, West Germany

1. INTRODUCTION

The formation and emission of soot by combustion processes pose problems which have long concerned scientist and engineer alike. Soot emission from a practical combustion appliance reflects poor combustion conditions and a loss of efficiency. It may result in an unsightly stack plume and contribute to reduced atmospheric visibility and increased particulate fallout. The emission of soot, or smoke, is however not only a problem of aesthetics or even energy conservation for these emissions are often associated with carcinogenic polycyclic aromatic hydrocarbons. This fact, and the increased particulate loadings of the atmosphere caused by smoke emissions, means that adverse health effects must also be considered.

Within the flame environment itself, the situation is not so clear cut. In internal combustion engines (particularly in diesel motors) and gas-turbine combustors the deposition of soot has deleterious consequences for the maintenance and efficiency of the device, so the designer has many good reasons to avoid soot formation altogether. This objective also applies in the case of fires, whose mechanism of propagation often involves radiant transfer from hot soot particles. On the other hand, this same ability to radiate is obviously desirable in a candle flame. Similarly, the presence of soot in a furnace flame promotes radiation and hence the efficiency of heat transfer from the flame. Under these circumstances, the technical problem is to generate the soot in such a way that the particles can be oxidized before they leave the furnace.

At the opposite extreme, the production of carbon black requires a maximum yield of soot from the flame pyrolysis of a hydrocarbon feedstock. However, we shall be paying little attention to this aspect of carbon formation in flames. The subject has received extensive coverage in the recent carbon black literature.¹⁻³

In brief, we are concerned here primarily with the generation of soot in combustion systems. Temperatures in such systems lie between 1500 and 2500 K and there is generally sufficient oxygen available for the substantial combustion of the fuel. The total amount of soot formed under these conditions is usually very small compared to the amount of carbon present in the fuel consumed.

Under these conditions, the time typically available for the formation of soot is of the order of a few milliseconds. During this time, some of the fuel is trans-

formed to give rise to the solid soot particles. The resulting aerosol can be characterized by the total amount of the condensed phase, often expressed as the soot volume fraction ϕ ($\text{cm}^3 \text{ soot}/\text{cm}^3$); the number of soot particles, N (cm^{-3}); and the size of the particles, d . The particles also possess a size distribution but this is usually relatively narrow and for the most part we shall consider here only an average size. The quantities ϕ , N and d are mutually dependent (for spherical particles, $\phi = \pi/6 \cdot Nd^3$) and any two are sufficient to characterize the system.

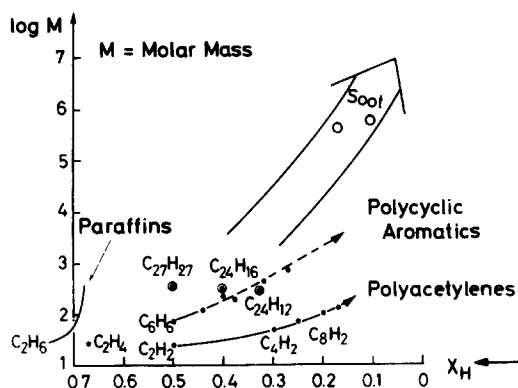
From a mechanistic point of view, it is most convenient to consider N and ϕ as the independent variables in the process as they are directly related to what appear to be the more-or-less separate stages of "soot particle formation" (the source of N) and "soot formation" (the source of ϕ). These stages can be summarized qualitatively as:

(1) Particle inception, whereby the first condensed phase material arises from the fuel-molecules via their oxidation and/or pyrolysis products. Such products typically include various unsaturated hydrocarbons, particularly acetylene and its higher analogues (C_{2n}H_2), and polycyclic aromatic hydrocarbons. These species are relatively stable with respect to decomposition to the elements⁴⁻⁹ and, compared with the paraffins and even olefines, they are also rather stable kinetically. These two types of molecule are often considered the most likely precursors of soot in flames.

The condensation reactions of gas phase species such as these lead to the appearance of the first recognizable soot particles (which are often called nuclei although this term should be used with caution because of its connotations of physical condensation phenomena). These first particles are very small ($d < 20 \text{ \AA}$) and the formation of even large numbers of them involves a negligible soot loading in the region of their formation, which is generally confined to the more reactive regions of the flame—i.e. in the vicinity of the primary reaction zone.

(2) Surface growth, by which the bulk of the solid-phase material is generated. Surface growth involves the attachment of gas phase species to the surface of the particles and their incorporation into the particulate phase. Some qualitative trends in this process can be obtained from Fig. 1, where the logarithm of the molecular weight of a species is plotted against its hydrogen mole fraction, x_H ¹⁰. Beginning with a typical fuel molecule of $x_H \gtrsim 0.5$, it is apparent that neither purely polyacetylene chain growth nor purely p.c.a.h. growth would lead to typical soot particles which have x_H in the range 0.1–0.2. What is needed is the condensation of species with the right hydrogen

*Present Address: Department of Chemical Engineering, Massachusetts Institute of Technology, Cambridge, MA 02139.

FIG. 1. Pathways to soot formation.¹⁰

content; or condensation of species with a higher hydrogen content followed by dehydrogenation; or a combination of both. Obviously some polyacetylenes and some polycyclics can satisfy these requirements, as can the saturated platelets (e.g. $C_{27}H_{27}$) proposed recently as soot intermediates.¹¹

Surface growth reactions lead to an increase in the amount of soot (ϕ) but the number of particles (N) remains unchanged by this process. The opposite is true for growth by coagulation, where particles collide and coalesce, thereby decreasing N , ϕ remaining constant. Particle growth (increasing d) is the result of simultaneous surface growth reaction and coagulation.

These stages of particle generation and growth constitute the soot-formation process. This is often followed by a phase of soot oxidation in which the soot is burnt in the presence of oxidizing species to form gaseous products such as CO and CO_2 . The eventual emission of soot from any combustion device will depend on the balance between these processes of formation and burnout.

It is the objective of this review to report, in greater detail than was possible in an earlier version,¹² on progress made in the study of soot formation in flames since the classic review of Palmer and Cullis¹³—i.e. since about 1964. Before discussing what is known of the details of the various stages outlined above we consider some more phenomenological aspects of soot formation under different conditions. Then, in Section 9, detailed kinetic results will be considered.

Inevitably, there are gaps in our coverage—as mentioned earlier, the literature on carbon black will not be considered; nor will the formation and deposition of carbon on surfaces. Furthermore, we consider the polycyclic aromatic hydrocarbons only in terms of their contribution to soot formation rather than as an undesirable emission in their own right. Other reviews which should be consulted on these areas and on soot formation in general are those of References 1–3 and 13–23. We also draw the reader's attention to some excellent new work presented at meetings too recently to be included in detail in this review—references 387, 388.

2. APPEARANCE OF SOOT

Soot generated in combustion processes is not uniquely defined. It normally looks black and consists mainly of carbon but it is quite different from graphite. Apart from carbon, soot particles also contain up to 10 mole % hydrogen, and even more when they are young. A good deal of this hydrogen can be extracted in organic solvents where it appears mostly in condensed aromatic ring compounds.

Sometimes, substances are emitted which, when cooled, look like tar or like glassy material, black, brown or even yellow in colour. Such materials may be the quenched intermediates of the soot formation process. Sometimes they result as a condensation product of the heavy hydrocarbons formed during combustion; or they may be fuel droplets which have passed through the combustion zone more or less untouched. Finally, they may be normal soot particles on which heavy hydrocarbons have condensed, as is the case with diesel smoke.

The inspection of soot under an electron microscope (Fig. 2) shows that the basic units of soot are spherical or nearly spherical particles with diameters often in the range 200–300 Å, corresponding to about one million carbon atoms. These particles are often called “elementary soot particles”.* Some of them are marked in Fig. 2 by white circles. These “elementary particles” are aggregated together to form the straight or branched chains to be seen in Fig. 2 (the bright spots are shadows of the particles in these chains). It is such chains, which form the fluffy soot flocculates, sometimes visible in the atmosphere.

The elementary soot particles exhibit a size distribution, usually not far from log-normal. However, as pointed out by Palmer and Cullis¹³ the particles collected from a wide variety of combustion processes (under normal operating conditions), such as furnace flames, piston engines, turbine combustors or premixed flames, do not differ much in size, being typically 200–400 Å in average diameter.

Information on the internal structure of soot particles has come mainly from investigations of carbon black particles generated in technical carbon black processes.† Early work with X-ray diffrac-

* Before the “elementary soot particles” reach their final size, smaller particles are present. They coagulate but do not form chains. During the formation of soot the product of coagulation and surface growth of these smaller particles are spherical particles. When in the following sections the growth of soot is considered it is mainly the growth of these elementary soot particles.

† These processes are not the same as combustion processes used for power generation but they are sufficiently closely related to be relevant in some cases. In the furnace process, hydrocarbons are injected into the burned gases of hydrocarbon-air diffusion flames. In the channel process, a natural gas flame impinges on a cold wall where reaction is quenched and carbon particles are precipitated. The lamp black process employs a pool-fire fed with aromatic oil and restricted air supply. We may thus safely assume that the structure of carbon black particles is at least related to that of soot particles of interest here.

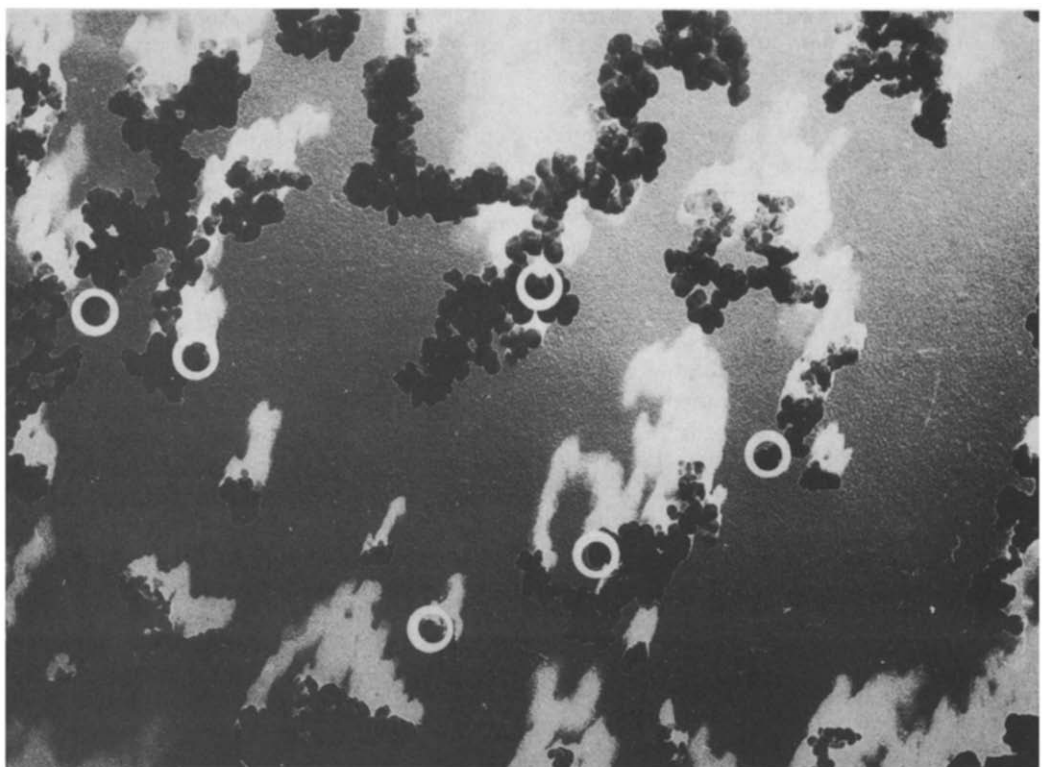


FIG. 2. Electron micrograph of soot particles of mean diameter 200 Å. The bright regions are the silhouettes of the particles created by heavy metal sputtering from the direction of the bottom right-hand corner.

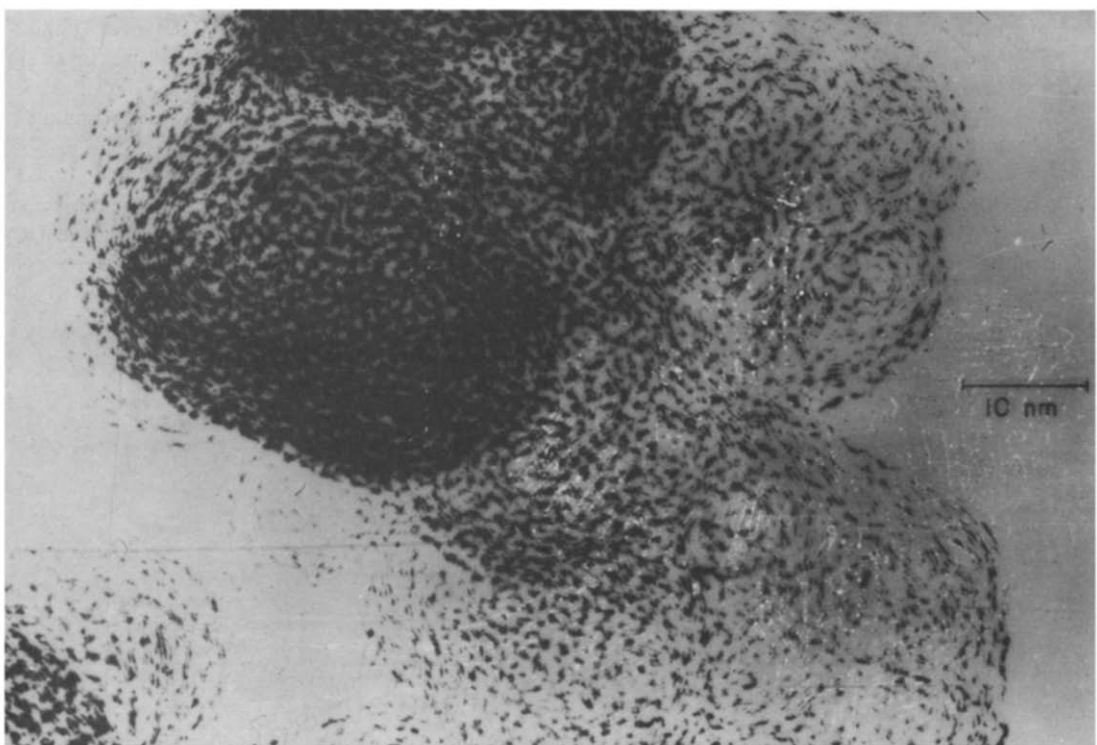


FIG. 3. Phase-contrast electron micrograph of carbon black.³³

tion²⁴⁻³¹ indicated that, within a particle, there are randomly disposed domains of graphite-like parallel layers. The spacing between these layers is somewhat larger than in graphite, however.

More recently, high-resolution phase-contrast electron microscopy of carbon black particles has been studied. The interpretation of the resulting images (see Fig. 3) can be summarized as follows:³²⁻³⁷ near the edge of the particle, bent carbon layers follow the shape of the particle surface. Inside the particles, lattice structures seem to be located more or less regularly around certain centres between which the structure is less ordered. Many dislocation and other lattice defects are present. The extension of the layers seems to be larger than indicated by the X-ray studies and the concept of crystallite formation, based on the X-ray results, is no longer favoured.^{26,35} The density of the particles may be less than 2 gm/cm³ due to large interplanar spacings. Electron diffraction indicates the presence of single C-C bonds.³⁸

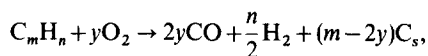
Heat treatment improves the internal order of the particles and the interplanar spacing approaches that of graphite. The rate of graphitization depends on temperature so that the age of a particle and its degree of order are closely linked.³⁹⁻⁴⁰ For soot particles at high temperatures, some ordering may occur as the particles continue to grow.

These observations pertain largely to comparatively old particles. Younger particles have a much higher hydrogen content and may have considerable radical character⁴¹⁻⁴⁴ so the situation may be rather different for them.

3. SOOT FORMATION IN PREMIXED FLAMES

3.1. The Sooting Limit

From a thermodynamic viewpoint, the formation of soot should only occur when, in



m becomes larger than $2y$ —i.e. when the C/O ratio exceeds unity.

Experimentally, limits of soot formation are usually equated with the onset of luminosity, and this occurs not at $C/O \approx 1$ but usually in the vicinity of $C/O = 0.5$. As shown in Table 1, the values of the critical C/O ratio found in Bunsen burner flames, flat flames, and stirred reactors are similar.

The influence of flame structural effects on the critical C/O ratio is shown by the familiar carbon streak emerging from the tip of Bunsen burner flames.¹⁹ Investigations of polyhedral flames have shown that the concentration above the flame zone varies from the ridges to the valleys, such that a richer mixture is burned over the ridges than in the valleys.⁵³⁻⁵⁹ Similarly, concentration measurements along the axis of a Bunsen burner flame show a pronounced maximum of C/O at the tip: for cyclohexene/air a maximum value of $C/O = 0.66$ was measured while in the input mixture $C/O = 0.52$.⁶⁰ For sufficiently rich input mixtures, this effect may lead to the rich limit of inflammability being exceeded at the tip, in which case soot formation occurs not over the tip but in a ring around it.⁴⁹

At the same time, diffusion of H and H_2 leads to a marked increase in the hydrogen content of the gases at the flame tip. As demonstrated by Homann, the appearance of soot formation in flames of higher hydrocarbons can be changed into that of C_2H_2 —or C_2H_4 —flames if sufficient H_2 is added so that the preferential diffusion of hydrogen becomes unimportant.¹⁰

These transport effects lead to the observation of somewhat higher critical C/O ratios for the heavier fuel molecules in flat-flame than in curved (e.g. Bunsen burner) flames (see Table 1 and References 61 and 62). However, even when these effects are taken into account, the experimentally observed critical C/O ratio remains well below that pertaining to equilibrium.

The departure from equilibrium is also shown by the fact that significant amounts of CO_2 and H_2O are observed at and even well beyond the critical C/O ratio, even though the concentrations of these species should be negligible in the presence of soot.⁶³ The

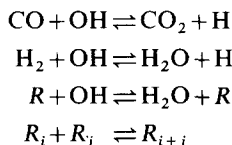
TABLE 1. Limits of soot formation ($T \approx 1800$ K)

	Bunsen-burner ^a	Well-stirred reactor ^b	Flat flame	
			$p = 1$ atm	$p \approx 20$ Torr
CH_4-O_2	—	—	0.45 ⁴⁸	—
C_2H_6 -air	0.48	—	0.47 ⁴⁹	—
C_3H_8 -air	0.47	—	0.53 ⁴⁹	—
C_2H_4 -air	0.61	0.70	0.60 ⁴⁹	—
$C_2H_4-O_2$	—	—	0.71 ⁵⁰	—
C_4H_8 -air	0.52	0.68	—	—
C_2H_2 -air	0.83	—	—	—
$C_2H_2-O_2$	0.95 ⁴⁵	—	—	0.95 ⁵²
$(T \approx 3000$ K)				
C_6H_6 -air	0.57	0.57	0.65 ⁵¹	—
$C_6H_6-O_2$	—	—	—	0.74 ⁵²
Methylnaphthalene air	0.42	0.50 ⁴⁷	—	—

^a Reference 14 unless otherwise specified.

^b Reference 46 unless otherwise specified.

explanation for this result lies in the nature of the processes occurring in the flame zone. The OH radical reacts with parent (aliphatic) fuel and with H_2 ^{64,65} to produce H_2O , and with CO to yield CO_2 . At the same time, the radicals H, O, and OH attack the parent fuel to produce a variety of hydrocarbon radicals. Some of these will be unsaturated and therefore capable of preserving their radical character and reactivity on undergoing the addition reactions necessarily preceding the production of soot:



Because the H-atom reactions to reduce H_2O and CO_2 have high activation energies (86 and 108 kJ/mole respectively⁶⁵), the oxygen contained in these materials is tied up for the time available in most combustion processes. Thus, the appearance of soot at rather low C/O ratios in premixed systems is a result of reaction kinetics and this is reflected in the success of phenomenological models for the onset of sooting in premixed flames.^{66,67} At very high temperatures, >3000 K, such kinetic considerations may be secondary and the physical condensation of carbonaceous species such as C_2 and C_3 is theoretically possible^{45,68} but we shall not consider these conditions further here.

The critical C/O ratio is only weakly, if at all, dependent on pressure—see Table 1 and References 17 and 69–74. Similarly, dilution of the combustible mixture at constant temperature does not have a marked effect on the sooting limit. Thus Millikan and Foss⁵⁰ measured a critical C/O = 0.71 at 1800 K in ethylene/oxygen flames while a value of 0.60 is found for the air flame at the same temperature.⁴⁹ The weak effects of backmixing (Table 1)^{46,47} are consistent with this picture.

Increasing temperature generally allows richer mixtures to be burned without the onset of sooting.^{14,49,50,70,72,75} However, as shown in Fig. 4 the effect is not marked. In flames the critical C/O seems always to be below unity but Radcliffe and Appleton,⁷² who shock heated acetylene/ and ethylene/oxygen mixtures found $(C/O)_{crit}$ approaching 2 at temperatures around 2500 K. This discrepancy may result from a difference in the measuring techniques as Radcliffe and Appleton measured extinction coefficients (which are insensitive to temperature). On the other hand, the onset of sooting in flames is usually determined from the luminosity of the flame, which presumably makes lower concentrations of soot visible at higher temperatures, thus weighting the high temperature data to lower C/O ratios.

The problem of defining and measuring the critical C/O ratio is, in fact, worthy of further consideration. As Homann¹⁹ has pointed out, "there is no property of the flame which shows a sudden change when the carbon limit is exceeded". This observation, in itself, implies that the definition of the critical C/O ratio is rather arbitrary; for example, for ethylene-air flames at 1750 K, the experimentally determined critical C/O ratio varies from 0.60 for the onset of yellow luminosity to 0.63 for the detection of above-background scattering, to 0.67 for 0.5% absorption (as used by Radcliffe and Appleton).⁵¹

Despite such drawbacks, the concept of the critical C/O ratio has proved useful as a means of characterizing various fuels in different laboratories under a variety of conditions. There is now a solid body of data in the literature on this aspect of soot formation and this provides a valuable reference point for further work in this field.

3.2. The Soot Yield

Beyond the carbon limit, the yield of soot in premixed flames initially increases rapidly with increasing C/O ratio.^{47,48,49,51,70,71,76,77} Eventually, when the rich limit of inflammability is approached, the yield falls again,⁷⁰ but such conditions appear to be of little interest technically.

The soot yield is not always well correlated with the critical C/O ratio. Thus for turbulent flames at 15 atm on Meker type burner, Macfarlane, Holderness and Whitcher⁷⁰ found that a C/O ratio of 0.8 produces ten times as much soot from benzene as it does from *n*-hexane, even though the critical C/O ratio for both fuels occurs at about 0.5. Similarly for flat benzene- and ethylene-air flames, benzene, with a critical C/O ratio of 0.65, appears to resist the onset of sooting more effectively than does ethylene (critical C/O = 0.60). However, as shown in Fig. 5, the actual soot volume fractions are the same at C/O = 0.68, and at C/O = 0.72, benzene forms three times as much soot as ethylene.⁵¹

As will be discussed in more detail in Section 9, it is not so much the particle number as the particle size which increases with increasing C/O.^{48,51}

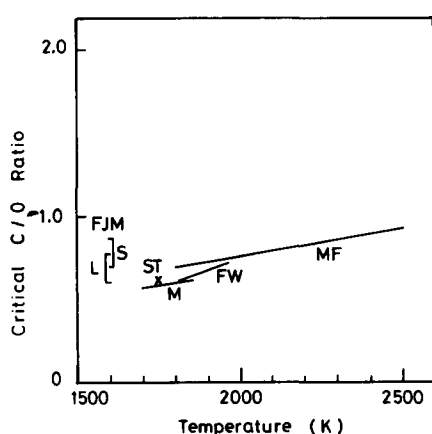


FIG. 4. Effect of temperature on the critical C/O ratio for soot formation in ethylene combustion. The symbols refer to the following conditions: ST,¹⁴ FW,⁴⁹ and M⁷⁵ all ethylene/air flames at 1 atm; MF⁵⁰ ethylene/oxygen flames at 1 atm; FJM⁶⁹ flames at 60–300 Torr on small (S) and large (L) burners.

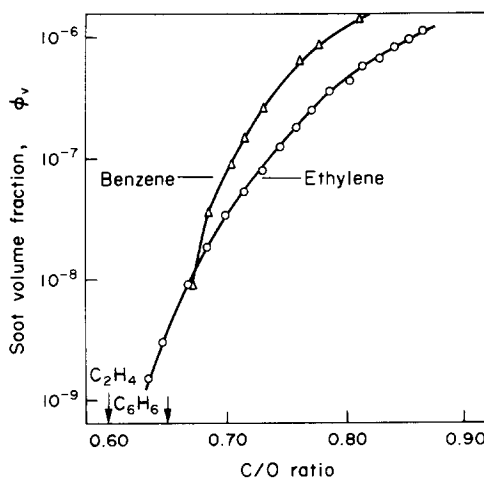


FIG. 5. Comparison of soot loadings from ethylene and benzene air flames for a range of C/O ratios.⁵¹

In contrast to the weak influence of pressure on the critical C/O ratio, the soot yield is usually strongly enhanced by increasing pressure.^{69,70,74} In their study of turbulent, premixed flames, Macfarlane *et al.*⁷⁰ found that the soot yield varied as P^{2-3} for fuels like hexane and hexene. (In the case of benzene, however, the effect of pressure was only weak.) The influence of pressure may result from a shifting of any gas-solid absorption balances to favour more condensation at higher pressures. This would be consistent with the weak pressure effect on the critical C/O ratio, i.e. in the absence of a surface on which such growth can occur.

In keeping with the influence of pressure, back-mixing brings about a profound reduction in the amount of soot produced at a given C/O ratio.^{47,77} Similarly, dilution of a premixed flame at constant temperature also reduces soot formation.⁷⁷

The effect of temperature on the production of soot appears to be complex. Near the critical C/O ratio, an increase in temperature reduces the amount of soot,^{49,51,70,75,78} and this has been interpreted as arising from differences in the activation energies of the steps forming soot and those opposing it (e.g. oxidation).⁷⁵ The magnitude of this effect is somewhat greater than the influence of temperature on the critical C/O ratio.^{49,75}

In very fuel rich flames, an increase in temperature has been observed to promote soot formation.⁷⁰ These results were obtained at elevated pressure (15 atm), where the rich limit of stability is significantly extended. The flames examined were probably fairly cool ($T \approx 1500\text{ K}$) and the effect is presumably due to enhanced pyrolysis at higher temperatures.⁷⁰

The structure of the flame zone also modifies the temperature effect: the appearance of a cellular structure changes the influence of increasing temperature from anti- to pro-soot.⁴⁹

3.3. The Influence of Additives

Additions of small quantities of most substances to premixed flames have little effect on carbon forma-

tion. Striking exceptions are some metals which affect sooting behaviour even when present at sub-ppm levels—these are discussed in Section 8. We are concerned here with the influence of additives effective at concentrations of the order of 1% of the fuel-air mixture.

Inert diluents tend to reduce the amount of soot at constant temperature.⁷⁷ However, dilution often produces a fall in temperature which promotes sooting, so the net result depends on the balance between these effects. Generally, rather high concentrations of inert diluents (> 5%) are required to produce significant changes in the soot concentration. Even this extent of dilution has practically no effect on the critical C/O ratio.^{14,79} Water vapour has practically no influence on either the soot threshold or the yield, except at very high concentration (> 10%).^{79,80}

Nitrogenous species such as NH₃, NO and NO₂ suppress the soot yield and raise the critical C/O ratio.^{17,79,81} For NH₃, the effect is as if the incoming mixture is made leaner by one C-atom for every N-atom added.⁷⁹ Such a result is consistent with the observation that NH₃ quantitatively forms unreactive HCN in fuel-rich hydrocarbon flames.⁸²

The sulphur compounds H₂S and SO₂ appear to be far more effective in reducing the soot yields, and raising the critical C/O ratio, than other species.^{14,79,83} Thus a 1% addition of either to a moderately sooting ethylene/air flame reduces the yield by about 85%.⁷⁹ The mode of action of the sulphur additions is not known.

The case of SO₃ additions to premixed flames is of special interest. Gaydon and Whittingham⁸³ found small (0.1% by volume) additions of SO₃ generally increased the luminosity of a premixed coal-gas/air flame. Similarly, a 0.2% addition of SO₃ increased sooting by 40% in an isobutane/air flame at low pressure.⁶⁹ Street and Thomas¹⁴ also observed an increase in sooting due to SO₃ and H₂SO₄, but found, at least in the case of benzene, that the acid gas can attack the fuel ahead of the flame zone. This question has received further attention recently.⁷⁹ For atmospheric-pressure premixed flames of propane-, ethylene-, and benzene-air, additions of 0.1–0.5% SO₃ and H₂SO₄ reduce the amount of soot formed. The magnitude of the decrease is only slightly stronger than that which would result from the addition of other sulphur compounds such as SO₂ and H₂S. The reason for the discrepancy between these results and the others is unknown—if, as suggested by Street and Thomas,¹⁴ SO₃ can attack the fuel in the mixing chamber, some specific burner dependence might arise depending on residence times and temperatures there.

The addition of H₂ or CO tends to promote sooting, but only rather weakly.^{14,17,79} The critical C/O ratio is depressed and the yield of soot rises.⁷⁹ These species presumably act as sinks for oxygen early in the flame, thus making it effectively richer.

Hydrocarbon additions also promote sooting, presumably by increasing the carbon content of the mixture.¹⁴

In all cases, additives of the type discussed here do not affect the number density of soot particles present in the flame.⁷⁹ Changes in the amount of soot present due to the additives are reflected in changes in particle size. Thus, in terms of the coagulation theory to be discussed in Section 9, these additives do not affect growth due to particle coalescence so much as surface growth.

4. SOOT FORMATION IN GASEOUS DIFFUSION FLAMES

4.1. Laminar Diffusion Flames

Most practical combustion devices use diffusion flame type burning. Fuel and oxidizer enter through separate inlets and the combustion process is diffusion controlled, or, in more general terms, mixing controlled. It is obvious, that under such circumstances the C/O ratio cannot everywhere stay below its critical limit.

It is thus obvious that the formation and emission of soot from diffusion flames depends *i.a.* on the flow situation. The first attempts at understanding the structure of diffusion flames were made by Burke and Schumann⁸⁴ who predicted the position of the ideal flame front (where stoichiometric proportions of fuel and oxidant prevail) based on a simple model of equal interdiffusion in a constant velocity field. If the flame is over-ventilated (i.e. more than the stoichiometric requirement of oxygen is available), then the flame surface of an axi-symmetric flame will terminate at the axis—i.e. the flame will close at the top. The great success of this theory has been the successful prediction of the visible heights of a variety of axi-symmetric flames when appropriate diffusion coefficients are assumed.⁸⁴⁻⁸⁸ This model has recently been extended to describe successfully flames on a variety of burner shapes.⁸⁷⁻⁸⁹

However, the visible height of a sooting flame is not necessarily the same as the ideal diffusion flame height.^{86,88,90-92} The problem is that the flame luminosity depends both on the overall production of soot as well as on its overall removal by oxidation. The former process occurs within the flame and is usually controlled by thermal and species diffusivities. Significant burnout of the soot particles in the laminar situation can only begin after the fuel is largely consumed—this burnout is, at least partly, chemically controlled^{91,92} so that high concentrations of soot cause an increase in visible flame size. Now whether the flame smokes or not depends on whether the soot, once formed, has time enough to burn out before radiation losses and diffusion of fresh cold air quench its oxidation. Roper *et al.*^{88,90} report that this can be expected to occur when the ratio of soot oxidation length to the true diffusion flame height reaches a value around one, regardless of the nature of the fuel.

Most experimental work on soot formation in diffusion flames has dealt with overall effects whereby the processes of formation and burnout are not considered separately. We examine the results of these

sorts of experiments first before going on to discuss the few detailed investigations of the sooting structure of diffusion flames.

4.1.1. The influence of fuel structure

The reciprocal value of the height at which a flame on a given burner starts to smoke and the limiting smoke-free fuel flow have been used to gauge the tendency of different fuels to smoke. This tendency increases from paraffin to mono- and di-olefines, benzenes and naphthalenes.^{15,93-95} Generally, the smaller the molecule, the greater the resistance to smoke emission. Similarly, more compact isomers such as branched chain forms are more prone to sooting. Acetylene soots copiously in diffusion flame.^{95,96}

Similar results are obtained from flame luminosity measurements⁹⁷ although this method strictly requires the same temperatures in different flames to enable correct comparisons to be made. Also, at high soot concentrations, the emissivity approaches unity and the luminosity becomes independent of the amount of soot.

Glassman and co-workers⁹⁵ have recently confirmed the importance of fuel structure in determining the smoking tendency and shown that the C/H ratio of the fuel is not of itself significant, although this quantity is used to correlate results from practical systems.^{98,99} Glassman^{100,387} has also pointed out the importance of temperature in determining the smoke point—at the same stoichiometric flame temperature, acetylene is actually more resistant to soot formation than ethylene, which is the order observed for the critical C/O ratio in premixed flames also. Similarly, when added in amounts of a few percent (not enough to alter the flame temperature significantly) to a hydrogen diffusion flame acetylene shows a weaker sooting tendency than cyclohexane.^{101,102} In the same experiment, Tesner^{101,102} found an increasing soot yield of larger particles for the series cyclohexane–benzene–toluene–naphthalene.

A similar technique has been applied by Scully and Davies^{103,104} who injected a large number of hydrocarbon/nitrogen mixtures (1 : 3 mole ratio) axially into the turbulent combustion of a fuel-rich town's gas/air flame at about 1300 K. Their measurements of the yield of soot also point to the efficacy of aromatic rings in producing soot under predominantly pyrolytic conditions. Hetero-atoms such as O, S, and N contained in or adjacent to the ring structure strongly inhibit soot formation, presumably by favouring ring rupture.

These largely qualitative descriptions of sooting tendency agree well with the detailed shock-tube pyrolysis results discussed in Section 9.1.

4.1.2. Pressure

The effect of pressure on soot formation in diffusion flames has been investigated over a wide range of

conditions. Generally speaking, low pressures reduce carbon formation^{96,105} while high pressures promote it.¹⁰⁶

4.1.3. Composition of oxidant

The effect on sooting of the composition of the oxidant has received some attention. McLintock¹⁰⁷ determined the fuel flow at the smoke point (Q_{smoke}) for ethylene flames burning on a circular port burner in a variety of co-flowing synthetic air mixtures. The composition of the oxidant was characterized by its oxygen index, $OI = \text{oxygen flow}/(\text{oxygen flow} + \text{inert flow})$.

When added to a constant flow of oxygen ($0.1 < OI < 0.4$), the various inert diluents (He, Ar, N₂) differ only slightly in their influences. The overall trend is for decreasing OI to lead to a slightly decreasing tendency to smoke, as shown in Fig. 6.

The importance of the flow situation is demonstrated by the results of similar experiments at nearly constant total flow of oxidizer¹⁰⁶⁻¹⁰⁸ (see Fig. 6). Now decreasing OI from high values (≈ 0.4) results in a marked increase in sooting tendency, with a maximum at $OI \approx 0.25$. Further decreases in OI reverse this trend and Q_{smoke} rises increasingly rapidly until the flame is extinguished at $OI \approx 0.10$. Increasing OI in this flow arrangement results in higher maximum temperatures in the flame zone. Therefore the increase in sooting tendency with increasing OI at low values of OI has been attributed to the predominance of pyrolysis over oxidation in this temperature range.¹⁰⁶⁻¹⁰⁸ As the temperature rises, pyrolytic (soot-forming) reactions are enhanced more strongly than oxidation processes. On the other hand, at higher temperatures and higher oxygen concentrations, burnout, with the higher activation energy of the

two processes, is gradually favoured over pyrolysis and the sooting tendency decreases again.

Such a description is consistent with the result that, when the nitrogen in the air is replaced by argon, thereby leading to a rise in maximum temperature of some hundreds of degrees K, an increase in soot yield is observed at low OI . At higher OI , the amounts of soot are less in the argon cases.^{106,108}

Further support for this qualitative picture is found in the results of Dearden and Long¹⁰⁹ who collected soot from within ethylene—and propane-air diffusion flames stabilized on a Wolfhard-Parker burner. In this way, they largely avoided oxidation effects and found no reduction of soot at higher OI , but rather a continuing slight increase. At lower values of OI , the sooting rate increased far more rapidly with increasing OI .

4.1.4. Influence of additives

The effects of addition of various gaseous substances to the fuel flow have also been investigated. Simple dilution by inert gases such as Ar, He and N₂ generally decreases the tendency to soot.^{86,95,107,109-113} If sufficient diluent is added, carbon luminosity can be suppressed altogether,¹¹⁴ possibly because of the substantial temperature reductions in the flame zone. Dilution is qualitatively similar to a reduction in pressure and some suppression of soot formation due to this effect can also be expected.

The addition of hydrogen to the fuel also suppresses soot emission.¹⁰⁹⁻¹¹² The effect may be only slightly greater than that of inert dilution.¹⁰⁹

When CO₂ or H₂O is added to the fuel, there is a considerable reduction in soot-forming tendency^{107,112} and a concentration of 45% CO₂ completely suppresses luminosity in methane/air diffusion flames.¹¹⁴ Similarly, replacement of the N₂ in the air by CO₂ has been observed to give rise to non-smoking flames for oxygen indices 0.17 (extinction) $< OI < 0.45$.¹⁰⁷ McLintock¹⁰⁷ has suggested that the influence of CO₂ and H₂O is exerted primarily in the soot oxidation zone where these species presumably promote soot burnout. A similar mechanism has been proposed for SO₂^{114,115} which is even more effective in opposing soot formation than are CO₂ and H₂O. However, recent studies of the effects of a variety of additives on the critical fuel flow has shown that, for the most part, reductions in sooting tendency are brought about thermally.⁹⁵ Thus such diverse additives as He, Ar, N₂, H₂O, CO₂ and SO₂ are all equally effective when considered on the basis of their heat capacities, as shown in Fig. 7.

Some additives promote soot formation. Foremost among these are the halogens, particularly bromine.^{95,116-118} It has been suggested that these species act by catalyzing radical recombination, thus neutralizing excess OH radicals which could otherwise oxidize soot or soot precursors. Ignition promoters such as organic nitrates have been reported

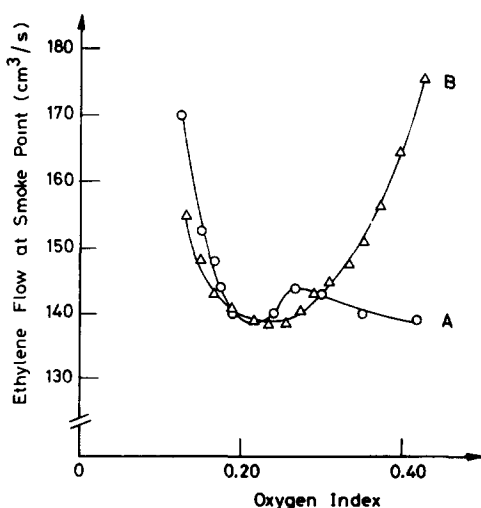


FIG. 6. Variation of fuel flow at the smoke point with oxygen index of the oxidant stream for axisymmetric ethylene diffusion flames in oxygen + nitrogen mixtures. For curve A the oxygen flow is held constant at 210 cm³/min and the nitrogen flow is varied while in B the total oxygen + nitrogen flow is fixed at 1000 cm³/min.¹⁰⁷

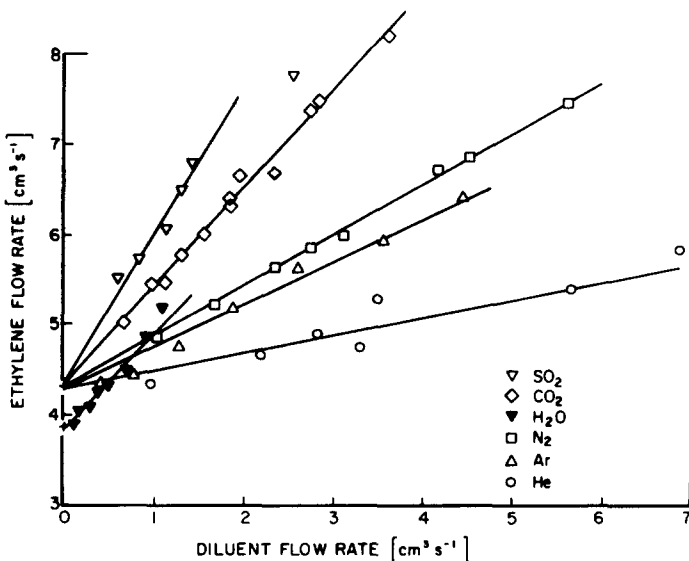


FIG. 7a. Effect of various additives to the fuel in suppressing soot, as determined by the increase in fuel flow at the smoke point with increasing additive flow.⁹⁵

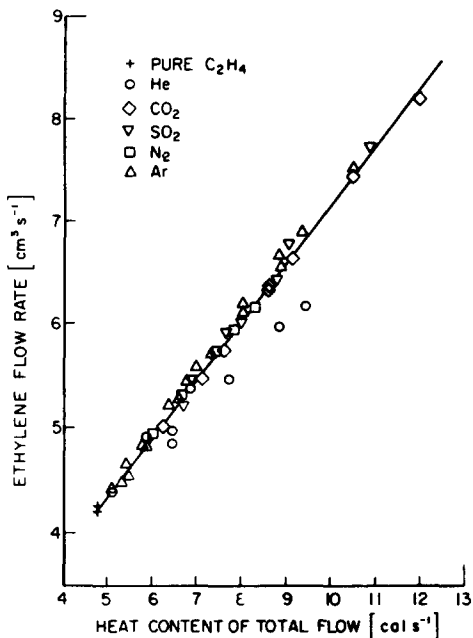


FIG. 7b. The same data as in (a) plotted against the total sensible heat content of the fuel + additive stream at the average flame temperature.⁹⁵

either to have no effect on soot emissions¹¹⁸ or to enhance them strongly.¹¹³

The effect of oxygen addition to the fuel is complex. In ethylene flames, small additions result in pronounced increased soot emissions^{86,95,109,111,113}. For over-ventilated flames, the maximum yield is achieved at an oxygen/carbon ratio in the mixture around 0.4.^{113,119} On an under-ventilated Wolfhard-Parker burner where there is limited subsequent oxidation of the carbon once formed, the soot yield increases continuously with further oxygen addition even up to the theoretical premixed sooting limit of O/C = 1.¹⁰⁹ This effect of increasing yield is not purely thermal as

it is far greater than that obtained at the same maximum flame temperature produced by oxygen enrichment of the air.¹⁰⁹ It has been suggested that the presence of oxygen accelerates the pyrolysis¹⁰⁹ or polymerization reactions¹¹³ occurring in the ethylene—at 800 K oxygen accelerates the pyrolysis without altering significantly the product distribution.¹²⁰ If the oxygen is added as air, the effects of such processes are apparently outweighed by those due to inert dilution and a net reduction in soot emissions is observed.¹¹³

In the case of other fuels, both soot promotion and inhibition have been observed as the result of oxygen addition. Jones and Rosenfeld⁸⁶ concluded that ethylene is the exception and that, for fuels such as propane, butane, and even propylene, oxygen suppresses soot emissions. In contrast to this result, others^{95,113} have found enhancement to be the rule when oxygen is added to ethane, propane, butane, propylene, and benzene diffusion flames. Enhancement of the sootting rate has also been observed by others¹¹⁹ for ethane as has the opposite effect in the case of propane.¹⁰⁹

As discussed in the following section (4.2.), probe analyses invariably indicate the presence of some oxygen on the fuel-side of a diffusion flame, presumably as a result of convective effects in the stabilization region near the burner. Judging by the oxygen-addition results, this oxygen may have significant effects on soot formation in the flame, these effects depending to some degree on the burner geometry.

Additions of other hydrocarbons to the fuel have also been examined. Invariably the soot yield is increased, the more so the greater the innate tendency of the additive to produce soot in a diffusion flame environment.^{95,109,110}

Perhaps the most intriguing influences of additives are observed for traces of some metals. These are discussed in more detail in Section 8.

4.2. The Sooting Structure of Laminar Diffusion Flames

It is apparent from the foregoing qualitative discussion of soot formation in diffusion flames that a number of opposing processes, most simply identified as pyrolysis and burnout, are involved. Therefore, investigation of overall effects such as flame height, smoke point, or even soot yield is unlikely to lead to a clear picture of how, and where, soot is formed in a diffusion flame. To fill this gap, a number of studies of the structure of the soot-forming zone have been undertaken.

Early work on this question was carried out by Wolfhard and Parker^{121,122} who developed the longitudinal slot burner now named for them, and examined methane and ethylene–oxygen flames. Broadly speaking, the flat diffusion flame consists of an oxidant side and a fuel side, separated by a reaction zone and the hot products. At a given height above the burner, the O₂ concentration falls steadily from the oxygen side to the fuel side, and this species is in low concentration at the position where carbon occurs. Similarly, the OH concentration, which reaches a maximum near the position of maximum temperature (corresponding approximately to the ideal flame zone) decreases rapidly towards the fuel side and, although the absolute OH concentrations reported have been questioned,¹²³ this species is obviously also in low concentration in the soot-forming zone.

The sooting zone itself occurs some millimetres to the fuel side of the region of maximum temperature. It is characterized by its familiar luminosity and by a strong absorptivity. A weaker absorption extends far into the relatively cool, unburned fuel but this cannot be attributed to a particle phase alone, for which the absorbance of small particles varies as $1/\lambda$. A similar “pyrolysis absorption” has been observed¹⁰⁵ in flow-tube pyrolysis experiments on a variety of pure hydrocarbons. More recently, a detailed spectroscopic examination of this region has shown generalized absorption maxima at 210, 300, 380 and 450 nm,¹²⁴ further supporting the interpretation that the absorption deep into the fuel side is not due to soot. There is as yet no indication as to the nature of the absorbers but they may be related to the species which produce a wide-band laser-excited fluorescence in the same region.¹²⁵

The carbon-forming zone in an axially symmetric propane-air diffusion flame has been examined spectroscopically in some detail by Kuhn and Tankin.¹²⁶ In such a system, lateral measurements of (integrated) emission and absorption must be inverted to yield radial profiles of extinction coefficient and temperature. In this way, the soot-forming region was shown to occur about two millimetres to the fuel side of the zone of maximum temperature. This region itself is only a few millimetres wide. The maximum concentrations of soot determined from their results (using appropriate optical constants for soot—see Section 9.1.2.3.) are very high, approaching

1×10^{-5} gm/cm³ in some regions. Particle diameters, inferred from the variation of extinction coefficient with λ , are in the range 400–600 Å.

In most of the soot-forming region, Kuhn and Tankin found good agreement between particle (Kurlbaum) and gas (Na-Dline reversal) temperatures. However, on the air side of this region, the particle temperatures are a few hundred degrees higher than the gas temperatures, perhaps due to a high rate of heat release at the particle surface as it burns out. On the other hand, on the fuel side, apparent particle temperatures are lower than the gas temperatures, which the authors consider may be a result of the particle formation process. Equally, if as described above, not all absorption in this zone is due to particles, then the apparent particle temperature will be lower than the true temperature, and there may in fact be no discrepancy.

Light scattering by soot particles has been used to probe the sooting region of axi-symmetric LPG (mostly butane) flames in air.¹²⁷ The particle size was determined from the angular variation of the scattered light intensity, but this is an unreliable technique, particularly if a large depolarized component such as fluorescence underlies the scatter signal.^{128,129} Thus, the large, and largely invariant, particle sizes ($d \approx 1500$ Å) reported by Kunugi and Jinno may not be real. Despite these problems, their results show quite clearly that soot does not reach the axis of the burner until some distance downstream of the burner port. At this point, there is a rapid formation of soot, followed by a slower burning-out further downstream. These effects are shown quantitatively in Fig. 8 for a hexane–air diffusion flame.¹³⁰

The structure of the early soot-forming region in a flat ethylene–air diffusion flame has been investigated

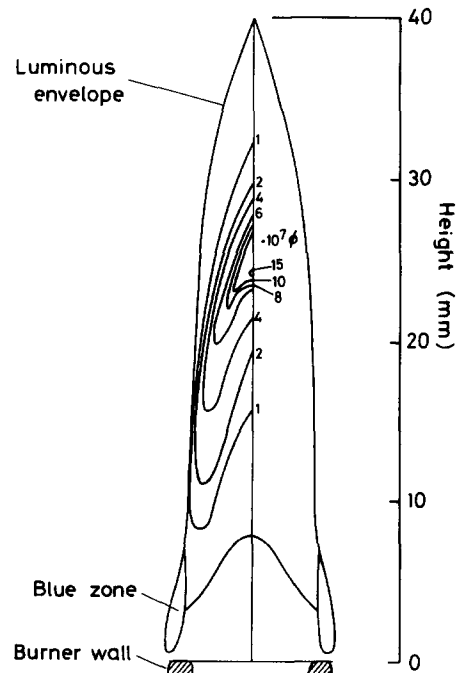


FIG. 8. Local soot loadings in an *n*-hexane/air diffusion flame.¹³⁰

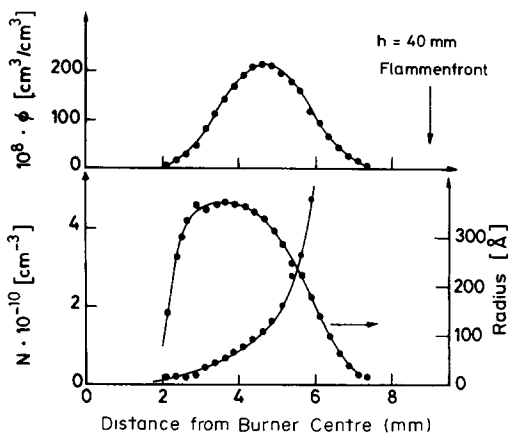


FIG. 9. Soot loading, particle size, and number density profiles across the sooting region in the early stages of a laminar ethylene/air diffusion flame established on a Wolfhard-Parker burner. The particle number density increases monotonically to exceed 10^{12} cm^{-3} at the edge of the sooting region nearer the air side. (The fuel-air partition in the burner occurs at 3 mm from the centre. The arrow marked "flame zone" indicates the position of the stoichiometric fuel-air interface at this height.)¹²⁵

recently using light-scattering and extinction measurements.^{125,131} In this way, the soot concentration as well as the particle number density and size fields are obtained, as shown in Fig. 9 for profiles across the flame at a height 40 mm above the burner. As found elsewhere^{121,122,126,130} the soot is contained in a region a few millimetres wide, to the fuel-side of the zone of maximum temperature. The particle number density is highest ($> 10^{12} \text{ cm}^{-3}$) nearest the reaction zone and decreases sharply into the fuel side, while particle formation (high N) and of soot formation (high ϕ) are distinct in this flame. Particles are formed in a fuel-rich mixture near the reaction zone where temperatures and radical concentrations are still high enough, much as in the flame zone of a premixed sooting flame (to be discussed in Section 9.1.2). The peak rates of particle formation are $10^{14} - 10^{15} \text{ cm}^{-3} \text{ sec}^{-1}$.¹³¹

An important structural feature of all typical hydrocarbon/air flames now comes into play to limit new particle formation to a narrow zone fairly close to the main reaction zone. Because one volume of fuel requires more than one volume of oxidant to complete combustion, the stoichiometric fuel-air interface moves outwards from the dividing streamline (that streamline emanating from the fuel-air partition of the burner) into the air side.^{84,90,125,130} Streamlines from the air-side passing through the flame zone will see increasingly higher fuel concentration at greater distances from the burner. However, away from the flame zone, the temperatures and radical concentrations soon fall to values too low to promote further new particle generation and the particle formation stage is complete although the soot loading is still negligible. (In very large flames or in easily pyrolyzed fuels, lower-temperature pyrolysis routes to soot, operating on a timescale of tens and hundreds of

milliseconds, could conceivably become important in the interior regions, away from the main reaction zone.)

The newly formed particles follow the streamlines into the fuel-rich interior of the flame. At the same time, thermophoresis¹²⁵ reinforces this effect by driving the particles deeper into the cooler fuel-side, away from the hot reaction zone. Under these conditions, oxidation of the particles can hardly be significant but surface growth (see Section 9.2.) occurs readily and the soot loading increases rapidly. Too far into the interior, even surface growth ceases and the soot loading falls off again. During this growth phase, the particles are coagulating and their number density is falling. Particle size increases both by coagulation and by surface growth. It seems from these results that there are strong parallels between soot formation in the laminar diffusion flame and the premixed flames discussed in depth in Section 9, in that the dominant overall processes of particle generation, surface growth and particle coagulation are identifiable in both systems.

For over-ventilated flames, the structure we have described pertains only to the lower regions of the flame. At some point, as the fuel is consumed and diluted by products, the stoichiometric interface begins to move back into the fuel region, eventually reaching the axis at the "flame height". Now the streamlines pass through increasingly leaner regions as the height above the burner increases, finally approaching and passing through the flame zone where particle oxidation becomes very rapid. As discussed by Roper,^{88,90} this process is partly kinetically controlled and some soot penetrates the flame front even in non-smoking flames. The particle burn-out time (Section 6) is significantly longer for larger particles so whether or not the flame smokes depends on the growth processes in the early stages of the flame, i.e. on surface growth and coagulation¹³³ — if the ratio of the soot oxidation length to the flame height exceeds about one, the soot oxidation is quenched before completion and the flame smokes.^{88,90}

Some light-scattering experiments on polymer diffusion flames have also been reported.¹³⁴ In the region of the flame zone, both polypropylene and polystyrene combustion produce trends which are qualitatively the same as those observed in the ethylene/air flames just described.^{125,131} However, there is also strong absorption and scattering of light from the interior regions of the polystyrene flame, which may indicate the presence of particles there too. Polystyrene is known to have an extraordinarily high propensity to form soot¹³⁵ and there may be some additional low-temperature particle formation mechanisms at work in this flame.

Analysis of samples withdrawn from diffusion flames has frequently been used to examine their chemical structure. In most cases, sooting conditions have been avoided in order to simplify the sampling operation. Nevertheless, the results gained are of

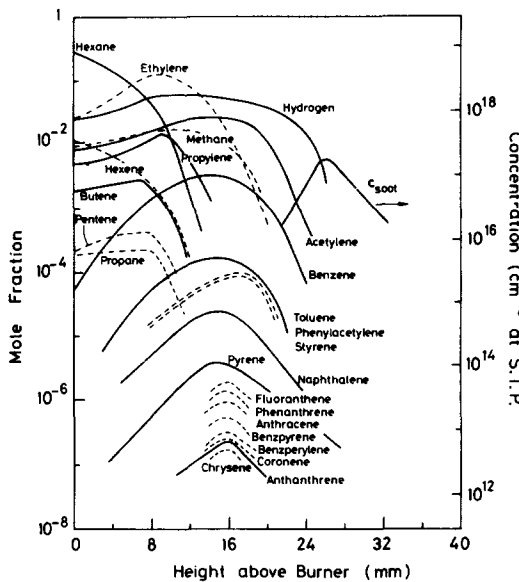


FIG. 10. Species concentration measurements along the axis of the *n*-hexane/air diffusion flame of Fig. 8.¹⁴⁰

direct relevance to an understanding of the process involved in sooting flames as well.

A variety of fuels have been investigated:

CH_4 ,¹³⁶⁻¹³⁸ C_2H_4 ,¹⁰⁹ C_3H_8 ,^{109,138} *n*-pentane,¹³⁹ *n*-hexane,^{130,140} *n*-heptane,¹⁴¹⁻¹⁴³ and various alcohols.^{137,144,145} In all cases, the parent fuel decomposes rapidly as it approaches the flame zone and a variety of hydrocarbon products arise, as shown in Fig. 10 for measurements along the axis of an *n*-hexane-air flame.¹⁴⁰

Typically, the main pyrolysis products are C_2H_2 , C_2H_4 , CH_4 and C_3H_6 . Benzene is also an important product in this region^{130,136,137,140,144,146} and it is here too that the polycyclic aromatics arise, albeit in low (< 10 ppm) concentrations.¹⁴⁰

There has been little attempt to relate the type and concentrations of these hydrocarbon degradation products to the formation of soot in the flame. Kern and Spengler¹⁴⁰ noted that C_2H_2 and C_6H_6 seemed most likely to persist into the carbon forming region and that either of these species is present in concentrations sufficient to account for the amount of soot arising as they disappear (Fig. 10). However, when benzene is added to a methane/oxygen diffusion flame, it breaks down (as indicated by the disappearance of its characteristic absorption) long before it reaches the carbon-forming zone.¹²² Similarly, the benzene in a benzene and hydrogen/air flame has almost completely disappeared before the onset of sooting.¹⁰² Smith and Gordon¹⁴⁴ found little correlation between sooting rates and the measured concentration of benzene, or of acetylene. Thus, ethanol diffusion flames produce only a weak yellow tip, whereas the propanols (*n*- and iso-) yield copious amounts of soot, even though the concentrations of benzene ($\approx 0.1\%$) and of acetylene (1-2%) are similar in all cases, as are the temperatures. Cole and Minkoff¹⁴⁷ measured the

$13.4 \mu\text{m}$ C_2H_2 absorption at various points in flames of methane and ethylene with oxygen on a Wolfhard-Parker burner. They found large amounts of C_2H_2 in all cases, particularly just to the fuel-side of the carbon zone. However, increases in the C_2H_2 absorption brought about by addition of C_2H_2 to the fuel did not change the luminosity of the flame and they concluded that C_2H_2 is not a precursor of soot. In contrast to this result, Dearden and Long¹⁰⁹ did find a dependence of their carbon formation rates on the amount of acetylene present in the pyrolysis region of C_2H_4 and C_3H_8 flames.

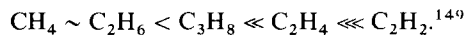
The behaviour of the oxidant is also of interest. The O_2 concentration in the air side decreases towards the flame zone, but it now seems established beyond doubt that some O_2 penetrates into the unburned fuel region without being consumed.^{136,138-140,142,148} Convective effects in the flame stabilization region, where reaction intensities are low, may be involved.^{132,143}

The products of combustion CO , CO_2 , H_2 and H_2O have also been measured (e.g. Refs. 109, 130, 136-146). The concentrations of CO_2 and H_2O peak in the zone of maximum temperature while CO and H_2 have their maximum concentrations more on the fuel side. As in the case of O_2 , these species persist far into the fuel region.

4.3. Turbulent Diffusion Flames

In a laminar diffusion flame, the visible flame height increases as the fuel flow is increased. Eventually when turbulent conditions are reached, the flame shortens again due to turbulence effects such as the entrainment of air.^{17,85} In the turbulent diffusion flame molecular diffusion is no longer controlling and eddy diffusion dominates the mixing process.

Qualitatively, soot formation in turbulent diffusion flames shows many similarities to that process in laminar flames. The effect of fuel type on the emission of soot varies as



Aromatic fuels also have a high sooting propensity.¹⁵⁰

Investigations of the average soot concentration field within the flame have been made by probe sampling and light scattering methods. Local concentrations of the order of 10^{-6} g/cm^3 have been reported for acetylene and propane flames.¹⁵¹⁻¹⁵⁵ Dilution of the fuel by N_2 reduces soot concentrations, as does the addition of water vapour.¹⁵⁶

Radial profiles of soot concentrations show a peak which moves closer to the axis further up the flame (Fig. 11), thus indicating that soot formation occurs predominantly at a conical surface concentric with the axis.^{151,154,155} The location of this maximum lies well within the visible flame boundary and reaches the axis at about 50% of the flame height.

Soot first appears on the axis at about 20% of the flame height and its concentration then increases rapidly to a maximum which coincides with the point

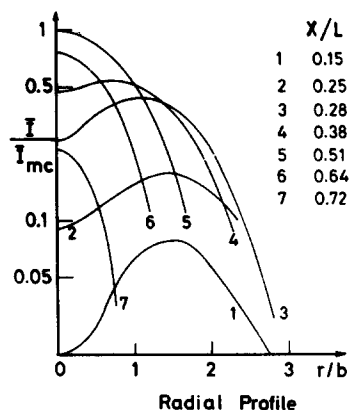


FIG. 11. Radial profiles of mean scattered light intensities (approximately proportional to mean soot concentration) at various distances downstream in turbulent propane/air flames of visible length L , and equivalent jet radius b . The intensities are normalized to the maximum mean intensity observed on the axis.¹⁵⁵

of maximum temperature.¹⁵⁵ Beyond the maximum, soot burnout dominates and the overall concentration decreases.^{150,151,154,155} Figure 12 shows that the axial profiles for flames stabilized with various velocities on nozzles of different diameters are well correlated in terms of the dimensionless distance $(x - H_u)/L$, where H_u is the upstream height at which the soot concentration reaches 50% of its maximum value and L is the visible flame length. The apparent insensitivity to nozzle conditions indicates that the flame is largely controlled by mixing.¹⁵⁵ This is in keeping with the observation by Becker and Yamazaki¹⁵⁵ that even at relatively low turbulent values of nozzle Re, the action of buoyancy in increasing the momentum flux with downstream distances was sufficient to make all their propane/air flames fully turbulent. They found the Richardson number Ri (which is the ratio of the buoyant to the momentum forces) to be the significant aerodynamic parameter in correlating their results. For example, the heights of

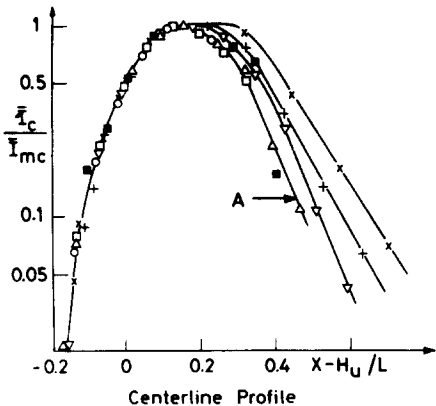


FIG. 12. Axial profiles of mean scattered light intensities relative to the maximum centreline value for various turbulent propane/air diffusion flames of visible length L . The height H_u is the height at which the scattering intensity upstream of the maximum reaches half of the maximum value.¹⁵⁵

the maximum temperature and maximum soot concentration are well correlated in terms of Ri and approach a constant value of 45% of the flame height in the natural convection limit ($Ri \rightarrow \infty$).

Average particle sizes have been determined from the angular variation of the scattered light intensity. Although there appears to be some difficulty in formulating an adequate model for evaluating the results,^{157,158} the particles in acetylene flames at least appear to grow to large sizes indeed. Dalzell *et al.*¹⁵¹ found an average diameter of 2000 Å in all regions of their flame while Magnussen¹⁵⁴ found that the particles grew as they moved downstream even into the soot combustion region. He reports apparent agglomerate sizes in excess of 5000 Å.

Although these descriptions of time-averaged quantities are important, it is the unsteady nature of turbulent flames which is of greatest fundamental significance. As can be seen in Fig. 13, the familiar, apparently homogeneous, brush-like appearance of these flames (long-exposure photograph 13A) belies the strongly fluctuating aspect of the soot distribution, particularly in the burnout zone where the soot-containing pockets appear to be separated by large zones free of soot (short exposures, B and C).

This question has recently been investigated using fast light-scattering measurements on turbulent acetylene¹⁵⁴⁻¹⁵⁶ and propane¹⁵⁵ flames in air. The most striking feature of the results in all cases is that the intensities of the fluctuations (i.e. the r.m.s. value of the fluctuating component relative to the mean of the scattered light intensity) are much higher than the concentration fluctuations typical of non-reactive jets. As suggested by Fig. 13, the soot concentration fluctuations are highest in the burnout region. Similarly, the intermittency factor for the scattered light intensity decreases rapidly to very low values in this region, further indicating strong inhomogeneity here. In contrast to the increasing intensity of the fluctuation in the soot combustion region, the integral scale of the scattered light intensity (which is a measure of the size of the largest soot-containing eddies) tends towards a constant value of the same magnitude as the integral scale of the axial turbulence velocity.¹⁵⁴⁻¹⁵⁶

Magnussen^{154,159} has interpreted these results as implying that the soot is formed and contained in eddies separated by regions of oxygen-containing gas. In the burnout zone, these eddies begin to break up into smaller ones that are rapidly burned away. The largest eddies, which determine the magnitude of the integral scale, resist this eddy dissipation process longest and the particles contained in them can continue to grow even well into this region. A similar description of these processes had earlier been given by Dalzell *et al.*¹⁵¹ based on their observations of average particle size. Such a model explains why the average rate of soot combustion in a turbulent flame is less than is observed under premixed conditions for the same mean values of temperature, oxygen partial pressure and soot concentration.¹⁶⁰

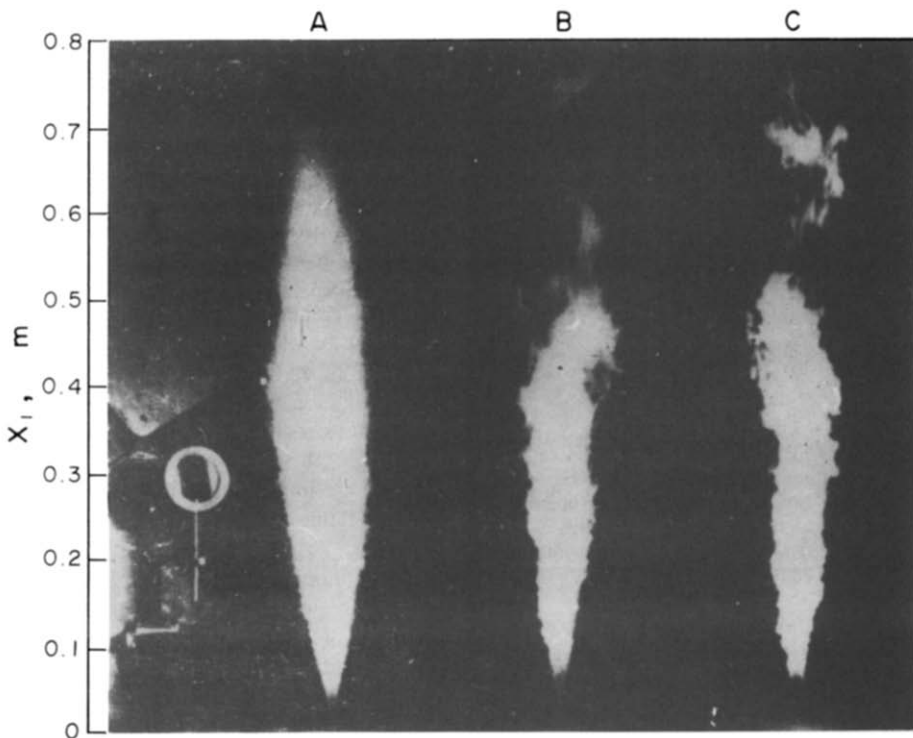


FIG. 13. A turbulent acetylene/air diffusion flame viewed (A) with long exposure time and (B) and (C) with 10^{-3} sec exposure time.¹⁵⁴

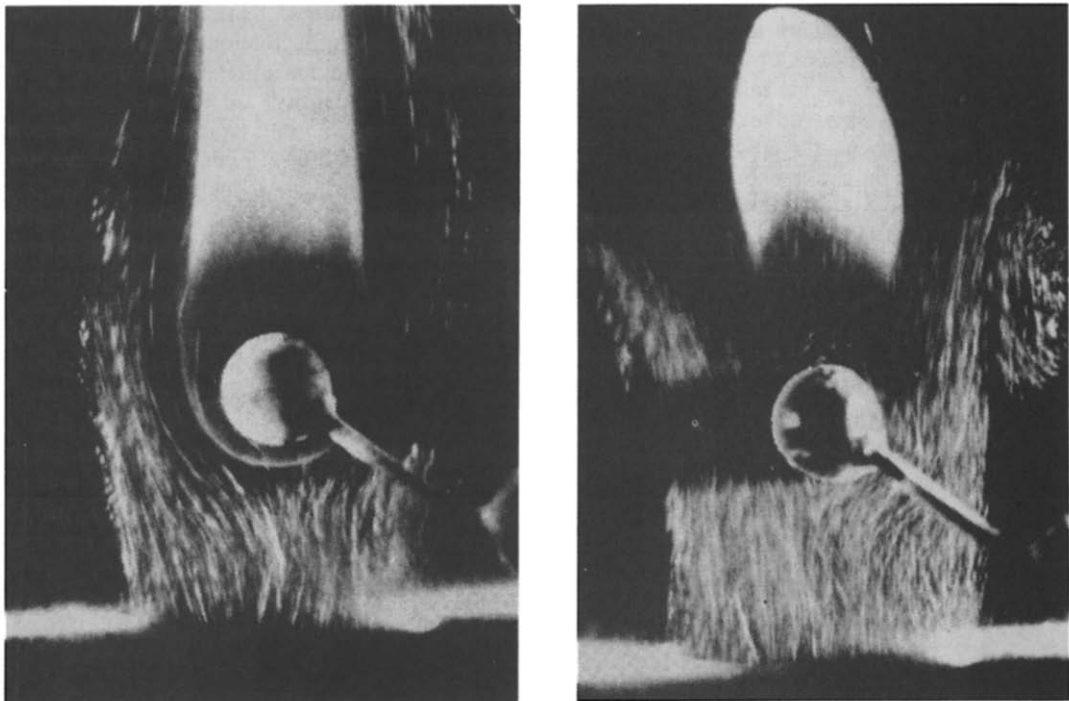


FIG. 14. Burning droplet models—envelope and wake flames on a 6 mm diameter *n*-pentane "droplet".¹³⁹

A word of warning on this interpretation has been given recently by Becker and Yamazaki.¹⁵⁵ They point out that turbulence/kinetics interactions could give rise to fluctuation intensities as high as those observed if the soot formation and combustion reactions are fast.

5. FUEL SPRAY FLAMES

Among the most important practical diffusion flames are the fuel-spray flames. The range of conditions under which these flames have to operate in diesel engines and continuous combustion chambers

such as turbines and furnaces is very wide indeed.

In the typical spray flame, fuel and air enter the combustion chamber separately and with different velocities so that the fuel droplets are not distributed evenly throughout the combustion zone. Thus the droplet size distribution, the trajectories of the droplets, their velocities and penetration depth, and their evaporation may each play an important role.

5.1. Soot Formation in Droplet Burning

In a gaseous diffusion flame, mixing is the rate-determining process. However, in the burning of droplets, evaporation of the fuel by heat transfer for the flame also plays a role. Thus, as the fuel spray approaches the flame, the smallest spray particles have time to evaporate completely before burning, while the larger ones may conceivably burn in a droplet flame.

Droplet combustion has been the subject of a number of comprehensive reviews.¹⁶¹⁻¹⁶⁵ At low relative velocities between the droplet and the surrounding oxidizer, the droplet is completely surrounded by the so-called envelope flame, as shown in Fig. 14a for a giant model droplet ($d = 6\text{ mm}$). In the lee of the droplet, the evaporated fuel burns as a gaseous diffusion flame. Above a critical air velocity, called the extinction or transition velocity, the envelope flame is extinguished and a much shorter, premixed type of flame, known as a wake flame is established downstream of the droplet (Fig. 14b). The extinction velocity increases with droplet diameter ($d^{1/2}$),^{166,167} with pressure ($P^{1/2}$)¹⁶⁸ and exponentially with oxygen concentration.^{166,167}

As could be expected, the envelope flame shows strong qualitative similarities^{139,169,170} to the gaseous diffusion flames discussed in Section 4. Thus, the soot yield shows a distinct maximum as the oxygen index is increased from low values to high. Also, replacement of the N_2 in the air by CO_2 strongly suppresses soot formation. Furthermore the yield increases sharply with increasing pressure. These similarities are borne out by probe sampling studies^{139,142} which show a region of fuel pyrolysis in the absence of oxygen, followed by a zone of soot combustion. In the pyrolysis zone, the heat release occurs at the fuel-vapour/air interface and it is likely that the soot is formed near here.

Quite different species concentration profiles are obtained in wake flames where a relatively high concentration of oxygen is present on the flow axis less than one diameter downstream of the droplet.¹³⁹ For their pentane flame, Gollahalli and Brzustowski¹³⁹ report concentrations consistent with an overall maximum C/O ratio of 1.0 in this region.

Not surprisingly, the amounts of soot formed in these two types of flame differ markedly, as is immediately evident from Fig. 14. Averaged over the flame at a given height, maximum concentrations of about $2 \times 10^{-6}\text{ gm/cm}^3$ are observed in the envelope flame, as against $0.6 \times 10^{-6}\text{ gm/cm}^3$ in the premixed

wake flame. The total amount of soot present in the wake flame as a whole is less than 10% of that in the envelope flame.¹³⁹

5.2. The Nature of Spray Flames

From the description of soot formation in the combustion of droplets, it appears that the suppression of soot formation may be achieved most easily by choosing conditions that lead to the extinction of the envelope flame.

However, there is an increasing body of evidence that individual droplet burning as such simply does not take place in the dense sprays typical of practical combustion systems. This evidence has been reviewed recently¹⁷¹ and we will outline here only the salient points. Near the nozzle exit, the fuel is dispersed in a dense spray region. There may be some oxygen present, particularly if an air-assist atomizer is used, but the temperatures are rather low and the overall gaseous-mixture ratios are so high, due to evaporation from the droplets, that combustion cannot occur. Only at the spray boundary are conditions found which will support combustion, much as in a gaseous diffusion flame. Further downstream, the fuel droplets become more dispersed, the mixture is more nearly homogeneous, and the reaction zone converges towards the burner axis. It is here that soot formation is most significant¹⁷²⁻¹⁷⁴ (see also Beretta *et al.*³⁸⁷ and cf. Section 4, particularly Fig. 8). Beyond this region, the burnout of soot and of CO predominates. Only towards the end of the flame can conditions arise where the few remaining droplets are in sufficient isolation, surrounded by air, to support individual envelope flames.

The overall analogy with gaseous diffusion flames has been emphasized strongly by the work of Onuma and co-workers^{172,175} who found that the shape of, and species concentration profiles in, their turbulent kerosene-spray flames are indistinguishable from those obtained in propane diffusion flames. The decrease in size of the droplets as they move away from the nozzle is consistent with their being evaporated within a hot gas environment. The completeness of the pure diffusion flame analogy has been questioned by

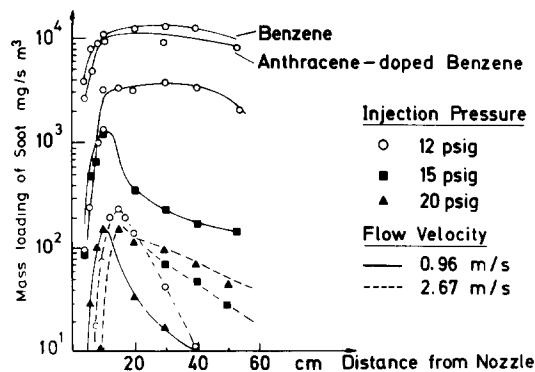


FIG. 15. Influence of atomizing pressure on axial profiles of soot mass loading in a continuous turbulent kerosene combustor at overall stoichiometric conditions.¹⁵⁰

Khalil and Whitelaw¹⁷⁶ who observed some droplet size effects in their studies. Nevertheless, the lower heat release rates which they observed reflect the influence of evaporation of larger or less volatile droplets on the mixing rate^{176,177} and do not imply any role for individual droplet flames.

Thus, the general consensus is that there is no evidence for individual droplet flames in laboratory scale burners. However, Breen¹⁷⁸ has estimated that from 1–10% of the droplets in a heavy fuel oil burner flame are consumed by droplet combustion outside the main fire ball. Although low, this percentage may be high enough to influence the overall soot loading if these droplet flames are quenched.

5.3. Soot Formation in Continuous Spray Combustion

Unfortunately little work has been directed towards determining the factors affecting the formation and behaviour of soot in well-defined spray flames. It is, however, becoming increasingly clear that measurements of exhaust concentrations are inadequate to providing any real insights.^{150,173,179–182}

Prado *et al.*¹⁵⁰ measured the axial soot distribution in turbulent, overall stoichiometric, kerosene flames in cylindrical flow reactors. Some of their profiles are reproduced in Fig. 15. At a low cold air velocity, soot formation occurs early in the flame, probably within the recirculation zone. The maximum and the exhaust values of the soot concentration decrease markedly with increasing nozzle pressure, due to improved atomization and better mixing. At the high flow velocities, the zone of soot formation is now downstream of the recirculation region and the maximum concentration observed is considerably less than for the low velocity case and more or less independent of the atomizing pressure.

Downstream of the reaction zone, the soot concentration decreases, presumably due to burnout, at a rate that is lower in the more poorly mixed low velocity flames. Curiously, the rate of soot disappearance in the high velocity flames varies inversely as the atomizing pressure. The explanation for this may be that, at higher atomizer pressures the downstream oxygen concentration is lower due to better mixing and more complete combustion in the main flame zone at higher atomizer pressures.

Close to the nozzle, the soot particles (maximum concentration again about 10^{-6} gm/cm³) have the appearance of partially coalesced units. Further downstream, the familiar lace-like agglomerates of nearly spherical units ($d \approx 200 \text{ \AA}$) are obtained.

These results indicate the importance of mixing and atomization in controlling soot formation in spray flames. In terms of the gas-type diffusion flame picture of a droplet spray flame, soot formation can be suppressed if mixing in the primary combustion zone is enhanced so as to encourage more pre-mixed, less fuel-rich combustion here. This has been the general, largely empirical approach, to the problem in technical

appliances also. In the following we consider briefly some relevant findings. The reader is referred to the literature for more detailed descriptions (e.g. Gill¹⁸³ on large-scale burners; Lefebvre,^{184,185} Mellor,¹⁸⁶ Toone,¹⁸⁷ and Blazowski⁹⁸ on gas turbine engines).

5.3.1. Overall fuel-air ratio

Overall stoichiometric or lean combustion is important in suppressing soot emissions. However, even under lean overall conditions, the presence of fuel-rich pockets in the primary zone may lead to significant soot emissions.¹⁸⁵

5.3.2. Droplet size

A decrease in droplet size which can be achieved by improved atomization, leads to more rapid evaporation of the fuel. In an air blast atomizer, this is accomplished by greatly increased thrust and mixing is therefore improved.¹⁷⁷ However, if improved atomization is accompanied by lower spray penetration because of the reduced momentum of the smaller particles, a very rich primary zone may be created which may actually encourage soot formation. This effect has been observed with pressure atomizers.¹⁸⁵ In the burning of heavy fuel oils, particularly those high in asphaltenes, the desire to avoid cenosphere formation is a further incentive to reducing particle size.¹⁶⁵

5.3.3. Swirl

Some degree of swirl imparted to the combustion air reduces particulate loadings. However, over-swirling promotes sooting by directing the air outwards and virtually separating it from the spray region.^{161,183}

5.3.4. Fuel spray cone angle

At low cone angles, the fuel spray region is condensed and therefore more fuel rich. Significant reductions in soot emissions can be achieved by increasing the cone angle.¹⁸⁷

5.3.5. Recirculation

Flue gas recirculation strongly reduces the tendency to soot formation in spray flames.^{167,188,189} Dilution of diffusion flames is known to reduce their production of soot (see Sections 4.1. and 4.3.), which may explain this result. The overall increase in gas flows can also be expected to promote mixing in the primary combustion chamber.

Sjögren¹⁶⁷ has interpreted this effect in terms of the extinction of individual droplet flames in vitiated air. As supporting evidence, he has pointed out that CO₂ dilution is particularly effective both in extinguishing envelope flames around single droplets and in inhibiting soot formation in a spray combustor. However, CO₂ also has this effect on gaseous diffusion flames (see Section 4.1.) and the argument is not conclusive.

5.3.6. Pressure

Increasing pressure favours soot formation in spray flames.^{173,187,190} This is in agreement with results from laboratory premixed⁷⁰ and diffusion flames⁹⁶ and from the burning of single droplets.¹⁷⁰

5.3.7. Fuel effects

The formation of soot in gas-turbine combustors correlates strongly with the H/C ratio of the fuel, increasing as the hydrogen content decreases.^{98,99,191} Influences of specific hydrocarbon types, e.g. aromatics, are secondary, especially at elevated pressures^{98,191} and high combustion intensities.¹⁹¹

The effects of volatility and viscosity are difficult to observe in isolation of other parameters. For a pressure-jet atomizer, higher volatility and lower viscosity tend to increase smoke formation.¹⁹² Such fuels are more rapidly vaporized and therefore form a less well-mixed, more fuel-rich primary zone.¹⁷⁷ For an air-blast atomizer, mixing is determined by the atomizing power,¹⁷⁷ and such effects may not arise.

Fuels of very low volatility may tend to form a carbonaceous residue.

5.3.8. Water injection

The combustion of an oil–water emulsion is known to produce significantly lower solids burdens than the burning of the oil alone, particularly in the case of medium heavy oils. This topic has been reviewed recently.¹⁹³ The major effect appears to be one of suppressing oil coke and cenosphere formation by the process of secondary, micro-explosive atomization due to the rapid expansion of the suspended water.^{193–195}

Reductions in the formation of soot can also be expected, based on the analogy with gaseous diffusion flames where addition of water vapour to the fuel strongly suppresses soot.^{95,107,156}

5.4. Soot Formation in Diesel Engines

One of the most widely used applications of fuel spray flames is that of diesel engine combustion. With increasing pressure for vehicles with lower fuel consumption, the use of these engines in passenger vehicles seems likely to become more common, and this possibly has highlighted the need for understanding the processes of smoke formation in diesel engine combustion.

Although Ricardo stated long ago that a well adjusted diesel need emit no visible smoke, soot emissions from these sources may contribute an important fraction to the overall particulate loading of the atmosphere. This occurs because, even under good operating conditions, the soot emission even if invisible is not negligible.

A comprehensive review of combustion and pollutant formation in diesel engines has been made recently by Henein.¹⁹⁶ The soot emission from these engines is influenced by spray atomization and con-

figuration, air motion, state of turbulence, pressure, etc. much as in the continuous spray flames discussed previously. For this reason, direct injection, pre-chamber and swirl chamber engines differ somewhat in their sooting characteristics. In general, the indirect injection systems emit less smoke than those with direct injection. At the exit of the pre-chamber in the indirect-type system, soot concentrations are actually very high because of the relatively rich mixtures formed there, but the high gas velocities and improved mixing in the main chamber lead to good burnout.

A description of the combustion process with regard to soot formation is as follows:¹⁹⁶ the fuel is injected at high pressure to produce a fine spray. The spray cone is very fuel rich and produces soot, especially under heavy load conditions. Some droplets may impinge on the walls, particularly in small high-speed direct-injection engines, and poor mixing in this region promotes pyrolysis and soot formation.¹⁹⁷ (In the Meurer engine, the fuel is sprayed deliberately onto the chamber walls—in this case, soot formation is avoided because combustion spreads through the chamber only as the fuel is evaporating from the walls and being mixed with the highly swirling air flow.) The last droplets of fuel to be injected (the spray tail) are usually somewhat larger due to the reduced pressure differential operating and they are therefore readily capable of producing soot.

Time-resolved measurements of the soot concentration made using UV-light absorption¹⁹⁸ show that soot formation commences in the region of the spray core immediately after ignition. The soot concentration increases rapidly to its maximum ($>10^{-7}$ gm/cm³) just 5° crank angle later, or 14° after the start of injection. Turbulent mixing, due mostly to the swirling air supply, ensures an even soot distribution at 21° crank angle angle after the start of injection.^{197,198}

The injection timing is very important as an earlier injection, with other parameters being kept constant, allows more fuel to be injected, vaporized and mixed before ignition. In this way, the exhaust smoke density is reduced.¹⁹⁹ A high rate of fuel injection (i.e. a short injection period) also reduces sooting.¹⁹⁹ Conversely, increasing inlet air temperature, which reduces spray penetration and cuts ignition delays,¹⁹⁶ promotes the production of soot.^{198–201}

When later in the cycle, the soot comes into contact with oxygen-containing regions, it burns out so that the eventual exhaust concentration is somewhat less than the maximum.^{197,204} The rate of burnout in diesel engines increases rapidly with increasing temperature and with the local oxygen concentration.^{199–202} (This subject is discussed more generally in Section 6).

The net exhaust emission varies in a complex fashion with engine speed and load.^{205,206} This is shown for a 2.4 l. 4-cylinder passenger car diesel engine in Fig. 16. At low speeds, the long soot combustion time available results in low particulate emissions. At high speeds, the soot emission is in-

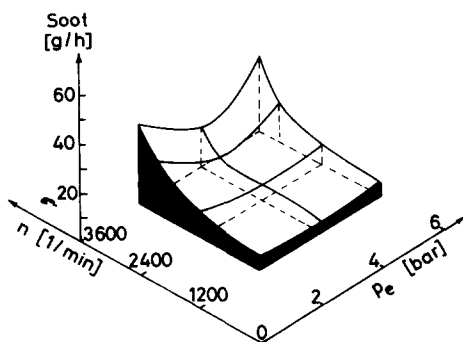


FIG. 16. Soot emission parameters for a 2.4 l. four cylinder passenger car diesel engine.²⁰⁵

creased as the burnout time is reduced. At these speeds, an increase in load raises chamber temperatures and promotes soot burnout so that the emission actually decreases. However, above a certain load, the increased formation of soot in the primary zone due to higher fuel concentrations outweighs this temperature effect and the net emissions climbs to very high values for heavy loads at high speeds.²⁰⁶

There have been many analyses of diesel exhaust particulates reported in the literature.^{202,205-210} Sizes of the sampled material vary widely in the range 0–30 µm but the large soot particles have been shown to consist of the individual spherical units of diameter around 300 Å typical of gas-phase soot formation. These primary units exhibit a nearly log-normal size distribution which varies hardly at all with the engine type or mode of operation, as shown in Fig. 17.^{206,210}

The agglomeration of the primary particles apparently begins within the combustion chamber,

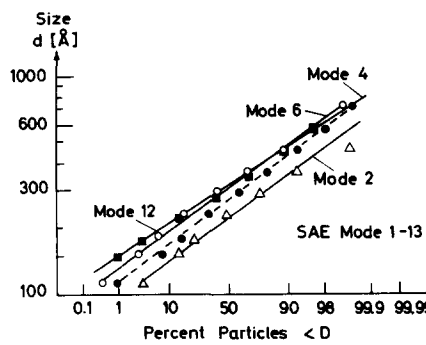


FIG. 17. Particle size distribution functions for soot emitted from an eight-cylinder direct-injection diesel engine for various modes of the SAE-J-1003 13-mode test cycle.²¹⁰

even within 50° crank angle after top dead centre.²⁰² Further agglomeration is likely to occur in the exhaust and sampling system.²¹⁰

Large hydrocarbon molecules may be formed in conjunction with the soot and these will condense on the particulate surface at typical exhaust temperatures. This condensation process changes the appearance of the agglomerates into that of tarry material and increases the H/C ratio towards one.^{197,210}

6. THE OXIDATION OF SOOT PARTICLES

The eventual emission of soot from a combustion device is usually much less than the amount actually generated within. The difference arises because of the combustion of soot particles in oxygen-containing regions beyond the soot-formation zone. In situations where soot formation is desirable for its ability to improve radiative heat transfer e.g. in a furnace, or a candle, this subsequent oxidation process assumes great importance.

The oxidation of soot aerosol particles in a flame environment has proven rather difficult to follow experimentally. The not unrelated subject of char and graphite gasification and combustion has been extensively studied (see, for example, References 211–215 for some recent reviews) but it is not yet clear how quantitatively these results can be applied to soot oxidation. Recently, however, Appleton^{216,217} has argued on the basis of structural similarities that the rates of oxidation of soot and of pyrographites should be the same. This is a considerable simplification in that, if care is taken to avoid diffusional resistance, studies of bulk samples of pyrographite may be used as a basis of our understanding of soot aerosol oxidation.

The semi-empirical formula of Nagle and Strickland-Constable²¹⁸ has been shown to correlate pyrographite oxidation for partial pressures of oxygen, $10^{-5} < P_{O_2} < 1 \text{ atm}$, and temperatures from 1100 to 2500 K. This formula is based on the concept that there are two types of site on the carbon surface available for O_2 attack. For the more reactive type A sites, the rate is controlled by the fraction of sites not covered by surface oxides, and is therefore of mixed order, between 0 and 1 in P_{O_2} . Type B sites are less reactive (desorption is rapid) and react with a rate first-order in the oxygen concentration. A thermal rearrangement of A sites into B is also allowed. A steady-state analysis of this mechanism yields a

TABLE 2. Empirical rate parameters for the Nagle and Strickland-Constable Model
($R = 1.987 \text{ cal/mole-K}$).^{218,219}

Rate constant	Value	Units
k_A	$20 \exp(-30,000/RT)$	$\text{gm-atom cm}^{-2} \text{ sec}^{-1} \cdot \text{atm}^{-1}$
k_B	$4.46 \times 10^{-3} \exp(-15,200/RT)$	$\text{gm-atom cm}^{-2} \text{ sec}^{-1} \cdot \text{atm}^{-1}$
k_T	$1.51 \times 10^{-5} \exp(-97,000/RT)$	$\text{gm-atom cm}^{-2} \text{ sec}^{-1}$
k_Z	$21.3 \exp(4100/RT)$	atm^{-1}

surface mass oxidation rate,

$$\frac{w}{12} = \left(\frac{k_A P_{O_2}}{1 + k_z P_{O_2}} \right) x + k_B P_{O_2} (1 - x) \text{ gm carbon/cm}^2 \cdot \text{sec}$$

where x is the fraction of surface occupied by type A sites, and is given by

$$x = \{1 + k_T / (k_B P_{O_2})\}^{-1}.$$

The empirical rate coefficients determined by Nagle and Strickland-Constable²¹⁸ for this model are listed in Table 2.

According to this mechanism, the reaction is first order at low oxygen partial pressures but approaches zero order at higher pressures. At a given pressure the rate initially increases exponentially with temperature (equivalent activation energy is that of k_A/k_z or 34100 cal/mole). However, beyond a certain temperature (which increases with increasing oxygen concentration) the rate begins to decrease as the thermal rearrangement favours formation of unreactive B sites. When, at sufficiently high temperature, the surface is completely covered with B sites, the rate is first order at all pressures, and increases again with temperature.

Radcliffe and Appleton²¹⁶ have shown how other results with pyrographite²¹⁹⁻²²¹ and the few available soot aerosol oxidation rates^{91,222,223} are surprisingly well correlated in terms of this model. More recently, elegant and extensive measurements of soot oxidation have been carried out by Park and Appleton.²¹⁷ They dispersed commercial carbon blacks (channel black, mean diameter 45 Å; furnace black, 180 Å) in a shock-tube and examined burnout for temperatures from 1700 to 4000 K and oxygen partial pressures from 0.05 to 0.5 atm. As shown in Fig. 18, their measurements are well correlated in terms of Nagle

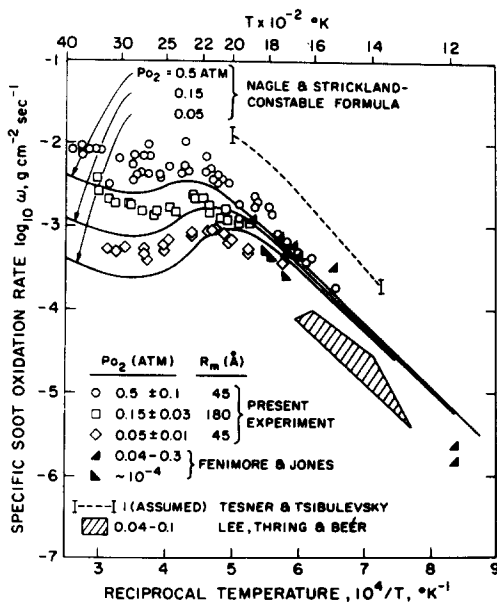


FIG. 18. Summary of experimental soot oxidation rates found in the literature and comparison with the Nagle and Strickland-Constable formula.²¹⁷ Authors identified are Lee, Thring and Beer;²¹ Fenimore and Jones;²²² and Tesner and Tsibulevsky.²²³

and Strickland-Constable formula and confirm that the reaction rate is first order in the oxygen concentration at low partial pressures, tending to zero order as P_{O_2} is increased. Also summarized in Fig. 18 are results obtained by other investigators for oxidation of soot aerosol particles. It is clear that the net activation energy for the lower temperatures ($T \lesssim 2000$ K) likely to occur in typical soot burnout environments is close to the value of 34.1 kcal/mole obtained from the Nagle and Strickland-Constable formula. Thus, Lee, Thring and Beer²¹ report $E_A = 39.3$ kcal/mole and this value is adequate to describe the experimental temperature dependence of soot combustion in a diesel-engine chamber also.²⁰² Other reported values are $E_A = 33^{224}$ and $E_A = 40$ kcal/mole.²²³

The influence of temperature and pressure on the burnout lifetime of a 100 Å diameter is shown in Fig. 19. At temperatures below about 1800 K the lifetime is largely insensitive to the oxygen concentration so the admixing of fresh, cold air will normally prolong the life of the particles due to a reduction in temperature.

Despite the obvious success of the semi-empirical Nagle and Strickland-Constable formula in correlating soot oxidation rates over a wide variety of conditions, it is by no means settled that the oxygen molecule is the dominant gasifying species in a flame environment. For graphite oxidation, high reaction probabilities have also been reported for O-atoms^{220,225,226} and for OH²²⁷ and the question is whether these species may not be important in soot oxidation in flames.

Millikan⁵⁰ found evidence that soot formation in a premixed flame can only occur after the OH concentration has approached its equilibrium value. Before that, the OH is presumed to inhibit sooting by consuming soot precursors and incipient particles. This process is suggested as explaining the characteristic dark space between the primary reaction zone and the onset of luminescence in sooting, pre-mixed flames.

Further support for OH attack is provided by Fenimore and Jones²²² who found that soot oxidation rates in flame gases containing from 10^{-4} to 0.3 atm partial pressure of oxygen are consistent with

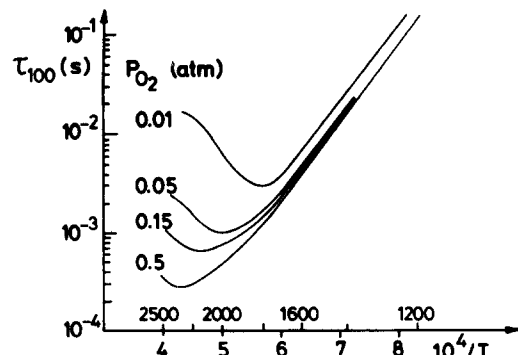


FIG. 19. Burnout lifetime τ for a 100 Å diameter soot particle as a function of oxygen partial pressure and temperature.

the assumption that about 10% of collisions of OH radicals with soot molecules are effective in removing a carbon atom. However, as discussed by Radcliffe and Appleton²¹⁶ these results are also quite consistent with the predictions of the Nagle and Strickland-Constable formula.

More direct support for the role of OH comes from a light-scattering study of soot particle combustion in very fuel-rich hydrogen flame environments at temperatures from 1850–2100 K.^{228,229} Under these conditions, the gasification rate appears to be significantly higher than the collision rate for O-atom or O₂ molecules with the soot. On the other hand, for OH, reaction probabilities of the order of 10% may be sufficient to account for the observation. This same conclusion has been reached recently by Neoh *et al.*³⁸⁸ who, in a meticulous study of soot burnout in flame gases containing from 10⁻⁵ to 0.05 atm O₂, at temperatures from 1600 to 1850 K, found a 20% reaction probability for OH collisions with soot. Under all conditions studied by Neoh *et al.*, soot oxidation is dominated by OH and only for very lean conditions or where the OH concentration is suppressed (lower temperatures) can O₂ be expected to become an important oxidant.

It is also conceivable that the major flame constituents CO₂ and H₂O oxidise soot to some extent. Based on char gasification results²¹¹ these reactions would only become significant under rather fuel-rich conditions.

Obviously, more work is needed to establish the mechanism of soot combustion in flames. Simultaneous measurements of particle size and number such as those achievable with laser-light scattering techniques, appear to be a useful means of investigation.

In conclusion, it appears that the kinetics of soot burnout are fairly well established. However, in the practical context, the results of Magnussen¹⁶⁰ are of interest as he found overall soot oxidation rates in turbulent flames rather less than those predicted. The discrepancy is believed to arise from turbulence-kinetic interactions whereby the soot and the oxygen containing eddies are separate so that the oxidation may actually be mixing-controlled in this situation.

7. SOOT AND IONS

A typical hydrocarbon flame zone produces chemions (see, for example, References 230–237) and it has long been a matter of conjecture as to whether such ions might influence the processes of soot particle formation and growth. Until recently, however, this subject has been approached through observations of macroscopic changes induced by the application of electric fields, or by extrapolation of small-ion chemistry results obtained in non-sooting flames. Only in the past few years have direct sampling studies of large ions from sooting flames been able to provide new, important insights into the electrical aspects of soot formation.

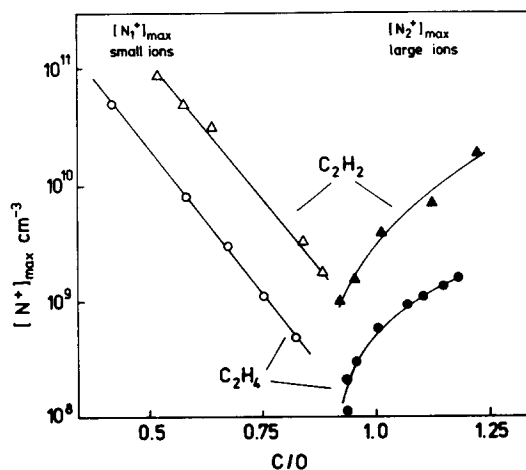


FIG. 20. Peak ion concentration in low-pressure ($p = 45$ Torr) acetylene ($\triangle, \blacktriangle$) and ethylene (\circ, \bullet) flames. The open symbols refer to N_1^+ , the small ions (e.g. $C_3H_3^+$) whose concentrations peak in the primary reaction zone. The filled symbols are for N_2^+ , the larger charged species (> 700 amu) arising downstream of the main reaction zone.²³⁴

It is now clear that the onset of sooting brings with it a new mechanism of ion formation, independent of the classical chemi-ionization mechanism operating in all hydrocarbon flame zones.^{234,238–241} (See also the recent work of Olson and Calcote^{387,388}.) This is clearly seen in Fig. 20 where $[N_1^+]_{\text{max}}$, the maximum concentrations of small (12–300 amu) positive ions arising in the flame zone (height $Z = 8$ mm above the burner), and $[N_2^+]_{\text{max}}$, the peak concentrations of heavy (> 700 amu) ions occurring in the sooting region ($Z \approx 15$ mm), are compared for low-pressure acetylene and ethylene–oxygen–nitrogen flames. The value of $[N_1^+]_{\text{max}}$ is highest in lean, non-sooting flames and decreases steadily as the flame is made more fuel-rich. On the other hand with the onset of sooting (which occurs at $C/O \approx 0.9$ for the acetylene series) $[N_2^+]_{\text{max}}$ rises rapidly to exceed $[N_1^+]$, increasing as the flame is made richer and the soot loading increases.

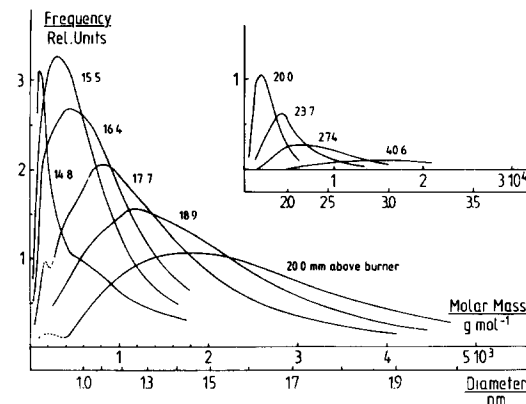


FIG. 21. Mass distribution of positively charged particles for different heights, z , in a low-pressure (20 Torr) acetylene/oxygen flame, $C/O = 1.12$. The end of the primary reaction zone occurs at $z = 12$ mm and the first soot particles appear at $z \geq 15$ mm.²⁴¹

As a function of distance from the burner, the positive charge concentration in the sooting region first rises steeply to a maximum and then falls more gradually further downstream.^{234,240,241} There is some discrepancy in the reported values of $[N_2^+]$ _{max}—Homann²⁴¹ and Delfau *et al.*²³⁴ find $[N_2^+] \approx 5 \times 10^9$ typically while Wersborg *et al.*²⁴⁰ report $[N_2^+] \approx 10^{12}$ under similar conditions. Beyond the maximum, the rate of decrease of ionization is so fast that a recombination with electrons must be responsible.²⁴¹

Mass spectra of the ions arising in the sooting region have been obtained by various electrical discrimination techniques.^{234,240,241} As shown in Fig. 21 for a weakly sooting low-pressure acetylene–oxygen flame,²⁴¹ the distribution of positive charge broadens and shifts to larger species—i.e. from large hydrocarbon ions, to the smallest soot particles, to larger soot particles—as the height above the burner increases. Although in the early regions there are many neutral molecules of the same masses as the charged species, the average size of the charged soot particles arising further downstream is somewhat less than that of particles collected and observed under the electron microscope.

The mechanism of formation of ions in the sooting region has been a point of some discussion. The very high levels of ionization found by Wersborg *et al.*²⁴⁰ are obviously inconsistent with the thermal ionization of hydrocarbon molecules or soot particles in this region.²⁴² However, other investigations^{234,241} show much lower ion concentrations and equilibrium thermal ionization may in fact be responsible. Thus Homann²⁴¹ finds that the relatively weak ionization of the large gaseous species early in the sooting region ($Z \lesssim 15$ mm in Fig. 21) can be explained in terms of the thermal ionization of hydrocarbon molecules with ionization energies of the order of 8–9 eV—this requires that about 1 in 10^7 hydrocarbon molecules be ionized.

When the first soot particles appear and $[N_2^+]$ rises steeply, the apparent ionization energy drops to about 5 eV. However, it is now not clear that equilibrium ionization is responsible because the charged particles are smaller than uncharged ones and one would in fact expect the opposite trend. Therefore, for the crucial ionization of small soot particles, Homann²⁴¹ proposes a kind of chemi-ionization due to the exothermicity of the surface growth reactions which dominate particle growth in this region (these reactions are discussed in Section 9).

Homann²⁴¹ has also observed the behaviour of negatively charged species in the sooting region. Early on, these appear to be predominantly free electrons but higher in the flame, at about the time that $[N_2^+]$ reaches its maximum, some larger negative ions are also observed. These show a bimodal mass distribution, with a pronounced peak at low masses (≈ 100 amu) and a broader peak at larger small-particle masses. The low mass peak probably corresponds to the charging of small hydrocarbon molecules

by deprotonation or electron attachment (see, for example, Reference 236 for a discussion of such processes).

At this stage, it appears that the high levels of ionization associated with soot in premixed flames are more a product of soot particle generation than a necessary precursor. Chemi-ions formed in the primary reaction zone may be less numerous than the small soot particles arising later on.²⁴¹ In this case “ionic nucleation” is unlikely to have been of importance but the data are not conclusive on this point and further work is required.

Once particles are formed, whatever the mechanism, they are subject to electrical effects. For example, electrostatic forces between charged particles have long been suspected of influencing their coagulation.^{234,244} Recently quantitative measurements of the coagulation rate constant in the presence of ionizing (alkali metal) additives have shown that coagulation is inhibited by these additives.^{78,245} When most particles are charged they will resist subsequent growth by coagulation and hence on average remain smaller. This work and others involving ionic mechanisms of additive activity are discussed in more detail in Section 8.

A further aspect of electrical effects in soot formation has been explored in great detail by Weinberg and co-workers^{244,246,252} who applied electric fields to opposed-jet diffusion flames. The most obvious result of applying a field in either direction on this burner is that the characteristic yellow luminosity of the soot disappears gradually as the voltage is increased. When the potential (over 1.5 cm flange separation) reaches 1 kV for positive, or 2 kV for negative, ion flux through the pyrolysis zone, virtually only the blue luminosity of the reaction zone remains visible. Similarly the amount of soot deposited from the flame decreases markedly. Apparently the same number of particles are collected, but they are rather smaller.²⁴⁶

At sufficiently high potentials, all the soot particles are similarly charged, either positively or negatively depending on the direction of the field. Just one charge is acquired per particle.²⁵⁰ This result applies for particles with diameters between 90 and 300 Å and would indicate that the equilibrium charging considerations (see e.g. References 253, 254) are not applicable.

Weinberg has interpreted these results as follows: particles normally tend towards being positively charged by thermionic emission (mature soot has an apparent work function of 4.6–5 eV^{241,249}). In a flux of positive charge carriers, this effect is reinforced by charge attachment. Under the influence of an electric field, charged particles are accelerated out of the pyrolysis zone and their growth stops. A stronger field reduces the residence time of the particles in this region of growth and smaller particles are collected. This interpretation is supported by the observation that at a certain field strength, particles can be held in the pyrolysis zone, against the gas flow, in which

case rapid growth to macroscopic clumps occurs.²⁴⁶

These observations provide an important general insight into the role of condensation reactions on the surface of existing particles in determining the total yield of soot from diffusion flames: a decreased residence time in the pyrolysis zone leads to smaller particles and less soot. Thus, in the present case,^{246,250} the mass of soot deposited on the burner is reduced by more than 90% although the number of particles appears unchanged. For a flux of negative charge through the pyrolysis zone thermionic emission opposes the attachment of negative charges and higher voltages (higher fluxes) are needed to produce the same particle size reductions observed for a positive flux.

In conclusion it is apparent that, regardless of their mechanism of formation, soot particles can, and often do, carry an electric charge. Weinberg's work shows how such charged particles can be manipulated by electric fields, and this may offer scope for emissions controls.^{246,248,252}

8. THE INFLUENCE OF ADDITIVES ON SOOT FORMATION

In this section we consider the influence of trace (<1%) amounts of certain additives in modifying the sooting behaviour of flames. Additives required in higher concentration to exert appreciable effects have been discussed for premixed flames in Section 3 and for diffusion flames in Section 4.

Where dilution is not significant, it seems generally true that non-metallic compounds have little effect, either in premixed or diffusion flames.^{14,17} As discussed in Section 3.1., sulphur (as H₂S, SO₂, SO₃, or H₂SO₄) appears to be the most effective element in this category.

By far the most striking effects of additives are those exhibited by various metals, some of which are used commercially as smoke suppressants in liquid fuel combustion. This aspect has been reviewed by Salooja²⁵⁵ who concluded that, although different additives are more effective under different conditions, manganese is generally very effective while iron and other transition metals such as nickel, cobalt and copper can significantly reduce smoke in some circumstances. Barium which is widely used as a diesel smoke suppressant, appears to be very effective at higher concentrations (0.5% by weight of the fuel) but at lower concentrations is less effective than other additives. The mode of action of these sorts of additives is unknown but there is evidence that nickel, on being incorporated into the soot phase, chemically catalyses the gasification of soot.²⁴³ A similar oxidation catalysis has been proposed for the action of manganese.^{69,222,256}

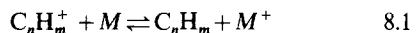
Many of these additive studies have used variations in the smoke point as their means of gauging the influence of the metal. This, however, may not be a reliable technique, as demonstrated recently in the case of manganese additions to a gas-turbine com-

bustor.²⁵⁷ There, the "smokiness" of the exhaust was definitely reduced by the action of the additive, but the effect was illusory as the total mass of particulate emissions actually increased, probably due to the contribution of solid manganese oxides. The explanation lies in the fact that the particles agglomerate far less in the presence of the additives than they do otherwise. The smaller particles scatter less and are therefore less visible.

Turning to studies on gaseous flames, where there is more chance of isolating the mechanisms involved in soot suppression (as opposed to smoke suppression from liquid-fuel flames) we generally find that the alkalis and alkaline earth metals are particularly effective.

Early studies by Bartholome and Sachsse²⁴³ showed that these metals could greatly reduce or even suppress soot emission from a diffusion-type partial combustor. They proposed that the metals promote ionization of the soot particles thus inhibiting their coagulation with the result that they are more easily oxidized.

Further evidence that the alkali metals and alkaline earths reduce soot by an ionic mechanism has been provided by Addecott and Nutt²⁵⁸ who found a loose correlation between measured ion concentration and smoke reduction. They proposed that more readily ionized additives reduce the concentration of "ionic precursors" by charge transfer,



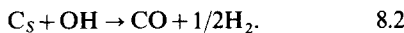
thereby suppressing soot formation.

A more complicated picture emerges from the results of Salooja^{259,260} who found both pro- and anti-smoke effects from the same additive introduced at different points in a Bunsen flame. The soot-promoting effect was strongest when a wire coated with the metal salt (particularly for low ionization potential metals such as caesium and potassium) was held at the base of the primary reaction zone, while soot inhibition was greatest at the tip of this zone. These results were explained by Salooja, and supported by Bowser and Weinberg,²⁵⁵ as arising from the ability of the additive to produce electrons. At the base of the flame the electrons reduce the concentration of natural flame ions, which could lead to a reduction in any ionic nucleation of soot; above the tip of the primary zone, the electrons might bring about neutralization of positively charged soot particles present there, thus promoting their coagulation and resistance to later oxidation.

Detailed examinations of propane- and acetylene-diffusion flames²⁶¹ have also shown the existence of both pro- and anti-smoke behaviour of metal additives. In these experiments, barium produces the most pronounced suppressions followed by other alkaline earths and alkali metals; molybdenum and tungsten are also rather effective, but most other metals show only slight effects. These results were explained qualitatively through an ionic mechanism, where low levels of additive (or additives of relatively

high ionization potential) could produce above-equilibrium metal ion concentrations, by reaction 8.1, which make further carbon-forming ionic nuclei available later in the combustion by the reverse process. On the other hand, high additive levels will drive this reaction to the left, thus destroying the postulated nucleation centres and leading to an anti-smoke effect.

The ionic theories described above rely largely on the assumed importance of ionic nucleation in soot formation (see Sections 7 and 9). In keeping with the considerable evidence for a neutral mechanism of soot formation, the influence of metal additives has also been described in terms of neutral chemistry. Thus Cotton *et al.*²⁶² who investigated a system very similar to that used by Bulewicz *et al.*²⁶¹ (and obtained qualitatively similar results) proposed that the activity of the alkaline earths is due to their known ability to catalyze the radical equilibrium $\text{H}_2\text{O} \rightleftharpoons \text{H} + \text{OH}$. If OH is suppressed below its equilibrium concentration in the sooting zone by rapid reaction with soot and unburnt hydrocarbons, the metal could thus improve the supply of OH and thereby promote soot oxidation.



Cotton *et al.*²⁶² supported this interpretation by showing that the anti-soot effect is quantitatively related to the ability of such widely varying substances as Ba, SO_2 , and NO to catalyze the radical equilibrium.

As usual, these studies in diffusion flames are unable to allow a distinction to be made between particle formation and burnout, since only the net emission is considered and a detailed description of the various processes can only be inferred. Such problems may be

partly resolved in premixed flames, where the burnout of particles can be avoided. Using relatively high concentrations of metal (up to 500 ppm) in premixed ethylene-air flames, Feugier^{263,264} found evidence for both ionic and chemical effects—the former supposedly predominate for the alkali metals Na, K and Cs and lead to an increase in the flame emissivity (i.e. soot loading) by creating “ionic nuclei” (reverse of reaction 8.1). A reduction in emissivity was found for the alkaline earths Ca, Sr and Ba as well as for Li—here the additive is seen as supplying OH radicals which could consume the (incipient) soot.

Rather different results have been obtained by Haynes *et al.*^{78,245} in a laser light scattering and absorption study of atmospheric pressure premixed ethylene/air flames seeded with low concentrations (<2 ppm) of various metal salts. Here the alkali metals and alkaline earths were both found to suppress soot, although in qualitatively distinct ways, and generally to an extent less than about 30%. More remarkably, the alkali metals strongly inhibited coagulation of the soot particles such that, as shown in Fig. 22, up to 25 times more, smaller particles were present in flames seeded with 1 ppm K. The potency of these metals in suppressing coagulation correlates strongly with the equilibrium ion concentration due to the metal and it was concluded that the additives promote the unipolar, positive charging of soot particles, thus inhibiting their coagulation. Of the alkaline earths, only Ba produces enough ions to suppress coagulation in the manner of the alkali metals. However, Ba, Sr and Ca all suppress soot formation, perhaps by the mechanism supported by Cotton *et al.*²⁶² Other than molybdenum and, perhaps, tungsten no other noticeably effective metals were found.^{78,245} The profiles for soot volume obtained in this work (Fig. 22) are also of some interest in that the very early stages of soot formation results for seeded and blank flames are indistinguishable. This result indicates that the primary soot formation steps may not be affected at all by the additive in pre-mixed flames.

The marked discrepancies between the results of Haynes *et al.*⁷⁸ and those of Feugier^{263,264} may arise by the very different metal concentrations used in the two studies (<2 ppm, <100 ppm respectively). However, the emission studies of Feugier may in fact be biased by his assumption that the additive does not change the gas temperature; Haynes *et al.* reported that even the mild suppressions they found were enough to reduce the total emissivity of the flame sufficiently for the temperature, and hence emission in the visible, to rise.

9. SOOT FORMATION KINETICS

Up to this point, we have reported largely phenomenological aspects of soot formation in various combustion environments. We now consider the kinetics of soot formation in more detail, based on the stages outlined in the Introduction:

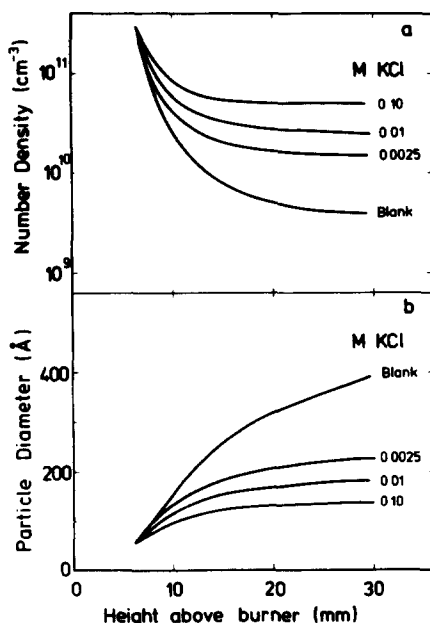


FIG. 22. Effect of potassium additions on soot particle size and number density in a premixed ethylene/air flame.⁷⁸ A 0.10M additive solution is equivalent to about 1 ppm K in the flame gases.

(1) particle inception, whereby the first "solid-phase" material is generated;

(2) particle growth, meaning the increase in size of the particles, (i) by surface growth, in which gas-phase species attach to the surface of existing particles. This brings about an increase in the amount of soot but the number of particles remains unchanged. This process may also operate in reverse in that material may also leave the surface to re-enter the gas-phase.^{265,266} Oxidation also represents a "negative growth" process. (ii) by coagulation, where two particles collide and fuse to form a single, larger particle. Although the particle number density decreases during coalescent coagulation, the amount of soot present remains unchanged.

These stages occur in pyrolyzing gases as well as in flames and we therefore consider both these situations. In the discussion of particle inception, we concentrate largely on kinetic descriptions, obtained from shock tube pyrolyses and flat, premixed flames. In the main, flow tube pyrolysis results are not considered—these have been discussed in detail recently by Lahaye and Prado.²

Finally, we consider some general, hopefully predictive, models of the soot formation process in the light of the detailed kinetic results.

9.1. Particle Inception

9.1.1. Shock tube pyrolysis

When a hydrocarbon–argon mixture is shock heated, it takes a certain induction period before soot formation is observed. The reactions occurring in this period are not well understood, and probably differ for different hydrocarbons. However, there is a general tendency, for a gaseous hydrocarbon at low concentration and high temperature, for the molecules to decompose in a uni-molecular reaction by breaking the weakest bond. Under these conditions, the rate of disappearance of hydrocarbon is first order and subsequent reactions are not important in determining this rate.

At lower temperatures and/or higher concentrations, the apparent rate of decomposition accelerates with time, the overall reaction may tend towards a higher order, and the apparent activation energy decreases. In the case of C_2H_2 , the reaction becomes second order in C_2H_2 , and the activation energy about 40 kcal/mole.^{267,268} For C_2H_4 even at low concentrations where the reaction remains first order, the apparent energy of activation quickly drops to 53 kcal/mole.²⁶⁹ Finally, for C_6H_6 decomposition, the second-order rate constant shows an activation energy between 40 and 70 kcal/mole.²⁷⁰⁻²⁷⁴

The transition from the description of the decomposition of the parent hydrocarbon to the appearance of the first soot particles is difficult to delineate experimentally. The induction period has been widely used as a descriptor of the overall process, where the first particles are signalled by the onset of continuous emission, of light absorption, or light scattering. For the pyrolysis of ethylene, induction periods for various

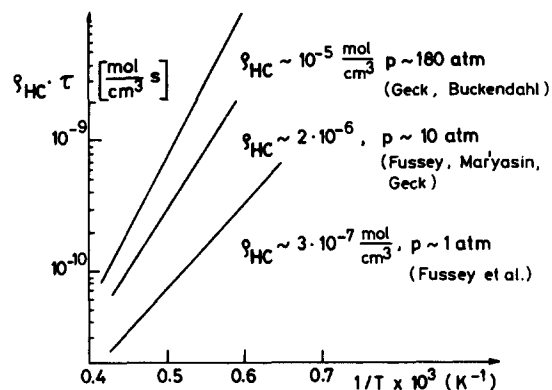


FIG. 23. Soot induction times for ethylene pyrolysis in shock tubes. The ethylene mole fraction is about 2% at the low pressures (results based on light emission) and medium pressures (light emission and absorption), and 0.5 to 1% for the high pressure runs (light emission). Data from Buckendahl,²⁷⁵ Geck,²⁷⁶ Fussey *et al.*^{277,278} and Maryasin and Nabutovskii.²⁸⁵

initial conditions are shown in Fig. 23 as a function of temperature. The apparent activation energy for an assumed first-order concentration dependence ranges from 30 kcal/mole at pressures near 1 atm to 50 kcal/mole at pressures in excess of 100 atm.²⁷⁵⁻²⁷⁸

Fussey *et al.*²⁷⁷ correlated induction periods for soot formation from the C_2 -hydrocarbons in terms of

$$\tau \cdot p^n_{HC} = A \exp\{E_A/RT\}$$

and obtained the results summarized in Table 3.

TABLE 3. Induction time correlation for C_2 -Hydrocarbons

	n	E_A (kcal/mole)
C_2H_6	0.42	36
C_2H_4	0.23	28
C_2H_2	0.41	31

For methane and propane, the apparent activation energies are 22 and 27 kcal/mole respectively²⁷⁹ while for toluene a value of 36 kcal/mole has been obtained.²⁸⁰

These results illustrate some of the problems in interpreting the real significance of the induction period. Not only is its definition somewhat arbitrary, there does not seem to be any indication of the nature of a rate determining step in the correlation obtained. Also, the results are of limited applicability in the understanding of diffusion flames because there the slow initiation reactions for thermal pyrolysis are replaced by reactions of H-atoms diffusing from the flame zone. Ideally, it is desired to establish the detailed kinetics of the processes at hand and these are almost certainly different for differing fuel types.

9.1.1.1. Aliphatic compounds Product analyses for pre-soot conditions show that paraffin hydrocarbons give rise initially to hydrogen, alkenes, and acetylenes.^{281,282} In the case of acetylene, higher acetylenes result.²⁸³⁻²⁸⁵

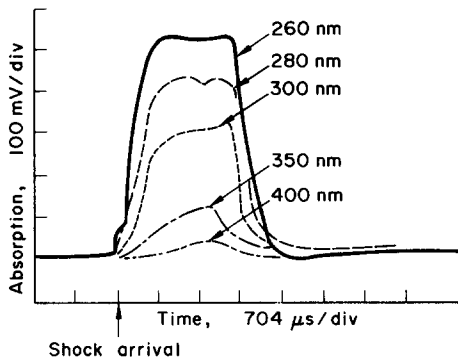
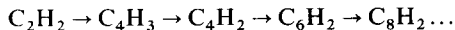


FIG. 24. Absorption profiles for "pre-soot" species in acetylene pyrolysis in shock-heated argon at 2100 K.²⁸⁷

Some indications of the changes occurring during this period come from absorption measurements which indicate the presence of species capable of absorbing in the visible and ultraviolet before soot becomes observable. This "pyrolysis absorption" was initially demonstrated by Parker and Wolfhard¹⁰⁵ for a heated flow reactor. They found that continuous UV-absorption could be detected in the pyrolysis products of various fuels at temperatures as low as 600 K for acetylene and 1100 K for methane. In subsequent work, the existence of a similar absorption deep into the fuel-side of a flat ethylene diffusion flame was also demonstrated;¹²² this flame-generated pyrolysis absorption has since been shown to possess generalized maxima at 210, 300, 380 and 450 nm.¹²⁴

More recently, such non-soot absorption has been observed in gases pyrolyzing behind shock waves, as shown in Fig. 24 for acetylene pyrolysis under conditions where no soot is formed. (Similar behaviour is observed when ethane, ethylene, or propylene is pyrolyzed.²⁸⁶⁻²⁸⁸) The absorption is detectable immediately after the passage of the shock front and climbs rapidly to a plateau level. It is strongest in the ultraviolet and decreases with increasing wavelength such that it is no longer detectable beyond 600 nm. Under these conditions, the height of the plateau is proportional to the fuel concentration and largely independent of temperature. The initial rates of increase of absorption, measured at temperatures from 1700 K to 2400 K, imply an energy of activation around 51 kcal/mole for the formation of the absorbing species from either ethylene or acetylene.

The identity of the absorbers is not established but, from the shape of the spectra, Cundall *et al.*²⁸⁶⁻²⁸⁸ suggest that they may be predominantly polyacetylenes, perhaps $C_{10}H_2$ or $C_{12}H_2$. Such species have in fact been measured mass-spectrometrically by Kistiakowsky and co-workers as products of C_2H_2 pyrolysis. They^{283,284} concluded that the reaction proceeds as



Recent experiments and kinetic modelling of C_2H_2 pyrolysis by Tanzawa and Gardiner²⁶⁸ support this interpretation.

Thus, at least in the case of C_2H_2 pyrolysis, the situation begins to look rather like that in the pre-mixed flames discussed in the next section.

In addition to the fast radical mechanisms available, some ionic processes may also be important, for it has been demonstrated recently that the shock tube pyrolysis of ethylene does lead to ion formation.²⁸⁹ Once formed, such ions may undergo very fast addition reactions without losing their ionic character.

How the larger species formed by either radical or ionic mechanisms organize themselves to form ring systems or even three-dimensionally linked structures such as platelets¹¹ before they dissociate again is still an open question. There will be a tendency towards those species most stable thermodynamically and kinetically (implying many internal bonds which may heal rapidly after breaking) and eventually polycyclic compounds will be favoured.

9.1.1.2. Aromatics During benzene pyrolysis, the reaction starts with the loss of a hydrogen atom from a benzene molecule. Further reactions lead to the formation of biphenyl radicals and their higher analogues as well as polycyclics.^{23,270,274} In the case of toluene pyrolysis, loss of an H-atom to form benzyl radical occurs initially. Subsequent reactions lead to higher molecular weight species including polycyclic aromatic hydrocarbons and higher polyacetylenes especially in the temperature range 1500–1700 K. Above 1700 K, the main products are acetylene and diacetylene.^{290,291}

Some qualitative insights into the mechanisms controlling soot formation from aromatic compounds come from investigations of soot yields as a function of hydrocarbon type and pyrolysis temperature. Graham *et al.*^{292,293} showed that, in the shock-tube pyrolysis of aromatic and related compounds at temperatures from 1600 to 2300 K, there is a pronounced maximum in the fractional conversion of hydrocarbon into soot at a temperature around 1750 K (Fig. 25). They interpret this behaviour as arising from the competition between two pathways for aromatic hydrocarbon pyrolysis—at lower temperatures, the molecules do not fragment but retain their underlying aromatic structure. These species rapidly and efficiently lead to soot so that, at about 1750–1800 K, a nearly complete conversion of hydro-

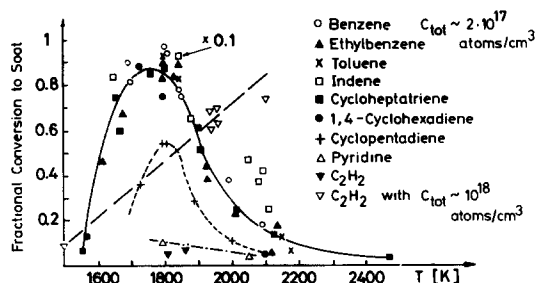


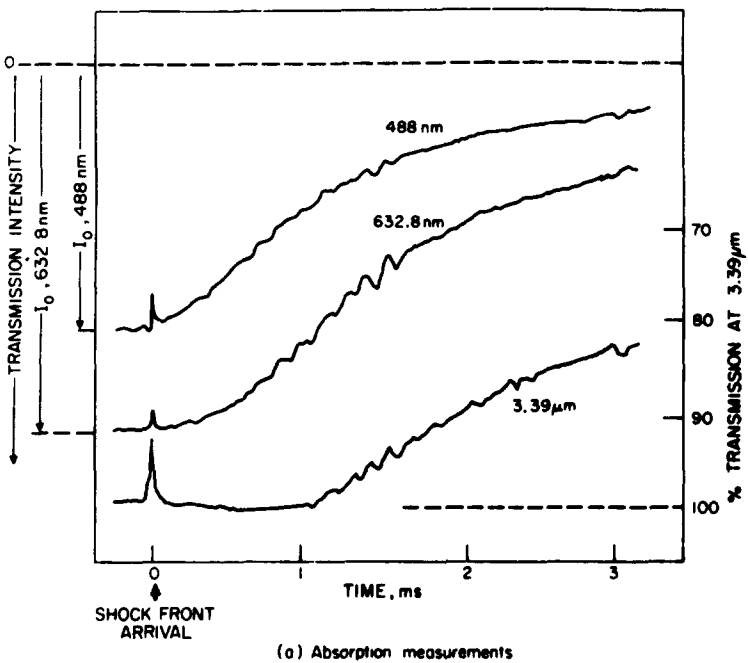
FIG. 25. Yields, after 2.5 msec of soot from various hydrocarbons (all with 2×10^{17} C-atoms/cm³) shock heated in argon. Also shown are results for acetylene at 10^{18} C-atom/cm³.²⁹³

carbon into soot occurs. Towards higher temperatures, thermal dissociation reactions begin to compete with polymerization, breaking the ring and generating smaller particles. These smaller species can only form soot rather slowly and inefficiently so the net yield drops at temperatures above 1800 K. This interpretation is borne out by the observation that acetylene first makes its appearance in the shock-tube pyrolysis products of benzene at temperatures above 1750 K, and rapidly becomes a major product as the temperature is increased.²⁷¹

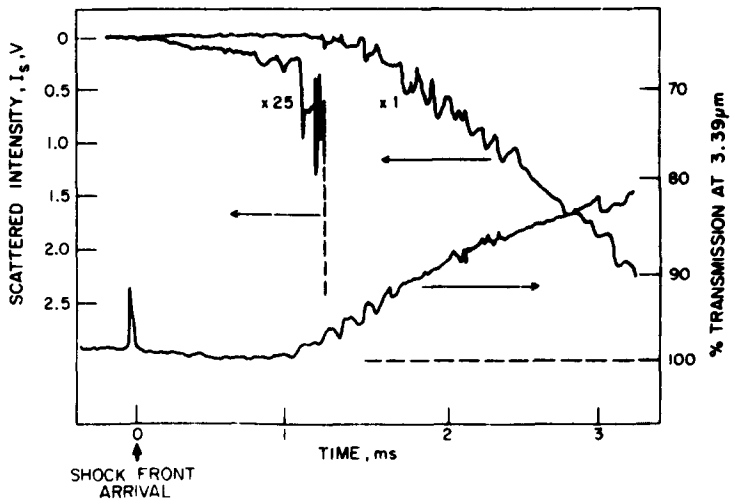
Some non-aromatic cyclic compounds such as cycloheptatriene and 1,4-cyclohexadiene behave very similarly to the aromatics, probably because they aromatize readily. Others, such as cyclopentadiene,

cyclopentane and 1,3-cyclohexadiene show an intermediate behaviour, characterized in Fig. 25 by the curve for cyclopentadiene; presumably ring rupture competes with aromatization in these species. Finally, cyclohexane and cyclohexene are obviously easily fragmented and they behave as small molecules such as acetylene. The heterocyclic aromatic pyridine is also in this category, as has also been observed for this compound in diffusion^{103,104} and premixed flames.⁵¹

Thus the first few steps in the pyrolysis are critical to the further progress of the reaction. If the aromatic ring remains intact, a high degree of conversion of the parent hydrocarbon to soot can be achieved. On the other hand, if ring-rupture occurs, the rate of soot formation is slowed and the eventual yield is reduced.



(a) Absorption measurements



(b) Absorption at 3.39 μm and scattering at 488 nm

FIG. 26. Transmission and scattering of light during shock tube pyrolysis of ethyl benzene in argon at 1750 K.²⁹²

This does not mean, however, that aliphatics cannot also give rise to high soot yields under some circumstances—this is shown in Fig. 25, where, for the pyrolysis of acetylene at a higher total C-atom concentration (10^{18} cm^{-3}), the fractional conversion to soot increases steadily as the temperature is increased.

Just as for aliphatic species, the pyrolysis of aromatic compounds also gives rise to pre-soot absorbers of light. Asaba and Fujii²⁷³ detected two absorption peaks, in the ultra violet ($\lambda \approx 300 \text{ nm}$) and red ($\approx 650 \text{ nm}$), after the passage of a shock-wave through non-sooting benzene/argon mixtures at temperatures from 1400 to 1800 K. There was no well defined induction period for the appearance of the UV absorption; the authors attributed this peak to biphenyl. For the red absorption, there was a clear induction delay, after which the intensity of the absorption increased rapidly—the rate of increase was approximately proportional to the initial benzene concentration and exhibited a 32 kcal/mole activation energy. This red absorption, and its associated emission, was ascribed to a radical species, perhaps the biphenyl radical $C_{12}H_9$. At best, these identifications must be considered tentative.

Graham *et al.*²⁹²⁻²⁹⁴ found absorption at 488 nm and 633 nm to begin immediately after the passage of a shock front through mixtures of aromatics such as benzene, toluene, and ethylbenzene (Fig. 26). In contrast to this there is no detectable absorption at $3.39 \mu\text{m}$ until particles are formed, as signalled by their light-scattering capacity. Low-resolution measurements of the pre-soot absorption spectrum²⁹⁵ showed a featureless absorption throughout the visible region, both just before and just after the appearance of soot particles. In addition to these non-soot absorption effects, Graham²⁹⁶ has shown that the light scattered from the particles in the early stages of their formation is appreciably depolarized (up to 2.5%). This may indicate the presence of fluorescing species as in the case of premixed^{51,129} and diffusion¹²⁵ flames—see also Section 9.1.2.3.

Graham *et al.*²⁹²⁻²⁹⁶ have provided an ingenious interpretation of their results for soot formation from aromatics:

(a) intermediates, presumably p.c.a.h., having a specific absorption at 488 nm similar to that of soot, are formed;

(b) a number of very small particles are generated from the gas phase

(c) these particles provide a surface for the condensation of the intermediates, whose gas phase concentration falls effectively to zero.

(d) the particulate phase now consists of soot and a fluid p.c.a.h., component. Of these only the former absorbs in the infra-red while both absorb in the blue (point (a)).

(e) an increase in the soot concentration, as indicated by increasing infra-red absorption results from the conversion of the (liquid) polynuclear aromatic hydrocarbon into soot, accompanied by the

evolution of hydrogen. Step (c) rules out the conversion of gaseous material into soot.

Such a mechanism explains the occurrence of the coalescent collisions undergone by young particles, and the eventual transition to chain-forming collisions (see Section 9.2.). Also the initial rate of increase of particle size and the differences between the absorption signals in the visible and infra-red can be resolved in these terms. However, further work is required before it can be accepted in general. An interesting approach would be to examine the possibility of fluorescing intermediates being present as these would then be detectable independently of the presence of a particulate phase.

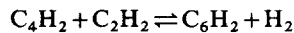
9.1.2. Premixed flat flames

Probably the most detailed kinetic information on the process of soot formation has been obtained from low-pressure, acetylene–oxygen flames. Here, measurements by the groups of Howard,^{240,297-301} Long³⁰²⁻³⁰⁵ and Wagner^{63,71,76,265,266,306-308} fit together quite well. Some quantitative differences are most probably due to slightly different conditions being studied by the different groups. We shall base our discussion on a standard flame with $C/O = 1.4$, $p = 20 \text{ Torr}$ and $v_0 = 50 \text{ cm/sec}$.

Light extinction measurements indicate that the first soot appears at around 15–20 mm in this flame. The amount of soot continues to increase up to a height of 40 mm where its formation effectively ceases.^{71,299,307}

The onset of particle formation can be approached either from the point of view of the chemical changes in the incoming gas; or by analysis of the particles collected after they are formed. There is something of a gap between these techniques which may be partly overcome by the use of optical techniques as well.

9.1.2.1. *Chemical changes* Molecular-beam sampling and analysis by mass spectrometry show that most of the oxygen has been consumed at about 12 mm above the burner. Already at this point, the water-gas components CO_2 , CO , H_2O and H_2 have nearly reached their final values and have established their equilibrium amongst themselves.^{63,265} Some acetylene remains unconsumed while the polyacetylenes pass through maxima at a height of about 15 mm above the burner, starting with diacetylene (C_4H_2) and followed, at successively lower concentrations, by the higher polyacetylenes.^{63,265,300} These species are apparently equilibrated amongst themselves, e.g.



This behaviour is common to different fuels such as methane, ethylene, propane and ethanol^{48,63,129,307,309} as well as to flames where N_2O is the oxidant.³⁰⁹ Benzene, to be discussed later, gives different results.

This region of peak polyacetylene concentration

appears to be very important in determining the subsequent reactions leading to the formation of soot. A variety of polycyclic aromatic hydrocarbons (p.c.a.h.) such as pyrene and acenaphthalene seem to originate here, as shown in Fig. 27a for the species $C_{14}H_8$. In contrast to the polyacetylenes, the concentrations of these species increase steadily

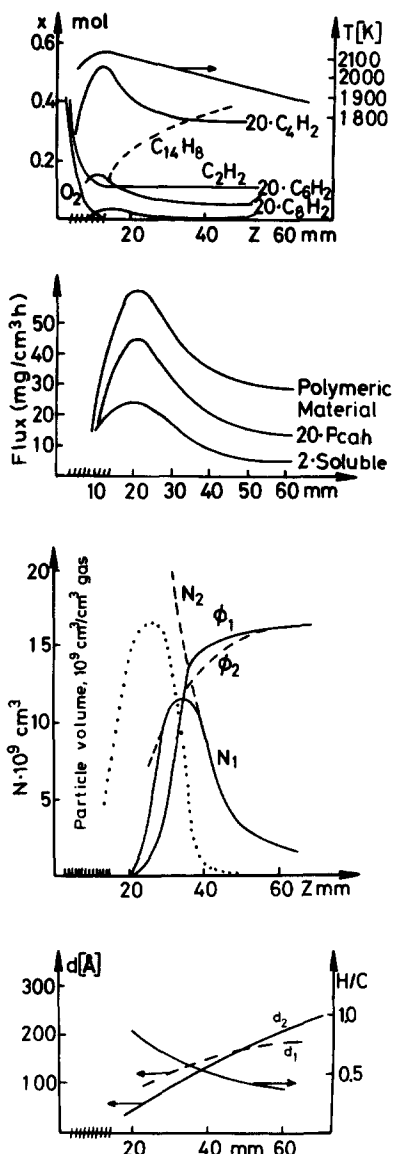
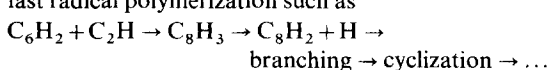


FIG. 27. (a) Temperature and concentration profiles of species of major importance in C_2H_2/O_2 flame ($C/O = 1.4$) burning at 20 Torr with a cold gas velocity $v = 50 \text{ cm/sec}$. The dashed region on the abscissa indicates the position of the visible reaction zone.²⁶⁵ (b) Fluxes of total polymeric material, polycyclic aromatics and chloroform-soluble material in an acetylene flame, as above except with $C/O = 1.5$.³⁰³ (c) Soot volume fractions ϕ_1 (after Howard *et al.*²⁹⁷) and ϕ_2 (after Bonne and Wagner⁷¹) and particle number densities N_1 and N_2 as a function of height above the burner for the same flame as in 27(a). The dotted curve represents absorbing gaseous hydrocarbons in and just beyond the flame zone.²⁹⁹ (d) Mean particle diameters d_1 ²⁹⁷ and d_2 ⁷¹ and atomic H/C ratio²⁶⁵ of soot particles, as a function of height above the burner for the same flame as in 27(a).

throughout the downstream region, which may mean these molecules are relatively unreactive and do not themselves go on to form soot^{266,308} later on.

Similar conclusions regarding the peak have been reached by D'Alessio *et al.*⁴⁸ in their studies of sooting methane/oxygen flames at atmospheric pressure. They found that some p.c.a.h. are unreactive throughout the flame; others have weak maxima in their concentration profiles but these occur long after the polyacetylene maximum and the appearance of the first soot particles. On the other hand, Long and co-workers³⁰²⁻³⁰⁵ observed polycyclic aromatic concentrations to have a sharp maximum in the region of the polyacetylene maximum in low pressure acetylene flames. On this basis, Long *et al.* concluded that the polycyclics could not be excluded as contributors to soot formation and growth. As known from a comparison with molecular beam sampling their batch sampling systems may have allowed composition changes to occur prior to analysis, particularly in samples from the radical-rich main reaction zone. The maximum concentration of total polymeric material collected by them³⁰³ exceeds the amount of soot appearing subsequently although oxidation reactions have ceased, Fig. 27b. Since the gas phase and the young soot molecules in this region are still extremely reactive, it may be that some material was collected here as polymeric material which later in the flame, where radical concentrations are lower and particles less reactive, would pass through the sampling device. On the other hand, some very recent results obtained by Bittner and Howard³⁸⁸ with a molecular-beam mass spectrometer system do provide qualitative support for Long's results, in that sharp maxima in the concentration profiles of various pcah are observed within the main reaction zone of an acetylene-oxygen flame. Bittner and Howard³⁸⁸ suggest that the pcah production mechanism operating here must differ from that giving rise to the increase in pcah concentration much later on, after the first particles have appeared. Obviously the whole question of pcah chemistry in flames requires further study.

A great many other hydrocarbons, mainly having molecular weights in excess of 250 appear at the end of the reaction zone in the region immediately preceding the appearance of the first particles.²⁶⁶ Unlike the pure polycyclic aromatics, these species disappear rapidly during the soot growth phase and are no longer detectable at a height above 35 mm. They may themselves be polycyclic in nature, but with side chains and perhaps some radical character.²⁶⁶ Their apparent reactivity indicates the likelihood of their being direct precursors of soot in these flames. Their formation, which is fast, is difficult to follow experimentally because so many different species are involved. Homann and Wagner²⁶⁶ suggest that they are derived from the acetylenes and flame radicals by a fast radical polymerization such as



—the acetylenes are known to be capable of undergoing cyclizations, for example, by Diels–Alder reactions.^{310,311} Similar mechanisms have been proposed for conjugated, resonance-stabilized species such as butadiene^{16,27} although such species are always found in rather low concentration in flames.^{62,265,300} The important feature of these early steps is that once the molecules are large enough, radical addition complexes will be less likely to dissociate before subsequent collisions, thus preserving the radical character of the large species which can then continue to grow rapidly by further addition reactions. The youngest soot particles sampled in this region have a rather high H/C ratio (Fig. 27d) indicating the attachment of many hydrogen containing branches to their largely polycyclic aromatic character. They also have many radical sites, as indicated by the strength of their e.s.r. signals, in keeping with a radical polymerization mechanism.

As discussed in Section 8, ions are observed in the primary reaction zones of these flames. It is a well-known feature of hydrocarbon ion-molecule reactions that addition reactions which lead to larger, charged species occur very rapidly, at rates approaching the collision frequency.^{312–317} It has often been suggested that such fast reaction might also occur to account for the rapid growth of molecules leading to the formation of the first soot particles, e.g. Refs. 240, 242, 308, 309, 311. However, recent evidence indicates there are relatively few chemi-ions formed in the fuel-rich flame zone of a sooting flame²³⁴ and the degree of ionization of the larger hydrocarbons preceding the appearance of the first particles is low, $< 10^{-7}$,²⁴¹ so that ionic mechanisms may not be important despite their excellent credentials.

Moving away from the reaction zone, the high temperatures will presumably cause rearrangement of the large polymer radicals (whether charged or not) into two and three dimensional arrangements such as platelets.¹¹ However, the mechanisms of such processes are not well understood. The hydrocarbon radical concentrations are reduced by addition reactions (recombinations are too slow in the low-pressure flames). The e.s.r. strengths of the soots decrease, as does their H/C ratio^{266,308} (Fig. 27d).

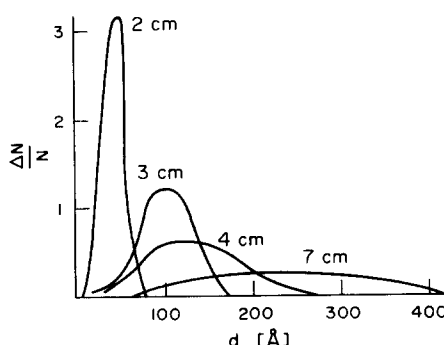


FIG. 28. Particle size distributions for various heights above the burner for the low-pressure acetylene–oxygen flame of Fig. 27(a).²⁹⁷

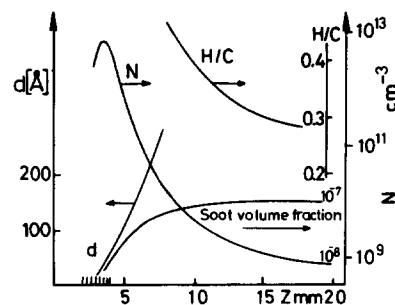


FIG. 29. Soot volume fraction, particle number density N , and particle diameter profiles obtained by light scattering and absorption measurements on an atmospheric-pressure CH_4/O_2 flame with $\text{C}/\text{O} = 0.64$. Also shown is the variation of the atomic H/C ratio of the soot with height above the burner.⁴⁸

The unreactive polycyclic aromatics probably arise by dissociations of the reactive species with side chains and can therefore be considered by-products of the soot formation process.²⁶⁶

9.1.2.2. Particle analysis The detailed kinetic measurements of Homann and Wagner²⁶⁶ could only be carried out for mass numbers up to 550 which was the upper limit for their mass spectrometer. On the other hand, the smallest particles detected under the electron microscope so far have been those with $d > 15 \text{ Å}$, corresponding to a mass number in excess of 2000.^{297,298} These measurements produced the particle size distribution shown in Fig. 28. As can be seen the average particle size increases and the particle number density (see Fig. 29) falls with height above the burner—these processes can be described quantitatively in terms of the coagulation phenomena discussed in the next section.

The gap between the two classes of measurements has been partially bridged by measurements of large, positively charged species^{234,240,241} by the adaptation of molecular beam sampling systems to allow electrical filtration of charged particles from the beam. In this way it is possible to observe (but not discriminate between) large hydrocarbon ions and charged soot particles with diameters ranging from 10 Å ($\approx 600 \text{ amu}$) to 25 Å ($\approx 10^4 \text{ amu}$) and larger. As discussed in Section 7, the sooting region produces its own ions, independently of those arising in the primary reaction zone. A comparison of the size distribution curves for the charged species²⁴¹ (Fig. 21) and particles obtained under similar conditions and analyzed under the electron microscope²⁴⁰ (Fig. 28) shows how the large hydrocarbon ions grow to be small, charged particles, whose further growth mirrors that of the uncharged particles. However, as Homann²⁴¹ has pointed out, only a few percent of the soot particles in the growth zone are actually charged and those which do carry a charge tend to be rather smaller than their neutral counterparts. Therefore, charging does not provide a truly representative tag to the particle. Nevertheless, the ability to bridge the gap between mass spectrometry and electron microscopy makes this technique a very useful one.

9.1.2.3. Optical techniques Non-intrusive optical methods provide an attractive means of examining sooting flames, particularly in the early stages of particle generation. The optical properties of soot particles are usually required for the evaluation of results. These are discussed in Refs. 71, 128, 292, 299 and 320–336. The most widely used value for the complex refractive index is that due to Dalzell and Sarofim³³² who established $\tilde{m} = 1.57 - 0.47i$ for a variety of soots in the visible wavelength.

Extinction: For spherical, absorbing particles in the Rayleigh regime ($\pi d/\lambda \lesssim 0.3$) the extinction of light is given by^{336,337}

$$k_{\text{ext}} = -\frac{\pi^2}{\lambda} \text{Im} \left\{ \frac{\tilde{m}^2 - 1}{\tilde{m}^2 + 2} \right\} N d^3 \quad 9.1$$

where N is the number density of particles of diameter d . Therefore, the extinction coefficient is proportional to the volume fraction of particulate and is widely used as a measure of soot loading.

Measurements of the optical dispersion, p , where $k_{\text{ext}} \propto \lambda^{-p}$ typically yield values of p in the range 1–1.6 with the highest values for the youngest particles.^{71,128,321,325,328} This could happen if \tilde{m} varies strongly with λ , which does not seem to be the case^{51,322,326,327,332} or if the particles become very large. However, as already mentioned in the discussion of pyrolysis, species other than soot are capable of broad-band absorption in the visible and UV, which may lead to the distortion of measurements of the true soot volume fraction, especially in the early stages of particle formation. Such an effect has been observed in acetylene^{71,299,307} methane,^{48,129} ethylene^{51,339} and benzene^{51,76} flames and it has been shown recently how this may explain the anomalous values of p .³³⁹

For the acetylene/oxygen flame at 20 Torr, Wersborg *et al.*²⁹⁹ compared the soot volume fraction measured by probe sampling and electron micrography with the optical extinction coefficient. They ascribed excess absorption early in the flame to the presence of heavy hydrocarbon species. As shown by the dotted line in Fig. 27c, these "intermediates" are present at heights from about 10–40 mm above the burner. The maximum concentration of these species occurs at a height of 25 mm and corresponds closely to the final soot volume fraction observed downstream.

Once the first particles appear, the soot volume fraction increases rapidly—Fig. 27c, ϕ_1^{298} and ϕ_2^{71} —by further particle generation and by surface growth. Measurements of the very small soot particles, with diameters as low as 15 Å, were made by Wersborg *et al.*²⁹⁸ who obtained the curve N_1 in Fig. 27c for their number density. This implies that new particle generation continues over an extended period (from $z \approx 20$ to $z \approx 40$ mm). On the other hand, when N is evaluated from optical absorption measurements (curve N_2 in Fig. 27c⁷¹), the particle number densities obtained are very much higher earlier on and the region where new particles are being generated may be considerably narrower. The discrepancy between

these two results may arise from the arbitrary definition in the electron micrography work²⁹⁸ (dictated by the limit of detection) of a particle as being a unit of $d > 15$ Å. Optical techniques take all particles into account—and, unfortunately, some gas phase species as well. These results indicate the difficulties in describing the behaviour of the particles when they are very young. The same difficulties apply to the definition and measurement of the average particle sizes shown in Fig. 27d.

Light scatter: For particles in the Rayleigh regime, the scattering coefficient, Q_{VV} , for vertically polarized incident and scattered beams is^{337,338}

$$Q_{VV} = \frac{1}{4} \left(\frac{\pi}{\lambda} \right)^4 \left| \frac{\tilde{m}^2 - 1}{\tilde{m}^2 + 2} \right|^2 N d^6. \quad 9.2$$

Ideally, vertically polarized incident light should give rise to no horizontal scattering component: $Q_{HV} = 0$. In practice, however, there is always some depolarization due to anisotropies of particle shape and polarizability. The depolarization ratio $\rho_V = Q_{HV}/Q_{VV}$ is a measure of these effects.

Light scatter is very sensitive to the onset of particle formation, the limit of detection being due largely to the molecular gases in which the particles find themselves. Combination of light scattering and extinction measurements allows average values of particle size, d , and number density, N , to be obtained from equations 9.1 and 9.2.⁴⁸

Unfortunately, this technique has not yet been applied to the otherwise well-studied, low-pressure, oxygen-acetylene flames. However, results obtained in atmospheric pressure methane,^{48,128,129,340,341} ethylene⁵¹ and benzene⁵¹ flames have been reported. Figure 29 shows how the particle size and number, as well as the total soot volume fraction, vary in a methane oxygen flame at atmospheric pressure.⁴⁸ The particle number density is initially very high and the region of new particle generation appears to be confined largely to the reaction zone. At the end of this zone, the soot volume fraction is still very low so that subsequent increases in the amount of soot would seem to arise mostly from condensational growth on the surface of the first particles generated, as is also implied by the curve N_2 in Fig. 27c. Further similarities between the low pressure acetylene/oxygen flame and this methane/oxygen flame are apparent from the behaviour of the curves for particle size, soot volume fraction and atomic H/C ratio in the sampled soot. This behaviour is in fact, quite general in that it applies also to ethylene/ and benzene/air flames at atmospheric pressure.⁵¹

At this point, we mention the recent application of time-resolved light-scattering to the determination of soot particle size and number densities in flames, although the technique is in its infancy.^{342–346} Light scattered from moving particles is spectrally broadened by the Doppler effect so a measurement of this broadening enables one to obtain the Brownian velocity of the particles, hence their diffusion velocities, and ultimately, by virtue of the Stokes–Einstein

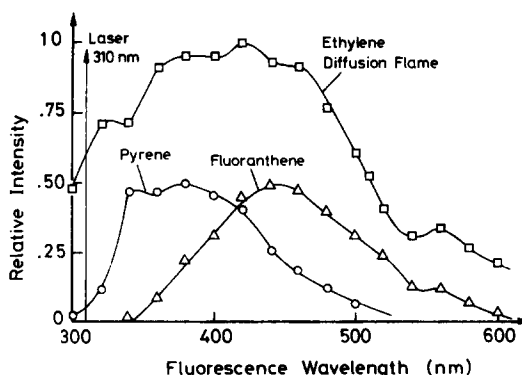


Fig. 30. Fluorescence spectra obtained from laser excitation at 310 nm of the fuel-rich region of an ethylene-air flat diffusion flame, and, for comparison, of pyrene and fluoranthene at 1400 K.³⁴⁹

relation, the particle diameter. This technique may be especially useful in conjunction with the scatter and extinction methods since it depends on a different moment of the particle size ($\simeq d^2$)³⁴⁶ and may help in establishing particle size distribution parameters.

Fluorescence: Recently, it has become apparent that a characteristic feature of a sooting flame is the presence of species capable of producing a broadband depolarized fluorescence when stimulated by laser irradiation. This has been observed in sooting flames of methane,^{129,347,348} ethylene,^{51,125,339,349} benzene⁵¹ and pyridine,⁵¹ starting in or just beyond the main reaction zone and always before the first particles appear. No such fluorescence is found in non-sooting premixed flames but it is found in diffusion flames.^{51,339,349} There is a strong correlation between the apparently non-soot continuum absorption and fluorescence in these flames^{51,339} so that the same species are probably responsible in both cases. The fluorescence has also been considered recently by DiLorenzo *et al.*³⁸⁷

Excitation wavelengths from 300 nm to 515 nm have been used and in all cases a broad-band, relatively featureless fluorescence spectrum results. A typical example is shown in Fig. 30 for excitation at 310 nm of an ethylene diffusion flame.

The identities of the fluorescing species have not been established directly but it is most likely that they represent, in the most general sense, the polycyclic aromatic hydrocarbons.^{51,125,339,349} The fluorescence spectra (at 1500 K) of pyrene and fluoranthene, typical of polycyclics known to occur in sooting flames^{62,265,300,301,303-305} are also shown in Fig. 30. It is not difficult to imagine how a complex mixture of similar species might give rise to the observed broad-band extinction and fluorescence.

Obviously the further identification of these phenomena could potentially yield valuable new information about the processes preceding the formation of the first soot particles.

9.1.2.4. Benzene flames There is no question that a benzene flame forms soot more readily than does

an acetylene flame.^{19,20,63,308} Not only is more soot formed but it is also formed more rapidly.

Mass spectrometric analyses of the main reaction zone and the regions immediately downstream thereof indicate a composition rather different from that which applies in general for aliphatic fuels.^{63,301} Acetylene and the polyacetylenes are still major products, albeit in reduced amounts, but their behaviour is now different in that their concentration does not decrease so markedly at the end of the reaction zone. The concentrations of various simple aromatic species, which now appear within the main reaction zone itself, are perhaps two orders of magnitude higher than for the aliphatic fuels.⁶³ While some of these species appear to be unreactive in this flame as they are in acetylene flames, others, such as phenyl-acetylene, indene, methylnaphthalene and biphenyl show a marked peak in their concentration profiles at the end of the primary reaction zone.

On examination of these trends, there is little doubt that aromatics do play an important role in the soot formation mechanism in benzene flames. Homann and Wagner^{19,266,308} suggested that a free radical polymerization process is probably responsible for the generation of the first particles. The fact that the particle formation zone overlies the main reaction zone to a much greater extent than in acetylene/oxygen flames^{51,52,265} means that many reactive radicals are readily available in a zone where the concentration of reactive polycyclics is already high. Thus a hydrocarbon radical can be expected to grow rapidly by adding such polycyclics which constitute much larger "building blocks" than are available at corresponding periods in acetylene flames.

Recently, in a mass-spectrometric study of a near-sooting benzene-oxygen flame at 20 Torr, Bittner and Howard³⁰¹ concluded that the sooting propensity of benzene derives chiefly from the presence of a high concentration of intact rings right in the main reaction zone which gives the smaller aliphatics arising from ring fragmentation (the most likely fate of the fuel) a site on which to add. The resulting addition complexes are presumably stabilized by internal aromatic substitution reactions leading to condensed ring systems, beginning with naphthalene. The p.c.a.h. therefore arise much earlier in these flames than in their acetylene counterparts and will presumably go on growing in the radical-rich environments in which they find themselves.

The high concentration of aromatics early in the benzene flame also raises the question of an ionic polymerization³¹⁸ as these species have relatively low ionization potentials.²⁴² Once again the evidence, which is discussed in detail by Bittner and Howard,³¹⁸ is inconclusive and the question remains open.

Despite the fact that the mechanism leading to the generation of the first particles in benzene flames differs from that for aliphatic fuels, the behaviour of the soot particles, once formed, is indistinguishable, as shown by the optical techniques discussed earlier. This is shown in Fig. 31 where the particle number

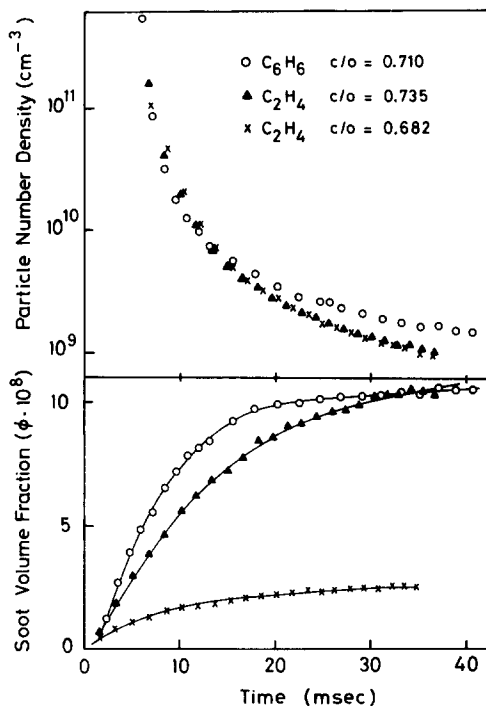


FIG. 31. Profiles of particle number density and soot volume fraction obtained by light scattering and extinction measurements on various atmospheric pressure flames at about 1800 K.

densities and soot volume fractions are compared for benzene- and ethylene-air flames. As is apparent, the benzene soot is formed more quickly and ceases forming sooner, indicating different processes of surface growth in the two flames. The particle number densities are largely indistinguishable however, as to be expected when coagulation is dominating. The effects of additives in the two types of flame are also the same.²⁴⁵

9.2. Particle Growth

9.2.1. By surface condensation

The surface of hot soot particles readily accepts hydrocarbons from the gas-phase. Some of this material may re-enter the gas phase;²⁶⁶ or it may be incorporated into the soot structure. This is clearly demonstrated by the appearance of macroscopic changes when soot particles are held (e.g. by electric fields^{246,247} or by a stream of gas²⁶⁵) in the carbon formation zone. Tesner³⁵⁰ pointed out that, for a given species, this can occur at rather lower temperatures than the generation of the particles themselves. Surface growth can also continue at hydrocarbon concentrations below the lower limit required for the inception of sooting.¹³

The high reactivity of the soot surface is such that the presence of soot can accelerate the decomposition of benzene²⁷⁰ and acetylene³⁵¹⁻³⁵⁴ in pyrolysis. In methane pyrolysis, the surface rate of deposition on soot particles is an order of magnitude higher than it is on alumina or graphite.³⁵⁵

There have been many studies, particularly in the Russian literature (reviewed recently by Tesner²¹) of surface reactions. By and large, these studies pertain to pyrocarbon growth (well after the initial induction period in which the first few molecular layers are set down) rather than to soot particle growth. However, there are sufficient similarities that these results should be at least qualitatively applicable to the growth of soot particles as well (see, for example, Refs. 13, 21, 355). In general, acetylene and aromatics are more effective growth species than are the aliphatics; larger molecules are only slightly more effective than their smaller homologues.²¹

Despite these studies, the detailed kinetics of surface growth are not well understood, largely because the pyrolysis of even such a simple species as methane gives rise to a complex mixture of hydrocarbons. Tesner^{350,356} suggested that, in these types of studies, the condensing species is usually the parent hydrocarbon, and that in a flame environment, because of their high concentrations, simple molecules such as acetylene and methane dominate surface growth reactions.²¹ However, at least in the case of methane, it appears that higher, perhaps unsaturated, hydrocarbons formed by pyrolysis are responsible.^{355,357}

Evidence for the importance of surface growth in determining the actual amount of soot formed in a flame comes from a comparison of the relative positions of the regions of new particle formation and of increasing soot loading. Thus, the particle number and soot concentration profiles in Figs. 29 and 31 show that the bulk of the soot appears after the end of the particle formation zone. This implies that surface growth, rather than the generation of new particles, is responsible for the additional solid phase material. This has also been confirmed for the oxygen/acetylene flame of Fig. 27c as well as for the laminar diffusion flames of Fig. 9 (Section 4.2.).

For the oxygen/acetylene flame, Homann and Wagner²⁶⁶ suggested that the main species being attached to the surface are acetylene and the polyacetylenes, as implied by the continual decrease of the concentrations of these species well beyond the main reaction zone. They also suggested that the decreasing atomic H/C ratio of the soot collected at increasing heights above the burner are in keeping with the addition of these species. Eventually surface growth slows, even though the concentration of polyacetylenes remains high. This occurs at a time when the concentration of radicals in the gas phase has dropped to a very low value and when the radical character of the particles has been greatly reduced (as indicated by e.s.r. measurements), perhaps by some process of tempering.²⁶⁶

Thus, once particles are formed, the nature and concentration of reactive species in the region control the eventual yield of soot. As discussed previously, the concentration of polycyclic species is much greater in benzene flames than in ethylene flames and this probably explains the differences in the curves for ϕ in Fig. 31—in the benzene flame, the soot is formed not

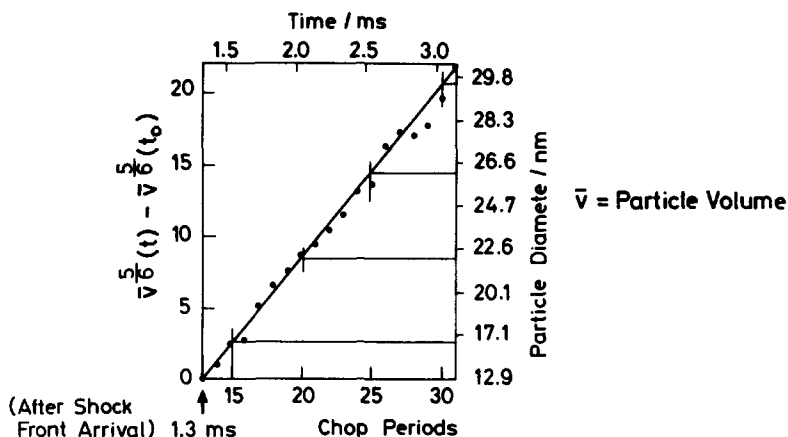


FIG. 32. Variation of the mean particle volume with time for soot formed by shock-heating ethylbenzene in argon at 1750 K—experimental verification of coagulation theory, equation 9.6.²⁹²

only more quickly but ceases forming earlier. The effect of increasing C/O is to increase the concentration of reactive intermediates while at the same time reducing the temperature. Because the apparent activation energies for surface growth reactions are very low,^{21,358} the net effect is an increase in soot loading. Only as the flame approaches its rich limit of stability is this trend reversed. Regardless of the changes in surface growth between different flames, the particle number density behaviour is practically invariant—this important result is a consequence of coagulation.

9.2.2. By coagulation

It was noted in early studies of low-pressure acetylene flames^{71,266} that a significant fraction of the observed particle growth is due to coagulation whereby particles collide and fuse, thus reducing their overall number concentration while increasing the average size of the particles. The importance of taking this phenomenon into account in all studies of soot particle dynamics is now well established.^{21,51,81,125,131,133,243,245,292-298,358} (See also Bockhorn *et al.* and Prado *et al.* in reference 387.)

A major part of Graham and co-workers' pyrolysis experiments^{292-296,360} has been the quantitative investigation of this process by light scattering and absorption techniques. Theoretically, the decrease in particle number can be expected to occur according to the Smoluchowski equation:

$$\frac{dN}{dt} = -k(d)N^2 \quad 9.3$$

where the rate constant k depends on the particle diameter d , or equivalently, on the mean volume \bar{v} . For particles small compared with gas mean free path (Knudsen number > 10), Brownian motion, and k , are described in terms of free molecule theory: for soot particles in a typical flame environment, this requires that $d \lesssim 600 \text{ \AA}$. For such a system in which uncharged spherical particles coalesce on every collision, this leads to a coagulation rate of³⁶¹⁻³⁶⁴

$$\frac{dN}{dt} = -\frac{6}{5}k_{\text{theory}}\phi^{1/6}N^{11/6} \quad 9.4$$

where

$$k_{\text{theory}} = \frac{5}{12}\left(\frac{3}{4\pi}\right)^{1/6}\left(\frac{6kT}{\rho}\right)^{1/2}G\cdot\alpha$$

and

- ϕ is the particulate volume fraction;
- ρ is the density of the particles;
- G is a factor to take account of interparticle dispersion forces and can be expected to have a value of about 2 for spherical particles;^{292,361}
- α is a weak function of the particle size distribution, reflecting the variation in collision rates with different particles sizes. For a mono-disperse system, $\alpha = 4\sqrt{2} = 5.66$; for the self-preserving size distribution, $\alpha = 6.55$.³⁶¹⁻³⁶⁵

When the soot volume fraction ϕ is constant, and coagulation alone determines particle growth, then the increase in the mean particle volume, $\bar{v} = \phi/N$, is given by

$$\frac{d\bar{v}}{dt} = \frac{6}{5}k_{\text{theory}}\phi\bar{v}^{1/6} \quad 9.5$$

which gives

$$\bar{v}^{5/6} - \bar{v}_0^{5/6} = k_{\text{theory}}\phi t. \quad 9.6$$

As shown in Fig. 32, Graham *et al.*²⁹² obtained a good straight line fit when they plotted $\bar{v}^{5/6}$ (here in arbitrary units) against t for their shock tube studies of aromatic hydrocarbon pyrolysis. Their experimental values for k agree well with the theoretical value, k_{theory} , thus indirectly substantiating the assumptions made in the theoretical development.

This work also provides evidence that the particle size distribution in these pyrolyzing gases tends towards a self-preserving form.^{292,361-365} As its name implies, a self-preserving size distribution (SPSD) is one whose form does not change with time in a coagulating system. Naturally it provides a considerable simplification in describing the dynamics of a purely coagulating aerosol; unfortunately it is un-

likely to take any simple form when simultaneous surface condensation is occurring to increase ϕ rapidly.³⁶⁶

For long reaction times ($N_o^{5/6}\phi^{1/6}k_{\text{theory}}t \gg 1$, or $t \gtrsim 1$ msec for Graham's conditions²⁹²), the particle number becomes independent of the initial number N_o and decreases as

$$N \simeq (k_{\text{theory}}\phi^{1/6}t)^{-6/5} \quad 9.7$$

which shows a rather weak dependence on ϕ , i.e. the number of particles is largely independent of the soot loading. Also, since k_{theory} is only a weak function of temperature, N at a given time should not be too strongly dependent on the gas temperature. As was seen in Fig. 31, the particle number density curves in ethylene flames containing different amounts of soot and in a benzene flame are barely distinguishable, as would be expected from the above equation. This behaviour has also been confirmed quantitatively in flames of CH_4-O_2 ⁴⁸ and $\text{C}_5\text{H}_5\text{N}-\text{air}$.⁵¹ The absolute magnitude of k_{theory} has also been determined to be close to that theoretically predicted.^{51,78,292} These and Graham's measurements establish that coagulation is a property of the soot itself and does not depend on the nature of the parent molecules, nor on the mode of its generation. Conflicting results have been obtained by Howard and co-workers²⁹⁷⁻²⁹⁸ who found coagulation rates at least an order of magnitude higher than predicted. They sampled particles and counted them under the electron microscope to determine particle number densities and coagulation rates. It is not clear yet why these results should differ so markedly from those obtained by the optical techniques.

It is expected that when particles are charged, their coagulation rate will be either weakly enhanced or somewhat reduced, depending on whether bipolar or homopolar charging occurs. The expected magnitude of the effect has been considered by Hidy and Brock³⁶³ and by Howard,²⁵³ amongst others. A demonstration of the effect has been provided recently by Haynes *et al.*^{78,245} who seeded sooting ethylene-air flames with ionizing additives such as caesium and potassium salts. They found that they were able practically to suppress particle coagulation in the presence of these additives (Fig. 22) presumably because the presence of the metal promotes charging of the small soot particles which subsequently resist coagulation by coulombic repulsion (see Section 8). This result could be of some practical interest for, as demonstrated by Fenimore,¹³³ a sooting flame smokes only when the soot particles coagulate to be too large to burn out in the time available.

Despite the considerable success in describing the growth of soot particles by coagulation in terms of collision and coalescence, there remain some open questions. Electron micrographs indicate that the elementary soot particles of which the chains are built (Fig. 2) are spherical, both the smaller ($d \simeq 50 \text{ \AA}$) and the larger ($d \simeq 500 \text{ \AA}$) ones. Graham²⁹⁶ has confirmed that the collisions occurring in his shock

flows are indeed coalescent for particle sizes at least up to a few hundred Ångstrom units. One way of explaining these results is to assume that the particles are present as liquid droplets^{2,105,293-296,367-372} capable of coalescing on collision to form larger drops which slowly pyrolyze. (The possibility that soot particles are liquid for at least part of their lives is discussed in the context of particle generation in the next section). However, it may not be necessary to postulate the formation of real "droplets" because young "solid" particles are very reactive so that continued surface growth will tend to blanket out asymmetries caused by "non-coalescent" collisions. Also, one would expect diffusion within young, highly disordered soot particles to be rather rapid so that the question as to whether the particles are liquid or solid may, in this respect, be insignificant.

Beyond a certain point, the collisions between particles do appear to change from being effectively coalescent to chain-forming. Much of the agglomeration observed in samples under the electron-microscope may have arisen during the sampling process, in the probe boundary layer, or on the collecting surface. However, optical evidence suggests that indeed some chain growth is occurring in the flame itself.^{48,151,154,373,374} The volume to be filled in to form symmetric particles after non-coalescent collision is proportional to the total particle volume, so that a resymmetrization of the particles is much faster with smaller than with larger particles. In addition, there is much more material in the gas-phase ready to add to the particle surface in regions where small particles occur than around the chain-forming "old" particles which are already tempered and exhibit generally reduced surface growth activity.²⁶⁵ Howard^{253,254,298} has suggested that the chain-form of the agglomerates reflects the influence of charging of the particles in that electrostatic lines of force at the ends of the particles will favour collisions there. However, chain growth may also be consistent with random collisions in the absence of electrical effects, since the exposed ends of a chain are more likely to come into contact with other particles.³⁷⁵⁻³⁷⁷

9.3. Some Models of Soot Formation

9.3.1. Liquid droplet models

The possibility that soot particles are formed by the carbonization of liquid droplets has been suggested many times—e.g. References 2, 105, 293-296, 367-372. One of the main attractions of this approach is that the transition from coalescent to chain-forming collisions during the growth of the particles may be explained by the carbonization of the droplets.

It is generally assumed that macromolecules are formed in a slow step by polymerization of the hydrocarbon pyrolysis products. These macromolecules can then undergo a classical condensation to produce liquid nuclei and droplets which subsequently pyrolyze to form soot.

Graham^{293,294} found definitive evidence that no droplets are present before soot appears, as signalled by the simultaneous onset of light scattering and infrared absorption. Thus, in place of a homogeneous nucleation, he suggested that as soon as some solid phase material is present, the (supersaturated) gas-phase species condense rapidly to give a two-phase, but predominantly liquid particle.

Homann³⁷⁸ has pointed out that, based on vapour pressure curves of large polycyclic aromatic hydrocarbons, the minimum size of polymers which could condense into liquid at high temperatures is rather large indeed. For example, under the conditions employed by Graham²⁹²⁻²⁹⁴ (2×10^{17} C-atom/cm³) the molecular weights of the first condensable species would be (without taking into account the change of vapour pressure with curvature or acquisition of electric charge):

T(K)	900	1300	1500	1800
M.W. (amu)	780	1450	1800	2700

At the higher temperatures, these single macromolecules constitute "particles" themselves, with equivalent spherical diameters of the order of 15 Å. The formation of such large molecules requires many polymerization steps and it is not clear why these molecules should not continue to condense in a chemical sense, to polymerize as long as free valencies are available. This would not necessarily mean that rigid bodies would be formed as such large macromolecules are likely to have a high degree of internal mobility themselves.

The situation becomes more favourable to the condensation of liquid droplets if the temperature is reduced. However, in the pyrolysis of acetylene at temperatures from 750 to 1250 K, Johnson and Anderson³⁷⁹ obtained evidence that soot does not arise by the carbonization of liquid droplets.

Recently, Lahaye and Prado^{2,368-371} have examined the formation of soot in benzene pyrolysis in terms of condensation to liquid droplets, following classical condensation theory. From this simple model, they predicted that

- (i) at constant benzene concentration the number of nuclei formed is independent of the reaction time at constant temperature.
- (ii) at a given temperature, the number of nuclei is independent of the benzene concentration.
- (iii) the number of nuclei formed increases with temperature.

To test their model they measured the particle number at the reactor exit and found it to behave as predicted for the number of nuclei, thus supporting their model.

However, in equating the number of particles collected (after reaction times in excess of 100 msec) with the number of nuclei generated, the authors appear to be neglecting the intervening effects of coagulation. In fact, their results may be explained

purely in terms of what is known of this phenomenon.⁵¹

We conclude that there is little firm evidence supporting the concept of liquid droplets being precursors of soot in combustion systems. Graham's²⁹²⁻²⁹⁴ ingenious interpretation is not far from a surface growth model—and only further work will clear up whether a liquid phase does exist in young "soot" particles.

9.3.2. Kinetic models

Tesner *et al.*^{98,99} have examined the formation of soot from small amounts of hydrocarbon in hydrogen diffusion flames at about 1800 K. They analyzed their results in terms of generation of radical nuclei which react to form new particles and which also interact with the surface of existing particles. For the radical nuclei, they write

$$\frac{dn}{dt} = n_o + (f-g)n - g_o Nn \quad 9.8$$

where

- n_o is the temperature-dependent rate of spontaneous generation of nuclei;
- f, g are branching and termination coefficients respectively;
- g_o is the rate of destruction of the nuclei on the soot particle surface.

For the number of particles, N :

$$\frac{dN}{dt} = (a - bN)n. \quad 9.9$$

Here a is the rate constant for the conversion of active centres to new particles. Presumably the corresponding term in the balance equation for n is contained in g . The physical significance of the term bNn is not made clear, but it implies a destruction of particles by active centres. No allowance is made for coagulation in this model.

There are many adjustable parameters in this model, which may mean that it has little predictive capability. For example, in an analysis of benzene pyrolysis in a flow reactor, totally different coefficients were obtained.³⁸⁰ On the other hand, Magnussen *et al.*¹⁵⁶ had only to modify slightly Tesner's coefficients to model their measurements of soot formation in turbulent acetylene/air flames.

Perhaps the strongest objection to this model is the fact that it offers no physical insights into the processes occurring in soot formation. In fact, Tesner himself seems to prefer a two stage (formation and growth) approach in his recent review.³¹ The first general models based on this approach were proposed by Gilyazetdinov³⁵⁹ and by Samkhan *et al.*³⁸¹ but in neither case is it altogether clear just what physical significance should be attached to the various terms.

A more recent analytical model by Surovkin³⁵⁸ recognizes three stages in the formation of a mature particle: (1) the formation of "radical nuclei"; (2) the

growth of the "radical nuclei" into "particle nuclei" which then grow (3) by surface growth. The first stage corresponds to the earliest reactions of the parent fuel and therefore has a high activation energy, while the last has practically no activation energy, corresponding to every collision's leading to growth and thus imitating a condensation phenomenon.

A more detailed model has been formulated by Jensen³⁸² who distinguished five processes controlling the production of soot: reactions forming nuclei; nucleation; coagulation; surface growth; and oxidation. He did not try to describe the first two steps in detail, but adopted the simplifying assumption that fragments such as C₂ or C₂H are the kinetic equivalent of condensed "nuclei" so that any species larger than C₂ are particles already. To these particles, gas-phase species such as C₂H₂ or C₂H can add. The particles can also coagulate.

With a relatively simple reaction set to describe C₁₋ and C₂₋ species pyrolysis chemistry, and neglecting oxidation, Jensen was able to calculate the rate of conversion of methane into soot under pyrolysis conditions at about 1500 K. As expected, the overall rate-controlling step determining the amount of soot formed is the initiation reaction CH₄ → CH₃ + H. By comparison of his predictions with measurements of the onset of sooting in a rocket motor exhaust, he concluded the principal growth species to be C₂H₂, although he was unable to identify any particular "nucleus".

Both this model and that of Surovkin³⁵⁸ bear strong overall resemblance to the stages of soot formation described earlier in this Section: particle inception, growth and coagulation. Unfortunately, they have only been tested on simple experiments performed under rather ill-defined conditions^{358,382,383} and it is not possible at this stage to evaluate their efficacy in general. It would not be surprising, however, to find in both cases that the chemistry of particle inception requires more detailed description than is offered, particularly in the case of a flame environment. On the other hand, since most of the soot loading arises by surface growth, detailed modelling of this stage may in fact not be required.

Acknowledgements—B.S.H. thanks the Alexander von Humboldt-Stiftung for support during his introduction to the study of soot formation. The hospitality of the Department of Mechanical Engineering at the University of Sydney is also gratefully acknowledged.

We are indebted to Professor Dr. K. H. Homann for many stimulating discussions.

REFERENCES

- DONNET, J. B. and VOET, A. *Carbon Black*. Marcel Dekker, New York (1976).
- LAHAYE, J. and PRADO, G. Mechanisms of carbon black formation, *Chemistry and Physics of Carbon*, (editors WALKER, P. L. and THROWER, P. A.), Vol. 14, pp. 168–294. Marcel Dekker, New York (1978).
- SCHWOB, Y. Acetylene black: manufacture, properties and applications, *Chemistry and Physics of Carbon*, (editors WALKER, P. L. and THROWER, P. A.), Vol. 15, pp. 109–227. Marcel Dekker, New York (1979).
- COWPERTHWAITE, M. and BAUER, S. H. Estimation of molecular parameters of C/H fragments, *J. Chem. Phys.* **36**, 1743–1753 (1962).
- DUFF, R. E. and BAUER, S. H. Equilibrium composition of the C/H system at elevated temperatures, *J. Chem. Phys.* **36**, 1754–1767 (1962).
- SHAW, R., GOLDEN, D. M. and BENSON, S. W. Thermochemistry of some six-membered cyclic and polycyclic compounds related to coal, *J. Phys. Chem.* **81**, 1716–1729 (1977).
- STEIN, S. E., GOLDEN, D. M. and BENSON, S. W. Predictive scheme for thermochemical properties of polycyclic aromatic hydrocarbons, *J. Phys. Chem.* **81**, 314–317 (1977).
- STEIN, S. E. On the high temperature chemical equilibria of polycyclic aromatic hydrocarbons, *J. Phys. Chem.* **82**, 566–571 (1978).
- LERSMACHER, B., LYDTIN, H., KNIPPENBERG, W. F. and MOORE, A. W. Thermodynamic considerations of carbon deposition in the pyrolysis of gaseous carbon compounds, *Carbon*, **5**, 205–217 (1967).
- HOMANN, K. H. Paper presented to the Dechema Fachausschuss für Gas und Flammenreaktionen, (1978).
- ABRAHAMSON, J. Saturated platelets are new intermediates in hydrocarbon pyrolysis and carbon formation, *Nature*, **266**, 323–327 (1977).
- WAGNER, H. GG. Soot formation in combustion, *Seventeenth Symposium (International) on Combustion*, pp. 3–19. The Combustion Institute, Pittsburgh, PA (1979).
- PALMER, H. B. and CULLIS, C. F. The formation of carbon from gases, *Chemistry and Physics of Carbon*, (editor WALKER, P. L.), Vol. 1, pp. 265–325. Marcel Dekker, New York (1965).
- STREET, J. C. and THOMAS, A. Carbon formation in premixed flames, *Fuel*, **34**, 4–36 (1955).
- SCHALLA, R. L. and HIBBARD, R. R. Smoke and coke formation in the combustion of hydrocarbon-air mixtures, *Basic Considerations in the Combustion of Hydrocarbons with Air*, Chap. 9, NACA Report 1300 (1957).
- THOMAS, A. Carbon formation in flames, *Comb. Flame*, **6**, 46–62 (1962).
- GAYDON, A. G. and WOLFHARD, H. G. *Flames: Their Structure, Radiation and Temperature*. Fourth Edition, Chapman and Hall, London (1979).
- PALMER, H. B. and SEERY, D. J. Chemistry of Pollutant Formation in Flames. *Ann. Rev. Phys. Chem.* **24**, 235–262 (1973).
- HOMANN, K. H. Carbon formation in premixed flames, *Comb. Flame*, **11**, 265–287 (1967).
- HOMANN, K. H. Russbildung in vorgemischten Kohlenwasserstoff–Flammen, *Angew. Chemie.* **80**, 425–438 (1968).
- TESNER, P. A. Soot formation during combustion, *Comb. Expl. Shockwaves*, **15**, 111–120 (1979).
- GUERIN, M. R. Energy sources of polycyclic aromatic hydrocarbons. *Polycyclic Hydrocarbons and Cancer: Environment, Chemistry and Metabolism*, pp. 3–44. Academic Press, New York (1978).
- FITZER, E., MUELLER, K. and SCHAEFER, W. The chemistry of the pyrolytic conversion of organic compounds to carbon. *Chemistry and Physics of Carbon*, (editor WALKER, P. L.), Vol. 7, pp. 237–383. Marcel Dekker, New York (1971).
- WARREN, B. E. X-Ray diffraction in random layer lattices. *Phys. Rev.* **59**, (Second Series), 693–698 (1941).
- WARREN, B. E. and BODENSTEIN, P. The diffraction pattern of fine particle carbon blacks, *Acta Cryst.* **18**, 282–286 (1965).
- AUSTIN, A. E. Crystal structural properties of carbon

- blacks, *Proceeding of the Third Conference on Carbon*, pp. 389–394, Pergamon, New York (1959).
27. FRANKLIN, R. E. The interpretation of diffuse X-ray diagrams of carbon, *Acta Cryst.* **3**, 107–121 (1950).
 28. FRANKLIN, R. E. The structure of graphite carbons, *Acta Cryst.* **4**, 253–261 (1951).
 29. FRANKLIN, R. E. Crystallite growth in graphitizing and non-graphitizing carbons, *Proc. Roy. Soc. A*, **209**, 196–218 (1951).
 30. HECKMAN, F. A. Microstructure of Carbon Black, *Rubber Chem. Tech.* **37**, 1245–1298 (1964).
 31. HECKMAN, F. A. and HARLING, D. F. Progressive oxidation of selected particles of carbon black: further evidence for a new microstructural model, *Rubber Chem. Tech.* **39**, 1–13 (1966).
 32. HALL, C. E. Dark-field electron microscopy II. Studies of colloidal carbon, *J. Appl. Phys.* **19**, 271–277 (1948).
 33. HESS, W. M. and BAN, L. L. High resolution dark field microscopy of carbon black, *Norelco Reporter*, **13**, 102–107, 132 (1966).
 34. BAN, L. L. Direct study of structural imperfections by high-resolution electron microscopy, *Surface and Defect Properties of Solids*, Vol. 1, pp. 54–94, The Chemical Society, London (1972).
 35. BAN, L. L. and HESS, W. M. Microstructure and morphology of carbon blacks, *Petroleum Derived Carbons*, (editors DEVINEY, M. L. and O'GRADY, T. M.), pp. 358–377, A.C.S. Symposium Series No. 21, A.C.S., Washington, D.C. (1976).
 36. MARSH, P. A., VOET, A., MULLENS, T. J. and PRICE, L. D. Electron micrography of interplanar spacings in carbon blacks, *Rubber Chem. Tech.* **43**, 470–481 (1970).
 37. MARSH, P. A., VOET, A., MULLENS, T. J. and PRICE, L. D. Quantitative micrography of carbon black microstructure, *Carbon*, **9**, 797–805 (1971).
 38. BAUER, S. H. Comment, *Tenth Symposium (International) on Combustion*, p. 511, The Combustion Institute, Pittsburgh (1965).
 39. FISCHBACH, D. B. The kinetics and mechanism of graphitization, *Chemistry and Physics of Carbon*, (editors WALKER, P. L. and THROWER, P. A.), Vol. 7, p. 105, Marcel Dekker, New York (1971).
 40. PACAULT, A. The kinetics of graphitization, *Chemistry and Physics of Carbon*, (editors WALKER, P. L. and THROWER, P. A.), Vol. 7, pp. 107–154, Marcel Dekker, New York (1971).
 41. MARCHAND, A. Variation thermique de la susceptibilité magnétique de quelques noirs de carbone, *Acad. Sci. Paris Comptes Rendus*, **238**, 1645–1647 (1954).
 42. MARCHAND, A. Variation thermique de la susceptibilité diamagnétique de quelques noirs de carbone, *Acad. Sci. Paris Comptes Rendus*, **239**, 1609–1611 (1954).
 43. UEBERSFELD, J., ETIENNE, A. and COMBRISSON, J. Paramagnetic resonance, a new property of coal-like materials, *Nature*, **174**, 614 (1954).
 44. INGRAM, D. J. E., TAPLEY, J. G., JACKSON, R., BOND, R. L. and MURNAGHAN, A. R. Paramagnetic resonance in carbonaceous solids, *Nature*, **174**, 797–798 (1954).
 45. JESSEN, P. F. and GAYDON, A. G. Estimation of carbon radical concentration in fuel-rich acetylene-oxygen flames by absorption spectroscopy, *Twelfth Symposium (International) on Combustion*, pp. 481–489, The Combustion Institute, Pittsburgh (1969).
 46. WRIGHT, F. J. The formation of carbon under well-stirred conditions, *Twelfth Symposium (International) on Combustion*, pp. 867–874, The Combustion Institute, Pittsburgh (1969).
 47. BLAZOWSKI, W. S. Dependence of soot production on fuel structure in backmixed combustion, *Combust. Sci. Tech.* **21**, 87–96 (1980).
 48. D'ALESSIO, A., DI LORENZO, A., SAROFIM, A. F., BERETTA, F., MASI, S. and VENTOZZI, C. Soot formation in methane-oxygen flames, *Fifteenth Symposium (International) on Combustion*, pp. 1427–1438, The Combustion Institute, Pittsburgh (1975).
 49. FLOSSDORF, J. and WAGNER, H. GG. Russbildung in normalen und gestörten Kohlenwasserstoff-Luft-Flammen, *Z. Phys. Chem. N.F.* **54**, 113–128 (1967).
 50. MILLIKAN, R. C. and FOSS, W. I. Non-equilibrium effects in soot deposition, *Comb. Flame*, **6**, 210–211 (1962).
 51. HAYNES, B. S., JANDER, H. and WAGNER, H. GG. Optical studies of soot formation processes in premixed flames, *Ber. Bunsenges. Phys. Chem.*, **84**, 585–592 (1980).
 52. MORGENEYER, W. Vergleichende Untersuchungen an russenden Acetylen und Benzol-Flammen mit optischen Methoden. *Dissertation*, Göttingen (1968).
 53. BEHRENS, H. Hydrogen diffusion and flame structure, *Naturwissenschaften*, **32**, 297–299 (1944).
 54. BEHRENS, H. Untersuchungen über Aussehen und Gestalt von Brennerflammen, *Z. Phys. Chem.* **196**, 78–101 (1950).
 55. JOST, W. Über die Möglichkeit des Auftretens räumlicher Periodizität in reagierenden homogenen Systemen, *Z. Phys. Chem.* **193**, 332–333 (1944).
 56. JOST, W. and KRISCHER, B. Gas-analytische Untersuchungen an gestörten Benzol-Luft-Flammen, *Z. Phys. Chem. N.F.* **5**, 298–401 (1955).
 57. MARKSTEIN, G. H. Instability phenomena in combustion waves, *Fourth Symposium (International) on Combustion*, pp. 44–59, (1953).
 58. MARKSTEIN, G. H. Composition traverses in curved laminar flame fronts, *Seventh Symposium (International) on Combustion*, pp. 289–295, Butterworth, London (1959).
 59. GARSIDE, J. E. and JACKSON, B. The formation and some properties of polyhedral burner flames, *Fourth Symposium (International) on Combustion*, pp. 545–552, (1953).
 60. FLOSSDORF, J., JOST, W. and WAGNER, H. GG. Entmischungseffekt in Flammen auf Bunsenbrennern, *Ber. Bunsenges. Phys. Chem.* **78**, 378–386 (1974).
 61. RYAN, P. W. Vergleich der Russgrenzen in flachen und kegelförmigen Kohlenwasserstoff-Flammen, *Diplomarbeit*, Göttingen (1968).
 62. HOMANN, K. H. Comment, *Twelfth Symposium (International) on Combustion*, p. 875, The Combustion Institute, Pittsburgh (1969).
 63. HOMANN, K. H., MOCHIZUKI, M. and WAGNER, H. GG. Über den Reaktionsablauf in fetten Kohlenwasserstoff-Sauerstoff-Flammen. I, *Z. Phys. Chem. N.F.* **37**, 299–313 (1963).
 64. BAULCH, D. L., DRYSDALE, D. D., HORNE, D. E. and LLOYD, A. C. *Evaluated Kinetic Data for High Temperature Reactions*. Vol. 1, *The H₂O₂ System*, Butterworth, London (1972).
 65. HOYERMANN, K. and SIEVERT, R. The reactions of alkyl radicals with oxygen atoms: identification of primary products at low pressure, *Seventeenth Symposium (International) on Combustion*, pp. 517–524, The Combustion Institute, Pittsburgh (1979).
 66. DANIELS, P. H. Carbon formation in premixed flames, *Comb. Flame*, **4**, 45–49 (1960).
 67. GLASSMAN, I. Phenomenological models of soot processes in combustion systems, Princeton University Department of Mechanical and Aerospace Engineering, Report 1450 (1979).
 68. GAY, N. R., AGNEW, J. T., WITZELL, O. W. and KARABELL, C. E. Thermochemical equilibrium in hydrocarbon–oxygen reactions involving polyatomic forms of carbon, *Comb. Flame*, **5**, 257–272 (1961).
 69. FENIMORE, C. P., JONES, G. W. and MOORE, G. E. Carbon formation in quenched flat flames at 1600 K, *Sixth Symposium (International) on Combustion*, pp. 242–247, Reinhold, New York (1957).
 70. MACFARLANE, J. J., HOLDERNESS, F. H. and WHITCHER, F. S. E. Soot formation rates in pre-mixed C₅– and C₆–

- hydrocarbon air flames at pressures up to 20 atm, *Comb. Flame*, **8**, 215–229 (1964).
71. BONNE, U. and WAGNER, H. GG. Untersuchung des Reaktionsablaufs in fetten Kohlenwasserstoff-Sauerstoff-Flammen. III—optische Untersuchungen an russenden Flammen, *Ber. Bunsenges. Phys. Chem.* **69**, 35–48 (1965).
 72. RADCLIFFE, S. W. and APPLETON, J. P. Shock-tube measurements of carbon to oxygen atom ratios for incipient soot formation with C_2H_2 , C_2H_4 and C_2H_6 fuels, *Combust. Sci. Tech.* **3**, 255–262 (1971).
 73. RECK, R. *Diplomarbeit*, T.V. Darmstadt (1972).
 74. MCARRAGHER, J. S. and TAN, K. J. Soot formation at high pressures: a literature review, *Combust. Sci. Tech.* **5**, 257–261 (1972).
 75. MILLIKAN, R. C. Non-equilibrium soot formation in premixed flames, *J. Phys. Chem.* **66**, 794–799 (1962).
 76. HOMANN, K. H., MORGENEYER, W. and WAGNER, H. GG. Optical measurements in carbon-forming benzene–oxygen flames, *Combustion Institute European Symposium*, (editor WEINBERG, F. J.), pp. 394–399, Academic Press, London (1973).
 77. WRIGHT, F. J. Carbon formation under well-stirred conditions: part II, *Comb. Flame*, **15**, 217–222 (1970).
 78. HAYNES, B. S., JANDER, H. and WAGNER, H. GG. The effect of metal additives on the formation of soot in premixed flames, *Seventeenth Symposium (International) on Combustion*, pp. 1365–1374, The Combustion Institute, Pittsburgh (1979).
 79. MÄTZING, H. *Diplomarbeit*, Göttingen (1979).
 80. MÜLLER-DETHLEFS, K. and SCHLADER, A. F. The effect of steam on flame temperature, burning velocity and carbon formation in hydrocarbon flames, *Comb. Flame*, **27**, 205–215 (1976).
 81. RECK, R. Untersuchung zum Einfluss von gasförmigen Zusätzen auf die Russbildung in Propan-Sauerstoff-Flammen, *Dissertation*, Darmstadt (1977).
 82. MORLEY, C. The formation and destruction of hydrogen cyanide from atmospheric and fuel-nitrogen in rich atmospheric-pressure flames, *Comb. Flame*, **27**, 189–204 (1976).
 83. GAYDON, A. G. and WHITTINGHAM, G. The spectra of flames containing oxides of sulphur, *Proc. Roy. Soc. A*, **189**, 313–325 (1947).
 84. BURKE, S. P. and SCHUMANN, T. E. W. Diffusion flames, *Ind. Eng. Chem.* **20**, 998–1006 (1928).
 85. HOTTEL, H. C. and HAWTHORNE, W. R. Diffusion in laminar flame jets, *Third Symposium on Combustion, Flame and Explosion Phenomena*, pp. 254–266, Williams and Wilkins, Baltimore (1949).
 86. JONES, J. M. and ROSENFELD, J. L. J. A model for sooting in diffusion flames, *Comb. Flame*, **19**, 427–434 (1972).
 87. ROPER, F. G. The prediction of laminar jet diffusion flame sizes: part I. Theoretical model, *Comb. Flame*, **29**, 219–226 (1977).
 88. ROPER, F. G., SMITH, C. and CUNNINGHAM, A. C. The prediction of laminar jet diffusion flame sizes: part II. Experiment verification, *Comb. Flame*, **29**, 227–234 (1977).
 89. ROPER, F. G. Laminar diffusion flame sizes for curved slot burners giving fanshaped flames, *Comb. Flame*, **31**, 245–250 (1978).
 90. ROPER, F. G. and SMITH, C. Soot escape from laminar air-starved hydrocarbon flames, *Comb. Flame*, **36**, 125–138 (1979).
 91. LEE, K. B., THRING, M. W. and BEER, J. M. On the rate of combustion of soot in a laminar soot flame, *Comb. Flame*, **6**, 137–145 (1962).
 92. HINOHARA, T. Carbon streaks in diffusion flames and the structure of diffusion flames, *Intern. Chem. Eng.* **5**, 175–179 (1965).
 93. MINCHIN, S. T. The chemical significance of tendency to smoke, *World Petr. Congress Proceedings*, **2**, 738–743 (1933).
 94. CLARKE, A. E., HUNTER, T. C. and GARNER, F. H. The tendency to smoke of organic substances on burning. Part I, *J. Inst. Petrol.* **32**, 627–642 (1946).
 95. SCHUG, K. P., MANHEIMER-TIMNAT, Y., YACCARINO, P. and GLASSMAN, I. Sooting behaviour of gaseous hydrocarbon diffusion flames and the influence of additives, *Combust. Sci. Tech.* **22**, 235–250 (1980).
 96. MILBERG, M. E. Carbon formation in an acetylene-air diffusion flame, *J. Phys. Chem.* **63**, 578–582 (1959).
 97. COWARD, H. F. and WOODHEAD, D. W. The luminosities of the flames of some individual chemical compounds, alone and mixed, *Third Symposium on Combustion and Flame and Explosion Phenomena*, pp. 518–522, Williams and Wilkins, Baltimore (1949).
 98. BLAZOWSKI, W. S. Future jet fuel combustion problems and requirements, *Prog. Energy Combust. Sci.* **4**, 177–199 (1978).
 99. NAEGLI, D. W. and MOSES, C. A. Effects of fuel properties in soot formation in turbine combustion, S.A.E. Technical Paper 781026 (1978).
 100. GLASSMAN, I. Private communication (1980).
 101. TESNER, P. A., SNEGIRIOVA, T. D. and KNORRE, V. G. Kinetics of dispersed carbon formation, *Comb. Flame*, **17**, 253–260 (1971).
 102. TESNER, P. A., TSYGANKOVA, E. I., GUILAZETDINOV, L. P., ZUYEV, V. P. and LOSHAKOVA, G. V. The formation of soot from aromatic hydrocarbons in diffusion flames of hydrocarbon–hydrogen mixtures, *Comb. Flame*, **17**, 279–285 (1971).
 103. SCULLY, D. B. and DAVIES, R. A. Carbon formation from aromatic hydrocarbons, *Comb. Flame*, **9**, 185–191 (1965).
 104. DAVIES, R. A. and SCULLY, D. B. Carbon formation from aromatic hydrocarbons II, *Comb. Flame*, **10**, 165–170 (1966).
 105. PARKER, W. G. and WOLFHARD, H. G. Carbon formation in flames, *J. Chem. Soc.* 2038–2049 (1950).
 106. SCHALLA, R. L. and McDONALD, G. E. Mechanism of smoke formation in diffusion flames, *Fifth Symposium (International) on Combustion*, pp. 316–324, Reinhold, New York (1955).
 107. McLINTOCK, I. S. The effect of various diluents on soot production on laminar ethylene diffusion flames, *Comb. Flame*, **12**, 217–225 (1968).
 108. CHAKRABORTY, B. B. and LONG, R. The formation of soot and polycyclic aromatic hydrocarbons in diffusion flames. Part I, *Comb. Flame*, **12**, 226–236 (1968).
 109. DEARDEN, P. and LONG, R. Soot formation in ethylene and propane diffusion flames, *J. Appl. Chem.* **18**, 243–251 (1968).
 110. TESNER, P. A., ROBINOVITCH, H. J. and RAFALKES, I. S. The formation of dispersed carbon in hydrocarbon diffusion flames, *Eighth Symposium (International) on Combustion*, pp. 801–806, Williams and Wilkins, Baltimore (1961).
 111. CHAKRABORTY, B. B. and LONG, R. The formation of soot and polycyclic aromatic hydrocarbons in diffusion flames—Part two, *Comb. Flame*, **12**, 237–242 (1968).
 112. HERBST, G. Über die Russbildung von Kohlenwasserstoffen in Koksofengas oder ähnlichen Brenngasen und eine Möglichkeit ihrer Beeinflussung, *Brennst.-Chemie*, **44**, 1–5 (1963).
 113. WRIGHT, F. J. Effect of oxygen on the carbon-forming tendencies of diffusion flames, *Fuel*, **53**, 232–235 (1974).
 114. ARTHUR, J. R. and NAPIER, D. H. Formation of carbon and related materials in diffusion flames, *Fifth Symposium (International) on Combustion*, pp. 303–316, Reinhold, New York (1955).
 115. WOLFHARD, H. G. and PARKER, W. G. Influence of sulphur on carbon formation in diffusion flames, *Fuel*, **29**, 235–240 (1950).
 116. GARNER, F. A., LONG, R., GRAHAM, A. J. and BADAKSHAN, A. The effect of certain halogenated methanes on premixed and diffusion flames, *Sixth*

- Symposium (International) on Combustion*, pp. 802–806, Reinhold, New York (1957).
117. IBIRICU, M. M. and GAYDON, A. G. Spectroscopic studies of the effect of inhibitors on counterflow diffusion flames, *Comb. Flame*, **8**, 51–62 (1964).
 118. RAY, S. K. and LONG, R. Polycyclic aromatic hydrocarbons from diffusion flames and diesel engine combustion, *Comb. Flame*, **8**, 139–151 (1964).
 119. CHAKRABORTY, B. B. and LONG, R. The formation of soot and polycyclic aromatic hydrocarbons in diffusion flames, III—Effect of additions of oxygen to ethylene and ethane respectively as fuels, *Comb. Flame*, **12**, 469–476 (1968).
 120. BACK, M. H. and MARTIN, R. The thermal reactions of ethylene at 500°C in the presence and absence of small quantities of oxygen, *Int. J. Chem. Kinetics*, **11**, 757–774 (1979).
 121. WOLFHARD, H. G. and PARKER, W. G. A new technique for the spectroscopic examination of flames at normal pressures, *Proc. Phys. Soc. A*, **62**, 722–730 (1950).
 122. WOLFHARD, H. G. and PARKER, W. G. A spectroscopic investigation into the structure of diffusion flames, *Proc. Phys. Soc. A*, **65**, 2–19 (1952).
 123. MELVIN, A., MOSS, J. B. and CLARKE, J. F. The structure of a reaction-broadened diffusion flame, *Combust. Sci. Tech.*, **4**, 17–30 (1971).
 124. LAUD, B. B. and GAYDON, A. G. Absorption spectra of ethylene diffusion flames, *Comb. Flame*, **16**, 55–60 (1971).
 125. HAYNES, B. S. and WAGNER, H. GG. Sooting structure in a laminar diffusion flame, *Ber. Bunsenges Phys. Chem.*, **84**, 499–506 (1980).
 126. KUHN, G. and TANKIN, R. S. Spectroscopic measurements to determine temperature and carbon particle size in an absorbing propane diffusion flame, *J. Quant. Spectrosc. Radiat. Transfer*, **8**, 1281–1292 (1968).
 127. KUNUGI, M. and JINNO, H. Determination of size and concentration of soot particles in diffusion flames by a light scattering technique, *Eleventh Symposium (International) on Combustion*, pp. 257–266, The Combustion Institute, Pittsburgh (1967).
 128. D'ALESSIO, A., DI LORENZO, A., BERETTA, F. and VENITOZZI, C. Optical and chemical investigation in fuel-rich methane–oxygen premixed flames at atmospheric pressure, *Fourteenth Symposium (International) on Combustion*, pp. 941–953, The Combustion Institute, Pittsburgh (1973).
 129. D'ALESSIO, A., DI LORENZO, A., BORGHESE, A., BERETTA, F. and MASI, S. Study of the soot nucleation zone of rich methane–oxygen flames, *Sixteenth Symposium (International) on Combustion*, pp. 695–708, The Combustion Institute, Pittsburgh (1977).
 130. SPENGLER, G. and KERN, J. Untersuchungen an Diffusionsflammen—Konzentrationsverteilung in einer Hexan—Diffusionsflamme, *Brennst. Chemie*, **50**, 321–324 (1969).
 131. KENT, J. H., JANDER, H. and WAGNER, H. GG. Soot formation in a laminar diffusion flame, *Eighteenth Symposium (International) on Combustion*, The Combustion Institute (to appear).
 132. MELVIN, A., MOSS, J. B. and CLARKE, J. F. Streamline deflection by a diffusion flame, *Combust. Sci. Tech.*, **6**, 135–142 (1972).
 133. FENIMORE, C. P. and JONES, G. W. Coagulation of soot to smoke in hydrocarbon flames, *Comb. Flame*, **13**, 303–310 (1969).
 134. JAGODA, I. J., PRADO, G. and LAHAYE, J. An experimental investigation into soot formation and distribution in polymer diffusion flames, *Comb. Flame*, **37**, 261–274 (1980).
 135. PAGNI, P. J. and BARD, S. Particulate volume fractions in diffusion flames, *Seventeenth Symposium (International) on Combustion*, pp. 1017–1028, The Combustion Institute, Pittsburgh (1979).
 136. SMITH, S. R. and GORDON, A. S. Studies of diffusion flames. I. The methane diffusion flame, *J. Phys. Chem.*, **60**, 759–763 (1956).
 137. GORDON, A. S., SMITH, S. R. and McNESBY, J. R. Study of the chemistry of diffusion flames, *Seventeenth Symposium (International) on Combustion*, pp. 317–324, Butterworths, London (1959).
 138. TSUJI, H. and YAMAOKA, I. The structure of counterflow diffusion flames in the forward stagnation region of a porous cylinder, *Twelfth Symposium (International) on Combustion*, pp. 997–1006, The Combustion Institute, Pittsburgh (1969).
 139. GOLLAHALLI, S. R. and BRZUSTOWSKI, T. A. Experimental studies of flame structure in the wake of a burning droplet, *Fourteenth Symposium (International) on Combustion*, pp. 1333–1344, The Combustion Institute, Pittsburgh (1973).
 140. KERN, J. and SPENGLER, G. Untersuchungen an Diffusionsflammen—Reaktionsprodukte in der Achse einer Hexan—Flame, *Erdöl Kohle—Erdgas—Petrochem.* **23**, 813–817 (1970).
 141. ALDRIDGE, J. W., PATEL, J. C. and WILLIAMS, A. The mechanism of combustion of droplets and spheres of liquid *n*-heptane, *Comb. Flame*, **17**, 139–148 (1971).
 142. ABDEL-KALIK, S. I., TAMARU, T. and EL-WAKIL, M. M. A chromatographic and interferometric study of the diffusion flame around a simulated fuel drop, *Fifteenth Symposium (International) on Combustion*, pp. 389–399, The Combustion Institute, Pittsburgh (1975).
 143. KENT, J. H. and WILLIAMS, F. A. Extinction of laminar diffusion flames for liquid fuels, *Fifteenth Symposium (International) on Combustion*, pp. 315–325, The Combustion Institute, Pittsburgh (1975).
 144. SMITH, S. R. and GORDON, A. S. Studies of diffusion flames. II. Diffusion flames of some simple alcohols, *J. Phys. Chem.*, **60**, 1059–1062 (1956).
 145. SMITH, S. R., GORDON, A. S. and HUNT, M. H. Studies of diffusion flames. III. The diffusion flames of the butanols, *J. Phys. Chem.*, **61**, 553–558 (1957).
 146. SMITH, S. R. and GORDON, A. S. Precombustion reactions in hydrocarbon diffusion flames: the paraffin candle flame, *J. Chem. Phys.*, **22**, 1150–1151 (1954).
 147. COLE, D. J. and MINKOFF, G. J. Carbon formation in diffusion flames and the role of acetylene, *Proc. Roy. Soc. A*, **239**, 280–287 (1957).
 148. MELVIN, A. and MOSS, J. B. Structure in methane–oxygen diffusion flames, *Fifteenth Symposium (International) on Combustion*, pp. 625–636, The Combustion Institute, Pittsburgh (1975).
 149. BECKER, H. A. and LIANG, D. Total emission of soot and thermal radiation by free turbulent diffusion flames, Paper presented at the Seventeenth Symposium (International) on Combustion, Leeds, England, August (1978).
 150. PRADO, G. P., LEE, M. L., HITES, R. A., HOULT, D. P. and HOWARD, J. B. Soot and hydrocarbon formation in a turbulent diffusion flame, *Sixteenth Symposium (International) on Combustion*, pp. 649–661, The Combustion Institute, Pittsburgh (1977).
 151. DALZELL, W. H., WILLIAMS, G. C. and HOTTEL, H. C. A light scattering method for soot concentration measurements, *Comb. Flame*, **14**, 161–170 (1970).
 152. MARAVAL, L. Characteristics of soot collected in industrial diffusion flames, *Combust. Sci. Tech.*, **5**, 207–212 (1972).
 153. HEIN, K. Recent results on the formation and combustion of soot in turbulent fuel oil and gas flames, *Combust. Sci. Tech.*, **5**, 195–206 (1972).
 154. MAGNUSEN, B. F. An investigation into the behaviour of soot in a turbulent free jet C_2H_2 -flame, *Fifteenth Symposium (International) on Combustion*, pp. 1415–1425, The Combustion Institute, Pittsburgh (1975).

155. BECKER, H. A. and YAMAZAKI, S. Soot concentration field of turbulent propane/air diffusion flames, *Sixteenth Symposium (International) on Combustion*, pp. 681-691, The Combustion Institute, Pittsburgh (1977).
156. MAGNUSEN, B. F., HJERTAGER, B. H., OLSEN, J. G. and BHADURI, D. Effects of turbulent structure and local concentrations on soot formation and combustion in C_2H_2 diffusion flames, *Seventeenth Symposium (International) on Combustion*, pp. 1383-1393, The Combustion Institute, Pittsburgh (1979).
157. JONES, A. R. Scattering of electromagnetic radiation in particulate-laden fluids, *Prog. Energy Combust. Sci.* **5**, 73-96 (1979).
158. JONES, A. R. Electromagnetic wave scattering by assemblies of particles in the Rayleigh approximation, *Proc. Roy. Soc. Lond. A*, **366**, 111-127 (1979).
159. MAGNUSEN, B. F. and HJERTAGER, B. H. On mathematical modeling of turbulent combustion with special emphasis on soot formation and combustion, *Sixteenth Symposium (International) on Combustion*, pp. 719-729, The Combustion Institute, Pittsburgh (1977).
160. MAGNUSEN, B. F. The rate of combustion of soot in turbulent flames, *Thirteenth Symposium (International) on Combustion*, pp. 869-877, The Combustion Institute, Pittsburgh (1971).
161. BEER, J. M. and CHIGIER, N. A. *Combustion Aerodynamics*, Applied Science Publishers, London (1972).
162. WILLIAMS, A. The mechanism of combustion of droplets and sprays of liquid fuels, *Oxidation and Combustion Revs.* **3**, 1-45 (1968).
163. WILLIAMS, A. Combustion of droplets of liquid fuels: a review, *Comb. Flame*, **21**, 1-31 (1973).
164. WILLIAMS, A. *Combustion of Sprays of Liquid Fuels*, Eleck, London (1976).
165. WILLIAMS, A. Fundamentals of oil combustion, *Prog. Energy Combust. Sci.* **2**, 167-179 (1976).
166. AGOSTON, G. A., WISE, H. and ROSSER, W. A. Dynamic factors affecting the combustion of liquid spheres, *Sixth Symposium (International) on Combustion*, pp. 708-717, Reinhold, New York (1957).
167. SJÖGREN, A. Soot formation by combustion of an atomized liquid fuel, *Fourteenth Symposium (International) on Combustion*, pp. 919-927, The Combustion Institute, Pittsburgh (1973).
168. GOLLAHALLI, S. and BRZUSTOWSKI, T. A. The effect of pressure on the flame structure in the wake of a burning hydrocarbon droplet, *Fifteenth Symposium (International) on Combustion*, pp. 409-417, The Combustion Institute, Pittsburgh (1975).
169. GOLLAHALLI, S. R. and BRZUSTOWSKI, T. A. Flame length in the wake of a burning hydrocarbon drop, *Comb. Flame*, **22**, 313-322 (1974).
170. KADOTA, T., HIROYASU, H. and FARAZANDEHMER, A. Soot formation by combustion of a fuel droplet in high pressure gaseous environments, *Comb. Flame*, **29**, 67-75 (1977).
171. CHIGIER, N. A. The atomization and burning of liquid fuel sprays, *Prog. Energy Combust. Sci.* **2**, 97-114 (1976).
172. ONUMA, Y. and OGASAWARA, M. Studies on the structure of a spray combustion flame, *Fifteenth Symposium (International) on Combustion*, pp. 453-465, The Combustion Institute, Pittsburgh (1975).
173. STYLES, A. C. and CHIGIER, N. A. Combustion of air blast atomized spray flames, *Sixteenth Symposium (International) on Combustion*, pp. 619-630, The Combustion Institute, Pittsburgh (1977).
174. JANOTA, M. S., CROOKES, R. J., DAEI, S. J., NAZHA, M. A. A. and SODHA, M. Soot and gaseous pollutant formation in a burning fuel spray in relation to pressure and air/fuel ratio, *J. Inst. Fuel*, **50**, 10-13 (1977).
175. ONUMA, Y., OGASAWARA, M. and INOUE, T. Further experiments on the structure of a spray combustion flame, *Sixteenth Symposium (International) on Combustion*, pp. 561-567, The Combustion Institute, Pittsburgh (1977).
176. KHALIL, E. E. and WHITELAW, J. H. Aerodynamic and thermodynamic characteristics of kerosene-spray flames, *Sixteenth Symposium (International) on Combustion*, pp. 569-576, The Combustion Institute, Pittsburgh (1977).
177. KOMIYAMA, K., FLAGAN, R. C. and HEYWOOD, J. B. The influence of droplet evaporation on fuel-air mixing rate in a burner, *Sixteenth Symposium (International) on Combustion*, pp. 549-560, The Combustion Institute, Pittsburgh (1977).
178. BREEN, B. P. Combustion in large boilers: design and operating effects on efficiency and emissions, *Sixteenth Symposium (International) on Combustion*, pp. 19-35, The Combustion Institute, Pittsburgh (1977).
179. MEIER ZU KÖCKER, H. Russ- und Stickoxidbildung in Flammen eines Ölvergasungsbrenners, *Brennst.-Wärme-Kraft*, **28**, 394-399 (1976).
180. MEIER ZU KÖCKER, H. Ausbrand und Russemission von Schwerölfämmen bei drallfreier Zerstäubung mit Luft, *Brennst.-Wärme Kraft*, **29**, 73-78 (1977).
181. MEIER ZU KÖCKER, H. Kinetics of soot formation: investigations into the mechanism of soot formation in hydrocarbon diffusion flames, *Comb. Sci. Tech.* **5**, 219-224 (1972).
182. GODRIDGE, A. M. and HORSLEY, M. E. Carbon formation in large residual-fuel-oil-fired burners, *J. Inst. Fuel*, **46**, 599-606 (1971).
183. GILLS, B. G. Production and emission of solids, SO_x and NO_x from liquid fuel flames, *J. Inst. Fuel*, **46**, 71-76 (1973).
184. LEFEBVRE, A. H. Progress and problems in gas-turbine combustion, *Tenth Symposium (International) on Combustion*, pp. 1129-1137, The Combustion Institute, Pittsburgh (1965).
185. LEFEBVRE, A. H. Pollution control in continuous combustion engines, *Fifteenth Symposium (International) on Combustion*, pp. 1169-1180, The Combustion Institute, Pittsburgh (1975).
186. MELLOR, A. M. Gas turbine engine pollution, *Prog. Energy Combust. Sci.* **1**, 111-133 (1976).
187. TOONE, B. A review of aero engine smoke emission, *Combustion in Advanced Gas Turbine Systems*, (editor SMITH, I. E.), pp. 271-294, Pergamon, London (1968).
188. COOPER, P. W., KAMO, R., MAREK, C. J. and SOLBRIG, C. W. Recirculation and fuel-air mixing as related to oil-burner design, American Petroleum Institute Publication No. 1723 (1964).
189. MEIER, J. G. and VOLLEN, B. L. The design of an integrated burner-boiler system using flue-gas recirculation, *Sixteenth Symposium (International) on Combustion*, pp. 63-76, The Combustion Institute, Pittsburgh (1977).
190. SCHIRMER, R. M. Effect of fuel composition on particulate emissions from gas turbine engines, *Emissions from Continuous Combustion Systems*, (editors CORNELIUS, W. and AGNEW, W. G.), pp. 189-210, Plenum Press, New York (1972).
191. FRISWELL, N. J. The influence of fuel composition on smoke emission from gas-turbine-type combustors: effect of combustor design and operating conditions, *Combust. Sci. Tech.* **19**, 119-127 (1979).
192. DODDS, W. J., PETERS, J. E., COLKET, M. B. and MELLOR, A. M. Preliminary study of smoke formed in the combustion of various jet fuels, *J. Energy*, **1**, 115-120 (1977).
193. DRYER, F. L. Water addition to practical combustion systems—concept and application, *Sixteenth Symposium (International) on Combustion*, pp. 279-295, The Combustion Institute, Pittsburgh (1977).
194. JACQUES, M. T., JORDAN, J. B., WILLIAMS, A. and HADLEY-COATES, A. The combustion of water-in-oil emulsions and the influence of asphaltene content,

- Sixteenth Symposium (International) on Combustion, pp. 307–319, The Combustion Institute, Pittsburgh (1977).
195. SJÖGREN, A. Burning of water-in-oil emulsions, Sixteenth Symposium (International) on Combustion, pp. 297–305, The Combustion Institute, Pittsburgh (1977).
 196. HENEIN, N. A. Analysis of pollutant formation and control and fuel economy in diesel engines, *Prog. Energy Combust. Sci.* **1**, 165–207 (1976).
 197. DUGGAL, V. K., PRIEDE, T. and KHAN, I. M. A study of pollutant formation within the combustion space of a diesel engine, S.A.E. Technical Paper 780227 (1978).
 198. GREEVES, G. and MEEHAN, J. O. Measurements of instantaneous soot concentration in a diesel combustion chamber, Paper C88/75 presented to Institution of Mechanical Engineers Conference on Combustion in Engines, Cranfield 1975.
 199. KHAN, I. M. Formation and combustion of carbon in a diesel engine, *Inst. Mech. Eng. Proc.* Vol. 184, Pt. 35, 36–43 (1969).
 200. KADOTA, T., HENEIN, N. A. and LEE, D. U. A new approach to study the formation of soot particulates in diesel sprays, Paper presented to the Spring Meeting, Central States Section of the Combustion Institute, March (1980).
 201. KADOTA, T., HENEIN, N. A. and LEE, D. U. Effect of fuel properties on the time resolved soot particulates in a simulated diesel spray, Paper presented to the Fifth International Automotive Propulsion Systems Symposium, April (1980).
 202. KHAN, I. M., WANG, C. H. T. and LANGRIDGE, B. E. Coagulation and combustion of soot particles in diesel engines, *Comb. Flame*, **17**, 409–419 (1971).
 203. KHAN, I. M., GREEVES, G. and WANG, C. H. T. Factors affecting smoke and gaseous emissions from direct injection engines and a method of calculation, S.A.E. Paper 730169 (1973).
 204. KHAN, I. M. and GREEVES, G. A method for calculating the formation and combustion of soot in diesel engines, *Heat Transfer in Flames*, (editors AFGAN, N. H. and BEER, J. M.), pp. 389–404, Scripta Book Co., Washington, D.C. (1974).
 205. HILBURGER, W. *Diplomarbeit*, Stuttgart (1976).
 206. LARESGOITI, A., LOOS, A. C. and SPRINGER, G. S. Particulate and smoke emission from a light duty diesel engine, *Environ. Sci. Tech.* **11**, 973–978 (1977).
 207. FREY, J. W. and CORN, M. Physical and chemical characteristics of particulates in a diesel exhaust, *J. Am. Indus. Hygiene Assoc.* Sept.–Oct (1967).
 208. DOLAN, D. F., KITTELSON, D. B. and WHITBY, K. T. Measurement of diesel exhaust particle size distribution, Paper presented at A.S.M.E. Winter Meeting, Houston (1975).
 209. DUGGAL, V. K. and HOWARTH, J. S. A preliminary study of the structure of diesel smoke, *J. Inst. Fuel*, **48**, 38–44 (1975).
 210. VUK, C. T., JONES, M. A. and JOHNSON, J. H. The measurement and analysis of the physical character of diesel particulate emissions, S.A.E. Technical Paper 760131 (1976).
 211. LAURENDEAU, N. M. Heterogeneous kinetics of coal char gasification and combustion, *Prog. Energy Combust. Sci.* **4**, 221–270 (1978).
 212. MARSH, H. How Oxygen molecules gasify carbons, *Oxygen in the Metal and Gaseous Fuel Industries*, pp. 133–174, Special Publication No. 32, The Chemical Society, London (1978).
 213. MULCAHY, M. F. R. The combustion of carbon, *Oxygen in the Metal and Gaseous Fuel Industries*, pp. 175–208, Special Publication No. 32, The Chemical Society, London (1978).
 214. LEWIS, P. F. and SIMONS, G. A. Char gasification: Part II. Oxidation results, *Combust. Sci. Tech.* **20**, 117–124 (1978).
 215. SMITH, I. W. The combustion rates of pulverized coal char particles, Paper presented to Conference on Coal Combustion Technology and Emission Control, Pasadena, February (1979).
 216. RADCLIFFE, S. W. and APPLETON, J. P. Soot oxidation rates in gas turbine engines, *Combust. Sci. Tech.* **4**, 171–175 (1971).
 217. PARK, C. and APPLETON, J. P. Shock-tube measurements of soot oxidation rates, *Comb. Flame*, **20**, 369–379 (1973).
 218. NAGLE, J. and STRICKLAND-CONSTABLE, R. F. Oxidation of carbon between 1000–2000°C, pp. 154–164, *Proceedings of the Fifth Conference on Carbon*, pp. 154–164, Pergamon Press, London (1962).
 219. WALLS, J. R. and STRICKLAND-CONSTABLE, R. F. Oxidation of carbon between 1000–2400°C, *Carbon*, **1**, 33–38 (1964).
 220. ROSNER, D. E. and ALLENDORF, H. D. Comparative studies of the attack of pyrolytic and isotropic graphite by atomic and molecular oxygen at high temperatures, *A.I.A.A. J.* **6**, 650–654 (1968).
 221. THOMAS, J. M. Microscopic studies of graphite oxidation, *Chemistry and Physics of Carbon*, (editor WALKER, P. L.), Vol. 1, pp. 121–202 (1965).
 222. FENIMORE, C. P. and JONES, G. W. Oxidation of soot by hydroxyl radicals, *J. Phys. Chem.* **71**, 593–597 (1967).
 223. TESNER, P. A. and TSIBULEVSKY, A. M. Gasification of dispersed carbon in hydrocarbon diffusion flames. III. Flames of acetylene–hydrogen and acetylene–water vapor mixtures, *Combustion, Explosion and Shock-waves*, **3**, 163–167 (1967).
 224. FEUGIER, A. Soot oxidation in laminar hydrocarbon flames, *Comb. Flame*, **19**, 249–256 (1972).
 225. ROSNER, D. E. and ALLENDORF, H. D. Kinetics of the attack of refractory materials by dissociated gases, *Heterogeneous Kinetics at Elevated Temperatures*, (editors BELTON, G. R. and WORRELL, W. L.), pp. 231–251, Plenum Press, New York (1970).
 226. WRIGHT, F. J. The oxidation of soot by O atoms, Sixteenth Symposium (International) on Combustion, pp. 1449–1460, The Combustion Institute, Pittsburgh (1975).
 227. MULCAHY, M. F. R. and YOUNG, B. C. The reaction of hydroxyl radicals with carbon at 298 K, *Carbon*, **13**, 115–124 (1975).
 228. ATES, H. F. and PAGE, F. M. The oxidation of soot particles in fuel-rich gases, *Deuxième Symposium Européen sur la Combustion*, pp. 380–384, The Combustion Institute (1975).
 229. PAGE, F. M. and ATES, H. F. Oxidation of soot in fuel-rich flames, *Evaporation-Combustion of Fuels*, (editor ZUNG, J. T.), pp. 190–197, A.C.S. Advances in Chemistry Series, No. 166, A.C.S., Washington, D.C. (1978).
 230. KNEWSTUBB, P. F. and SUGDEN, T. M. Mass spectrometry of the ions present in hydrocarbon flames, *Seventh Symposium (International) on Combustion*, pp. 247–253, Butterworths, London (1959).
 231. CALCOTE, H. F. Ions in flames, *Ion-Molecule Reactions*, (editor FRANKLIN, J. L.), Vol. 2, pp. 673–706, Plenum Press, New York (1972).
 232. HAYHURST, A. N. and KITTELSON, D. B. The positive and negative ions in oxy-acetylene flames, *Comb. Flame*, **31**, 37–51 (1978).
 233. TSE, R. S., MICHAUD, P. and DELFAU, J. L. Initial pyrolysis ions in hydrocarbon flames, *Nature*, **272**, 153–155 (1978).
 234. DELFAU, J. L., MICHAUD, P. and BARASSIN, A. Formation of small and large positive ions in rich and sooting low-pressure ethylene and acetylene premixed flames, *Combust. Sci. Tech.* **20**, 165–177 (1979).
 235. GOODINGS, J. M., BOHME, D. K. and NG, C.-W. Detailed ion chemistry in methane oxygen flames. II. Negative ions, *Comb. Flame*, **36**, 45–62 (1979).
 236. GOODINGS, J. M., BOHME, D. K. and NG, C.-W. Detailed

- ion chemistry in methane-oxygen flames. I. Positive ions, *Comb. Flame*, **36**, 27–43 (1979).
237. BOHME, D. K. Chemical ionization in flames, *Kinetics of Ion-Molecule Reactions*, (editor AUSLOOS, P.), pp. 323–343, Plenum Press, New York (1978).
 238. SINGER, J. M. and GRUMER, J. Carbon formation in very rich hydrocarbon-air flames—I. Studies of chemical content, temperature, ionization and particulate matter, *Seventh Symposium (International) on Combustion*, pp. 559–569, Butterworths, London (1959).
 239. NAKAMURA, J. Effect of the electric field upon the spectra of the hydrocarbon diffusion flame, *Comb. Flame*, **3**, 277–284 (1959).
 240. WERSBORG, B. L., YEUNG, A. C. and HOWARD, J. B. Concentration and mass distribution of charged species in sooting flames, *Fifteenth Symposium (International) on Combustion*, pp. 1439–1448, The Combustion Institute, Pittsburgh (1975).
 241. HOMANN, K. H. Charged particles in sooting flames. I. Determination of mass distributions and number densities in $C_2H_2-O_2$ flames, *Ber. Bunsenges. Phys. Chem.* **83**, 738–745 (1979).
 242. PRADO, G. P. and HOWARD, J. B. Formation of large ions in sooting flames, *Evaporation-Combustion of Fuels*, (editor ZUNG, J. T.), pp. 153–166, Advances in Chemistry Series No. 166, Am. Chem. Soc. Washington, D.C. (1978).
 243. BARTHOLOME, E. and SACHSSE, H. Katalytische Erscheinungen an Aerosolen, *Z. Elektrochem.* **53**, 326–331 (1949).
 244. BOWSER, R. J. and WEINBERG, F. J. Electrons and the emission of soot from flames, *Nature*, **249**, 339–341 (1974).
 245. HAYNES, B. S., JANDER, H., MÄTZING, H. and WAGNER, H. GG. The influence of various metals on carbon formation in premixed flames, *Comb. Flame*, **40**, 101–103 (1981).
 246. PLACE, E. R. and WEINBERG, F. J. Electrical control of flame carbon, *Proc. Roy. Soc. A*, **289**, 193–205 (1965).
 247. PLACE, E. R. and WEINBERG, F. J. The nucleation of flame carbon by ions and the effect of electric fields, *Eleventh Symposium (International) on Combustion*, pp. 245–255, The Combustion Institute, Pittsburgh (1967).
 248. WEINBERG, F. J. Electrical aspects of aerosol formation and control, *Proc. Roy. Soc. A*, **307**, 195–208 (1968).
 249. BOOTHMAN, D., LAWTON, J., MELINEK, S. J. and WEINBERG, F. J. Rates of ion generation in flames, *Twelfth Symposium (International) on Combustion*, pp. 969–978, The Combustion Institute, Pittsburgh (1969).
 250. MAYO, P. J. and WEINBERG, F. J. On the size, charge and number-rate of formation of carbon particles in flames subjected to electric fields, *Proc. Roy. Soc. A*, **319**, 351–371 (1970).
 251. WEINBERG, F. J. Smokes, droplets, flames and electric fields, *Symposium of the Faraday Society*, **7**, 120–132 (1973).
 252. HARDESTY, D. R. and WEINBERG, F. J. Electrical control of particulate pollutants from flames, *Fourteenth Symposium (International) on Combustion*, pp. 907–918, The Combustion Institute, Pittsburgh (1973).
 253. HOWARD, J. B. On the mechanism of carbon formation in flames, *Twelfth Symposium (International) on Combustion*, pp. 877–887, The Combustion Institute, Pittsburgh (1969).
 254. BALL, R. T. and HOWARD, J. B. Electric charge of carbon particles in flames, *Thirteenth Symposium (International) on Combustion*, pp. 353–362, The Combustion Institute, Pittsburgh (1971).
 255. SALOOJA, K. C. Burner fuel additives, *J. Inst. Fuel*, **45**, 37–42 (1972).
 256. FRISWELL, N. J. Emissions from gas-turbine-type combustors, *Emissions from Continuous Combustion Systems*, (editors CORNELIUS, W. and AGNEW, W. G.), pp. 141–182, Plenum Press, New York (1972).
 257. GIOVANNI, D. V., PAGNI, P. J., SAWYER, R. F. and HUGHES, L. Manganese effects on emissions from a model gas turbine combustor, *Combust. Sci. Tech.* **6**, 107–114 (1972).
 258. ADDECOTT, K. S. B. and NUTT, C. W. Mechanism of smoke reduction by metal compounds, *Preprints, Amer. Chem. Soc., Div. Pet. Chem.* **14** (4), A69–71, Sept (1969).
 259. SALOOJA, K. C. Combustion control by novel catalytic means, *Nature*, **240**, 350–351 (1972).
 260. SALOOJA, K. C. Carbon formation in flames: control by novel catalytic means, *Combustion Institute European Symposium*, (editor WEINBERG, F. J.), pp. 400–405, Academic Press, London (1973).
 261. BULEWICZ, E. M., EVANS, D. G. and PADLEY, P. J. Effect of metallic additives on soot formation processes in flames, *Fifteenth Symposium (International) on Combustion*, pp. 1461–1470, The Combustion Institute, Pittsburgh (1975).
 262. COTTON, D. H., FRISWELL, N. J. and JENKINS, D. R. The suppression of soot emission from flames by metal additives, *Comb. Flame*, **17**, 87–98 (1971).
 263. FEUGIER, A. The effect of alkali metals on the amount of soot emitted by premixed hydrocarbon flames, *Combustion Institute European Symposium*, (editor WEINBERG, F. J.), pp. 406–411, Academic Press, London (1973).
 264. FEUGIER, A. Effect of metal additives on the amount of soot emitted by premixed hydrocarbon flames, *Deuxième Symposium Européen sur la Combustion*, pp. 362–367, The Combustion Institute, Orleans (1975).
 265. HOMANN, K. H. and WAGNER, H. GG. Untersuchung des Reaktionsablaufs in fetten Kohlenwasserstoff-Sauerstoff-Flammen. III. Versuche an russenden Acetylen-Sauerstoff-Flammen bei niedrigem Druck, *Ber. Bunsenges. Phys. Chem.* **69**, 20–35 (1965).
 266. HOMANN, K. H. and WAGNER, H. GG. Some new aspects of the mechanism of carbon formation in premixed flames, *Eleventh Symposium (International) on Combustion*, pp. 371–379, The Combustion Institute, Pittsburgh (1967).
 267. BACK, M. H. Mechanism of the pyrolysis of acetylene, *Can. J. Chem.* **49**, 2199–2204 (1971).
 268. TANZAWA, T. and GARDINER, W. C. Thermal decomposition of acetylene, *Seventeenth Symposium (International) on Combustion*, pp. 563–573, The Combustion Institute, Pittsburgh (1979).
 269. ROTH, P. and JUST, TH. Messungen zum homogenen thermischen Zerfall von Äthylen, *Ber. Bunsenges. Phys. Chem.* **77**, 1114–1118 (1973).
 270. HOU, K. C. and PALMER, H. B. The kinetics of thermal decomposition of benzene in a flow system. *J. Phys. Chem.* **69**, 863–868 (1965).
 271. MARYASIN, I. L. and NABUTOVSKII, Z. A. An investigation of the kinetics of the pyrolysis of benzene in shock waves, *Kinetics and Catalysis*, **10**, 800–806 (1969).
 272. MARYASIN, I. L. and NABUTOVSKII, Z. A. Investigation of the kinetics of carbon black formation during the thermal pyrolysis of benzene and acetylene in a shock wave, *Kinetics and Catalysis*, **14**, 139–144 (1973).
 273. ASABA, T. and FUJII, N. Shock-tube study of high-temperature pyrolysis of benzene, *Thirteenth Symposium (International) on Combustion*, pp. 155–164, The Combustion Institute, Pittsburgh (1971).
 274. BROOKS, C. T., PEACOCK, S. J. and REUBEN, B. G. Pyrolysis of benzene, *J.C.S. Faraday Trans. I*, **75**, 652–662 (1979).
 275. BUCKENDAHL, W. *Diplomarbeit*, Göttingen (1970).
 276. GECK, C. C. *Diplomarbeit*, Göttingen (1975).
 277. FUSSEY, D. E., GOSLING, A. J. and LAMPARD, D. A shock-tube study of induction times in the formation of

- carbon particles by pyrolysis of the C₂ hydrocarbons, *Comb. Flame*, **32**, 181–192 (1978).
278. HOOKER, W. J. Shock tube studies of acetylene decomposition, *Seventh Symposium (International) on Combustion*, pp. 949–952, Butterworths, London (1959).
279. GOSLING, A. J., LAMPARD, D. and FUSSEY, D. E. A shock-tube study of the formation of carbon particles during the pyrolysis of hydrocarbons, *Combustion Institute European Symposium*, (editor WEINBERG, F. J.), pp. 388–393, Academic Press, London (1973).
280. WANG, T.-S., MATULA, R. A. and FARMER, R. C. Soot formation from toluene, Paper presented at the 1980 Spring Meeting of the Central States Section of the Combustion Institute, March (1980).
281. BRADLEY, J. N. A general mechanism for the high-temperature pyrolysis of alkanes. The pyrolysis of isobutane, *Proc. Roy. Soc. A*, **337**, 199–216 (1974).
282. BRADLEY, J. N. and WEST, K. O. Single pulse shock tube studies of hydrocarbon pyrolysis, Part 5—pyrolysis of neopentane, *J.C.S. Faraday I*, **72**, 8–19 (1976).
283. BRADLEY, J. N. and KISTIAKOWSKY, G. B. Shock-wave studies by mass spectrometry. II. Polymerization and oxidation of acetylene, *J. Chem. Phys.*, **35**, 264–270 (1961).
284. GAY, I. D., KISTIAKOWSKY, G. B., MICHAEL, J. V. and NIKI, H. Thermal decomposition of acetylene in shock waves, *J. Chem. Phys.*, **43**, 1720–1726 (1965).
285. MARYASIN, I. L. and NABUTOVSKII, Z. A. Investigation of the kinetics of the pyrolysis of acetylene in a shock wave, *Kinetics and Catalysis*, **11**, 706–711 (1970).
286. CUNDALL, R. B., FUSSEY, D. E., HARRISON, A. J. and LAMPARD, D. An investigation of the precursors to carbon particles during the pyrolysis of acetylene and ethylene, Paper presented to the Eleventh International Shock-tube Symposium, Seattle, July (1977).
287. CUNDALL, R. B., FUSSEY, D. E., HARRISON, A. J. and LAMPARD, D. Shock tube studies of the high temperature pyrolysis of acetylene and ethylene, *J.C.S. Faraday Trans. I*, **74**, 1403–1409 (1978).
288. CUNDALL, R. B., FUSSEY, D. E., HARRISON, A. J. and LAMPARD, D. High temperature pyrolysis of ethane and propylene, *J.C.S. Faraday Trans. I*, **75**, 1390–1394 (1979).
289. BOWSER, R. J. and WEINBERG, F. J. Chemi-ionization during pyrolysis, *Comb. Flame*, **27**, 21–32 (1976).
290. SMITH, R. D. A direct mass-spectrometric study of the mechanism of toluene pyrolysis at high temperatures, *J. Phys. Chem.*, **83**, 1553–1563 (1979).
291. SMITH, R. D. Formation of radicals and complex organic compounds by high-temperature pyrolysis: the pyrolysis of toluene, *Combust. Flame*, **35**, 179–190 (1979).
292. GRAHAM, S. C., HOMER, J. B. and ROSENFIELD, J. L. J. The formation and coagulation of soot aerosols generated by the pyrolysis of aromatic hydrocarbons, *Proc. Roy. Soc. Lond. A*, **344**, 259–285 (1975).
293. GRAHAM, S. C., HOMER, J. B. and ROSENFIELD, J. L. J. The formation and coagulation of soot aerosols, *Modern Developments in Shock-Tube Research: Proceedings of the Tenth International Shock Tube Symposium*, (editor KAMIMOTO, G.), pp. 621–631 (1975).
294. GRAHAM, S. C., HOMER, J. B. and ROSENFIELD, J. L. J. Shock-tube study of the formation and growth of soot particles, *Deuxième Symposium Européen sur la Combustion*, pp. 374–379, The Combustion Institute, Lyons (1975).
295. GRAHAM, S. C. The formation and coagulation of soot aerosols, Presented at Euromech 85, Symposium on Processes in High Temperature Gases, Aachen, March (1977).
296. GRAHAM, S. C. The collisional growth of soot particles at high temperatures, *Sixteenth Symposium (International) on Combustion*, pp. 663–669, The Combustion Institute, Pittsburgh (1977).
297. HOWARD, J. B., WERSBORG, B. L. and WILLIAMS, G. C. Coagulation of carbon particles in premixed flames, *Symp. Faraday Soc.*, **7**, 109–119 (1973).
298. WERSBORG, B. L., HOWARD, J. B. and WILLIAMS, G. C. Physical mechanisms in carbon formation in flames, *Fourteenth Symposium (International) on Combustion*, pp. 929–940, The Combustion Institute, Pittsburgh (1973).
299. WERSBORG, B. L., FOX, L. K. and HOWARD, J. B. Soot concentration and absorption coefficient in a low pressure flame, *Comb. Flame*, **24**, 1–10 (1975).
300. BITTNER, J. D. Formation of soot and polycyclic aromatic hydrocarbons in combustion systems, *Proceedings of the Stationary Source Combustion Symposium; Vol. I, Fundamental Research*, EPA Report 600/2-76-152a (1976).
301. BITTNER, J. P. and HOWARD, J. B. Composition profiles and reaction mechanisms in a near-sooting premixed benzene/oxygen/argon flame, *Eighteenth Symposium (International) on Combustion* (to appear).
302. LONG, R. and TOMPKINS, E. E. Formation of polycyclic aromatic hydrocarbons in pre-mixed acetylene–oxygen flames, *Nature*, **213**, 1011–1012 (1967).
303. TOMPKINS, E. E. and LONG, R. The flux of polycyclic aromatic hydrocarbons and insoluble material in pre-mixed acetylene–oxygen flames, *Twelfth Symposium (International) on Combustion*, pp. 625–634, The Combustion Institute, Pittsburgh (1969).
304. CRITTENDEN, B. D. and LONG, R. Formation of polycyclic aromatics in rich, premixed acetylene and ethylene flames, *Comb. Flame*, **20**, 359–368 (1973).
305. CRITTENDEN, B. D. and LONG, R. The mechanisms of formation of polynuclear aromatic compounds in combustion systems, *Carcinog.–Compr. Surv.*, **1**, 209–223 (1976).
306. BONNE, U. and HOMANN, K. H. Die Zusammensetzung von Russ aus Acetylen-Sauerstoff-Flammen Kurznachrichten der Akademie der Wissenschaften in Göttingen, April (1965).
307. BONNE, U., HOMANN, K. H. and WAGNER, H. GG. Carbon formation in premixed flames, *Tenth Symposium (International) on Combustion*, pp. 502–512, The Combustion Institute, Pittsburgh (1965).
308. HOMANN, K. H. and WAGNER, H. GG. Chemistry of carbon formation in flames, *Proc. Roy. Soc. A*, **307**, 141–152 (1968).
309. FENIMORE, C. P. and JONES, G. W. Comparative yields of soot from premixed hydrocarbon flames, *Comb. Flame*, **12**, 196–200 (1968).
310. BASTIDE, J. and HENRI-ROUSSEAU, O. Cycloadditions and cyclizations involving triple bonds, *Chemistry of the Carbon–Carbon Triple Bond*, Part 1, (editor PATAI, S.), pp. 447–473, John Wiley and Sons, New York (1978).
311. FUKS, R. and VIEHE, H. G. Cyclic compounds from acetylenes, *Chemistry of Acetylenes* (editor VIEHE, H. G.), pp. 425–595, Marcel Dekker, New York (1969).
312. AUSLOOS, P., LIAS, S. G. and SCALA, A. A. Investigating ion-molecule reactions by analyzing neutral products formed in the radiolysis and photo-ionization of hydrocarbons, *Ion-Molecule Reactions in the Gas-Phase*, (editor GOULD, R. F.), pp. 264–277, A.C.S. Advances in Chemistry Series No. 58, A.C.S., Washington, D.C. (1966).
313. WEXLER, S., LIFSHITZ, A. and QUATTROCHI, A. High press mass spectrometry with a m.e.v. proton beam–ethylene, acetylene and methylene, *Ion-Molecule Reactions in the Gas-Phase*, (editor AUSLOOS, P. J.), pp. 193–209, Advances in Chemistry Series 58, A.C.S., Washington, D.C. (1966).
314. MEISELS, G. G. Formation and reactions of ions in ethylene radiolysis, *Ion-Molecule Reactions in the Gas-Phase*, (editor AUSLOOS, P. J.), pp. 243–263, Advances in Chemistry Series 58, A.C.S., Washington, D.C. (1966).
315. LIFSHITZ, C. and MANDELBAUM, A. Mass-spectrometry

- of acetylenes, *Chemistry of the Carbon-Carbon Triple Bond*, Part 1, (editor PATAI, S.), pp. 157-198, John Wiley and Sons, New York (1978).
316. SMITH, D. and ADAMS, N. G. Ion-molecule reactions in low-temperature plasmas: formation of interstellar species, *Kinetics of Ion-Molecule Reactions*, (editor AUSLOOS, P.), pp. 345-376, Plenum Press, New York (1978).
317. TALROSE, V. L., VINOGRADOV, P. S. and LARIN, I. K. On the rapidity of ion-molecule reactions, *Gas-Phase Ion Chemistry*, (editor BOWERS, M. T.), Vol. 1, pp. 305-347, Academic Press, New York (1979).
318. BITTNER, J. D. and HOWARD, J. B. Role of aromatics in soot formation, *Alternative Hydrocarbon Fuels: Combustion and Chemical Kinetics*, (editors BOWMAN, C. T. and BIRKELAND, J.), pp. 335-358, Progress in Aeronautics and Astronautics, Vol. 62, American Institute of Aeronautics and Astronautics, New York (1978).
319. CALCOTE, H. F. Ionic mechanisms of soot formation in flames, Paper presented to 1978 Fall Technical Meeting, Eastern States Section, Combustion Institute, Miami, November (1978).
320. SENFTLEBEN, H. and BENEDICT, E. Über die optische Konstante und die Strahlungsgesetze der Kohle, *Ann. Physik.* **54**, 65-78 (1971).
321. RÖSSLER, F. and BEHRENS, H. Bestimmung des Absorptionkoeffizienten von Russsteinchen verschiedener Flammen, *Optik*, **6**, 145-151 (1950).
322. STULL, V. R. and PLASS, G. N. Emissivity of dispersed carbon particles, *J. Opt. Soc. Am.* **50**, 121-129 (1960).
323. MILLIKAN, R. C. Measurement of particle and gas temperatures in a slightly luminous premixed flame, *J. Opt. Soc. Am.* **51**, 535-542 (1961).
324. MILLIKAN, R. C. Optical properties of soot, *J. Opt. Soc. Am.* **51**, 698-699 (1961).
325. MILLIKAN, R. C. Sizes, optical properties, and temperatures of soot particles, *Temperature, Its Measurement and Control in Science and Industry*, Vol. 3, Part 2, pp. 497-507, Reinhold, New York (1962).
326. TAFT, E. A. and PHILIPP, H. R. Optical properties of graphite, *Phys. Rev.* **138A**, 197-202 (1965).
327. HOWARTH, C. R., FOSTER, P. J. and THRING, M. W. The effect of temperature on the extinction of radiation by soot particles, *Proc. Third International Heat Transfer Conference*, Vol. 5, pp. 122-128 (1966).
328. SIDDALL, R. G. and MCGRATH, I. A. The emissivity of luminous flames, *Ninth Symposium (International) on Combustion*, pp. 102-110, Academic Press, New York (1963).
329. ECHIGO, R., NISHIWAKA, N. and HIRATA, M. A study on the radiation of luminous flames, *Eleventh Symposium (International) on Combustion*, pp. 381-389, The Combustion Institute, Pittsburgh (1967).
330. FOSTER, P. J. and HOWARTH, C. R. Optical constants of carbons and coals in the infrared, *Carbon*, **6**, 719-729 (1968).
331. BONYTON, F. P., LUDWIG, C. B. and THOMSON, A. Spectral emissivity of carbon particle clouds in rocket exhausts, *A.I.A.A. Journal*, **6**, 865-871 (1968).
332. DALZELL, W. H. and SAROFIM, A. F. Optical constants of soot and their application to heat flux calculations, *Trans A.S.M.E.-J. Heat Transfer*, **91**, 100-104 (1969).
333. MURRAY, I. and SERGEANT, G. D. The onset of luminosity in propane/air flames, *Fuel*, **51**, 267-271 (1971).
334. GRAHAM, S. C. The refractive indices of isolated and aggregated soot particles, *Combust. Sci. Tech.* **9**, 159-163 (1974).
335. CHIPPERT, S. and GRAY, W. A. The size and optical properties of soot particles, *Comb. Flame*, **31**, 149-159 (1978).
336. JANZEN, J. The refractive index of colloidal carbon, *J. Colloid Interface Sci.* **69**, 436-447 (1979).
337. KERKER, M. *The Scattering of Light*, Academic Press, New York (1969).
338. VAN DE HULST, H. C. *Light Scattering by Small Particles*, Wiley, New York (1957).
339. MÜLLER-DETHLEFS, K. Doctoral Thesis, Imperial College, London (1979).
340. AMBROSIO, M., BERETTA, F., D'ALESSIO, A. and DILORENZO, A. Analytical techniques in the study of pollutants evolution in rich methane-oxygen flames, *La Rivista des Combustibili*, **29**, 337-348 (1975).
341. D'ALESSIO, A. and AMBROSIO, M. Metodi ottici nello studio di fiamme contenenti particelle di fuliggine, *La Termotecnica*, **30**, 460-472 (1976).
342. PENNER, S. S., BERNARD, J. M. and JERSKEY, T. Power spectra observed in laser-scattering from moving, polydisperse systems in flames—I. Theory. *Acta. Astro.* **3**, 69-92 (1976).
343. PENNER, S. S., BERNARD, J. M. and JERSKEY, T. Laser scattering from moving polydisperse particles in flames—II. Preliminary experiments. *Acta. Astron.* **3**, 93-105 (1976).
344. BERNARD, J. M. and PENNER, S. S. Determination of particle sizes in flames from scattered laser power spectra, *Experimental Diagnostics in Gas-Phase Combustion Systems*, (editor ZINN, B. T.), pp. 411-420, Progress in Aeronautics and Astronautics, Vol. 53, American Inst. of Aeronautics and Astronautics, New York (1977).
345. PENNER, S. S. and CHANG, P. On the determination of log-normal particle-size distributions using half-widths and detectabilities of scattered laser power spectra, *J. Quant. Spectr. Rad.* **20**, 447-460 (1978).
346. DRISCOLL, J. F., MANN, D. M. and McGREGOR, W. K. Submicron particle size measurements in an acetylene-oxygen flame, *Combust. Sci. Tech.* **20**, 41-47 (1979).
347. BERETTA, F., BORGHESE, A., D'ALESSIO, A. and VENITOZZI, C. Laser light scattering investigations in rich methane-oxygen flames, Paper presented at the Workshop on Laser Measurement Methods in Combustion, Urbino, September (1977).
348. CAVALIERE, A., D'ALESSIO, A. and VENITOZZI, C. Tecniche di Fluorescenza ed Assorbimento nell' U.V. per la caratterizzazione di Composti ad alto peso Molecolare in Fiamme in Eccesso di Combustibile. Risultati Preliminari, Paper presented to the Congresso dell' Associazione Termotecnica Italiana, Palermo, September (1979).
349. COE, D. Private communication.
350. TESNER, P. A. Formation of dispersed carbon by thermal decomposition of hydro carbons, *Seventh Symposium (International) on Combustion*, pp. 546-553, Butterworths, London (1959).
351. TESNER, P. A., KNORRE, V. G., KAMENSCHIKOVA, V. I. and SNEGIREVA, T. D. Formation of soot from acetylene under shock-tube conditions. *Comb. Expl. Shock Waves*, **12**, 649-653 (1976).
352. GRANOVSII, E. A., KNORRE, V. G. and TESNER, P. A. Role of soot in propagation of a laminar acetylene decomposition flame, *Comb. Expl. Shock Waves*, **12**, 644-649 (1976).
353. KNORRE, V. G., KOPYLEV, M. S. and TESNER, P. A. Role of soot in acetylene detonation. *Comb. Expl. Shock Waves*, **13**, 732-736 (1977).
354. STEHLING, F. C., FRAZEE, J. D. and ANDERSON, R. C. Mechanisms of nucleation in carbon formation, *Eighth Symposium (International) on Combustion*, pp. 774-784, Williams and Wilkins, Baltimore (1962).
355. DUGWELL, D. R. and FOSTER, P. J. Carbon formation from methane in combustion products, *Carbon*, **11**, 455-467 (1973).
356. TESNER, P. A. The activation energy of gas reactions with solid carbon, *Eighth Symposium (International) on*

- Combustion*, pp. 807–814. Williams and Wilkins, Baltimore (1962).
357. NARASIMHAN, K. S. and FOSTER, P. J. The rate of growth of soot in turbulent flow with combustion products and methane. *Tenth Symposium (International) on Combustion*, pp. 253–257, The Combustion Institute, Pittsburgh (1965).
358. SUROVIKIN, V. F. Analytical description of the processes of nucleus-formation and growth of particles of carbon black in the thermal decomposition of aromatic hydrocarbons in the gas phase. *Solid Fuel Chemistry*, **10**, (1), 92–101 (1976).
359. GILYAZETDINOV, L. P. Coagulation growth of soot aerosol particles. *Adv. Aerosol Phys.* **7**, 49–54 (1973).
360. GRAHAM, S. C. and HOMER, J. B. Light-scattering measurements on aerosols in a shock tube. *Recent Developments in Shock Tube Research*, (editors BERSHADER, D. and GRIFFITH, W.), pp. 712–719, (Proceedings of the Ninth International Shock Tube Symposium), Stanford University Press (1973).
361. GRAHAM, S. C. and HOMER, J. B. Coagulation of molten lead aerosols. *Symp. Faraday Soc.* **7**, 85–103 (1973).
362. GRAHAM, S. C. and ROBINSON, A. A comparison of numerical solutions to the self-preserving size distribution for aerosol coagulation in the free-molecule regime. *J. Aerosol Sci.* **7**, 261–273 (1976).
363. HIDY, G. M. and BROCK, J. R. *The Dynamics of Aerocolloidal Systems*, Pergamon Press, Oxford (1970).
364. LAI, F. S., FRIEDLANDER, S. K., PICH, J. and HIDY, G. M. The self-preserving particle size distribution for brownian coagulation in the free-molecule regime. *J. Colloid. Interface Sci.* **39**, 395–405 (1972).
365. ULRICH, G. D. Theory of particle formation and growth in oxide synthesis flames. *Combust. Sci. Tech.* **4**, 47–57 (1971).
366. McMURRAY, P. H. and FRIEDLANDER, S. K. Aerosol formation in reaction gases: relation of surface area to rate of gas-to-particle conversion. *J. Colloid. Interface Sci.* **64**, 248–257 (1978).
367. SWITZER, C. W. and HELLER, G. L. The formation of carbon black in hydrocarbon flames. *Rubber World*, **134**, 855–865 (1956).
368. PRADO, G. and LAHAYE, J. Mécanisme de Formation de Particules de Noir de Carbone lors de la Décomposition Thermique de Benzene. I. Etude Cinétique. *J. Chim. Phys.* **70**, 1678–1683 (1973).
369. LAHAYE, J., PRADO, G. and DONNET, J. B. Nucleation and growth of carbon black particles during thermal decomposition of benzene. *Carbon*, **12**, 27–35 (1974).
370. LAHAYE, J. and PRADO, G. Formation of carbon particles from a gas phase: nucleation phenomenon. *Water, Air and Soil Pollution*, **3**, 473–481 (1974).
371. PRADO, G. and LAHAYE, J. Mécanisme de Formation de Particules de Noir de Carbone lors de la Décomposition Thermique d'Hydrocarbones, II. Phénomène d'Association de particules. *J. Chim. Phys.* **72**, 483–489 (1975).
372. JINNO, H., FUKUTANI, S. and AKIKO, T. Estimation of the stability of droplet as nuclear of soot formation in hydrocarbon flames. *Sixteenth Symposium (International) on Combustion*, pp. 709–718, The Combustion Institute, Pittsburgh (1977).
373. ERICKSON, W. D., WILLIAMS, G. C. and HOTTEL, H. C. Light scattering measurements on soot in a benzene-air flame. *Comb. Flame*, **8**, 127–132 (1964).
374. JONES, A. R. and WONG, W. Direct optical evidence for the presence of sooty agglomerates in flames. *Comb. Flame*, **24**, 139–140 (1975).
375. MEDALIA, A. I. Morphology of aggregates. I. Calculation of shape and bulkiness factors: application to computer-simulated random flocs. *J. Coll. Interface Sci.* **24**, 393–404 (1967).
376. SUTHERLAND, D. N. A theoretical model of floc structure. *J. Coll. Interface Sci.* **25**, 373–380 (1967).
377. ULRICH, G. D. Comments in *Twelfth Symposium (International) on Combustion*, p. 884, The Combustion Institute, Pittsburgh (1969).
378. HOMANN, K. H. Comments in *Sixteenth Symposium (International) on Combustion*, p. 717, The Combustion Institute, Pittsburgh (1977).
379. JOHNSON, G. L. and ANDERSON, R. C. An electron microscope study of carbon formation in the pyrolysis of hydrocarbon. *Proceedings of the Fifth Conference on Carbon*, Vol. 1, pp. 395–405, Pergamon Press, New York (1962).
380. SUROVIKIN, V. F., ROGOV, A. V. and VERSHININ, L. V. Carbon black formation in the incomplete combustion of benzene. *Comb. Expl. Shock Waves*, **11**, 202–209 (1975).
381. SAMKHAN, I. I., TSVETKOV, Y. V., PETRUNICHEV, V. A. and GLUSHKO, I. K. Theory of the formation of carbon black. *Colloid Journal (U.S.S.R.)*, **33**, 740–745 (1971).
382. JENSEN, D. E. Prediction of soot formation rates: a new approach. *Proc. Roy. Soc. A*, **338**, 375–396 (1974).
383. COATS, C. M. and WILLIAMS, A. Investigation of the ignition and combustion of *n*-heptane–oxygen mixtures. *Seventeenth Symposium (International) on Combustion*, pp. 611–621, The Combustion Institute, Pittsburgh (1979).
384. BECKER, R. and DÖRING, W. *Ann. Phys.* **24**, 719 (1935).
385. ABRAHAM, F. F. Homogeneous Nucleation Theory, *The Pretransition Theory of Vapor Condensation*, Academic Press, New York and London (1974).
386. BAUER, S. H. et al. *J. Phys. Chem.* **81**, 984, 1015, 1001, 1007 (1977).
- Some recent research papers on soot formation are to be found in:
387. *Eighteenth Symposium (International) on Combustion*, The Combustion Institute, Pittsburgh, PA; 1981 (to appear).
388. *Particulate Carbon–Formation During Combustion*, Proceedings of the General Motors Symposium held 14–16 October 1980, Warren, Michigan, U.S.A. (to appear).

(Manuscript received 7 January 1981)